REVIEW

Check for updates

A dual experimental–theoretical perspective on ESPT photoacids and their challenges ahead†

Niklas Sülzner, [ID] *a Gregor Jung [ID] *b and Patrick Nuernberger [ID] *c

Photoacids undergo an increase in acidity upon electronic excitation, enabling excited-state proton transfer (ESPT) reactions. A multitude of compounds that allow ESPT has been identified and integrated in numerous applications, as is outlined by reviewing the rich history of photoacid research reaching back more than 90 years. In particular, achievements together with ambitions and challenges are highlighted from a combined experimental and theoretical perspective. Besides explicating the spectral signatures, transient ion-pair species, and electronic states involved in an ESPT, special emphasis is put on the diversity of methods used for studying photoacids as well as on the effects of the environment on the ESPT, illustrated in detail for 8-hydroxypyrene-1,3,6-trisulfonate (HPTS) and the naphthols as examples of prototypical photoacids. The development of exceptionally acidic super-photoacids and magic photoacids is subsequently discussed, which opens the way to applications even in aprotic solvents and provides additional insight into the mechanisms underlying ESPT. In the overview of highlights from theory, a comprehensive picture of the scope of studies on HPTS is presented, along with the general conceptualization of the electronic structure of photoacids and approaches for the quantification of excited-state acidity. We conclude with a juxtaposition of established applications of photoacids together with potential open questions and prospective research directions.

1 Introduction

Proton transfer (PT) is omnipresent in chemistry and its related fields, including countless examples from biochemistry, chemical synthesis, and catalysis, as well as industrial applications.[1–3] It is at the heart of acid–base catalysis[4–7] and continues to be relevant in today's research, *e.g.*, in the development of fuel cells.[8] In biochemical systems, to name a few examples, the structure and functioning of proteins is determined by the protonation states of the amino acid side chains,[9,10] proton gradients along biomolecular membranes act as driving forces for the ATP synthesis,[11] and many enzymes either directly catalyze—at least in one step of their catalytic cycle—an acid–base reaction[12] or their activity involves proton transfer along a conduction wire, *i.e.*, a preformed hydrogen-bond network of amino acids and water molecules (*e.g.*, in photosystem II[13]). Proton transfer can also take place in an electronically excited state, *e.g.*, as in fluorescent proteins[14–28] or in the chromophore of Firefly's D-luciferin.[29–36] Moreover, such

an excited-state proton transfer (ESPT) of anthocyanin pigments in plants is biologically relevant for the protection from photodamage since the ESPT provides a fast deactivation channel, efficiently converting the absorbed light energy into heat.[37,38]

Owing to this fundamental importance, there has been a huge interest in the study of proton-transfer reactions since the beginnings of chemistry,[39,40] both with respect to the underlying thermodynamics as well as the chemical kinetics. From a thermodynamic perspective, the acid dissociation constant K_a or the pK_a, *i.e.*, its negative decadic logarithm, is the most important quantity as it quantifies the Brønsted acid strength.[41] While the experimental determination of pK_a has nowadays become a standard in aqueous solution owing to a broad variety of well-established techniques (*e.g.*, potentiometric, NMR-spectroscopic, or spectrophotometric titrations),[42] the situation is much more complicated in non-aqueous solution since the drastically lower acidity constants in combination with other complications such as low solubilities or homo-conjugation challenge the accuracy of experimental detection methods.[43,44] Due to these difficulties, computational pK_a predictions have become much more important in these environments, providing an alternative path to pK_a.[45,46]

Regarding the kinetics, a molecular probe is typically required to experimentally obtain information on the PT mechanisms including relevant intermediates as well as rate constants for the individual steps. For this task, so-called photoacids have established as particularly powerful tools during

aLehrstuhl für Theoretische Chemie, Ruhr-Universität Bochum, 44780 Bochum, Germany. E-mail: niklas.suelzner@rub.de; Tel: +49 234 32 24523

bBiophysikalische Chemie, Universität des Saarlandes, 66123 Saarbrücken, Germany. E-mail: g.jung@mx.uni-saarland.de; Tel: +49 681 302 71320

cInstitut für Physikalische und Theoretische Chemie, Universität Regensburg, 93040 Regensburg, Germany. E-mail: patrick.nuernberger@ur.de; Tel: +49 941 943 4487

† Dedicated to the late Professor Dan Huppert on the occasion of his 80th birthday.

the last decades (Fig. 1 and *vide infra*). These photoacids are molecules that exhibit an increase in acidity (*i.e.*, a decrease in pK_a) upon electronic excitation.[47,48] In other words, such a photoacid is a stronger acid in its electronically excited state (usually the lowest-lying singlet state S_1) compared to the (singlet) ground state S_0. Thus, the excited-state pK_a (from now on referred to as pK_a^*) is smaller than the ground-state pK_a. As a consequence, photo-excitation can trigger an excited-state proton transfer (ESPT)[49] from the photoacid to a nearby proton acceptor, *e.g.*, the solvent or any other Brønsted base.[50] While most (weak) photoacids ($pK_a^* > 0$) are—due to limited acid strength—restricted to ESPT in neat water[51,52] and aqueous solutions containing an additional base[53] or co-solvent,[54–57] those with a negative pK_a^* can also perform an ESPT in other protic (*e.g.*, alcohols)[58,59] or even aprotic solvents such as dimethyl sulfoxide (DMSO).[60,61] In particular, the use of pulsed lasers has made it possible to temporally initiate the ESPT event, which conveniently allows to investigate the associated dynamics in real time using time-resolved spectroscopy.[62,63]

Research on light-induced triggering of processes involving proton transfer is rather broad and also covers many phenomena beyond ESPT. The area of metastable-state photoacids[64–68] or generally photacid generators (PAGs)[69–72] is closely related, and so is the relation between electron and proton transfer[73] and proton-coupled electron transfer (PCET)[74–78] in the widest sense, however these topics are not within the scope of this review, and neither are triplet photoacids,[79–84] Lewis photoacids,[85–87] nor intramolecular ESPT (ESIPT).[88–90] Rather, within the spectrum of existing photoacid reviews (*e.g.*, ref. 2, 47, 48, 50 and 91–98) the purpose of this article is to give an up-to-date overview on photoacids from an experimental–theoretical perspective (including their upcoming challenges) with a focus on the kinetics and the thermodynamics of the ESPT process.

2 A brief history of photoacids

2.1 The phenomenon of photoacidity

Photoacids have been the subject of ongoing scientific studies (see Fig. 1 for a selection of milestones in experimental photoacid research) since their initial description in the first half of the 20th century by Weber (1932),[99] Terenin and Kariakin
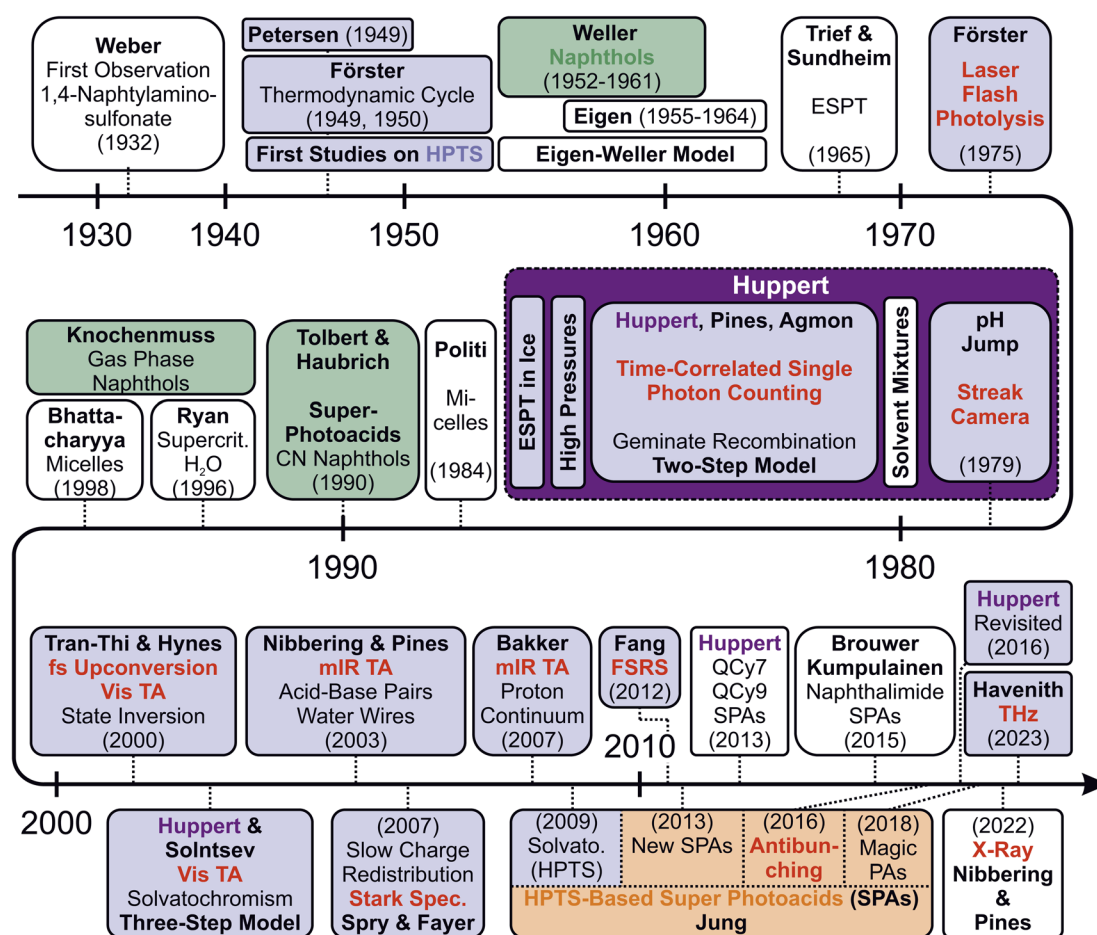

Fig. 1 Milestones of experimental research on photoacids exhibiting ESPT. Color coding: studies involving 8-hydroxypyrene-1,3,6-trisulfonate (HPTS) (blue), naphthols (green), or the recent HPTS-based super-photoacids introduced by Jung (orange); contributions from the Huppert group (purple); application of novel experimental techniques (red). Abbreviations: femtosecond (fs), visible (Vis), mid infrared (mIR), femtosecond Raman scattering (FSRS), terahertz (THz), spectroscopy (spec.), solvatochromism (solvato.), super-photoacids (SPAs), new inspection and analysis of the ultrafast time-resolved fluorescence data on HPTS (Huppert Revisited).
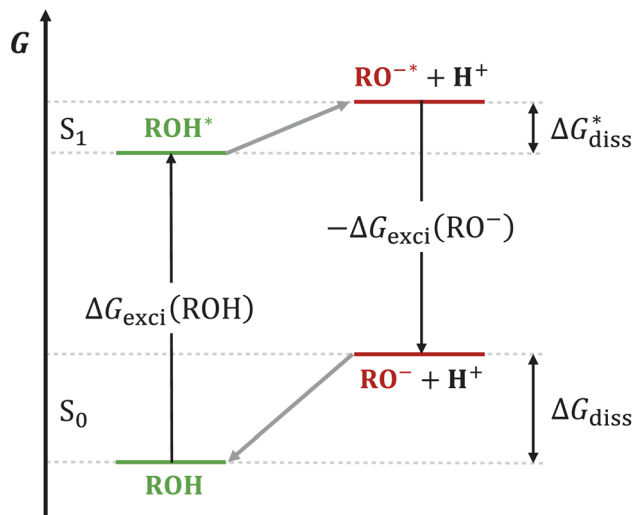
Fig. 2 The Förster cycle. A simple thermodynamic cycle to account for an increased acidity, i.e., a decreased (Gibbs free) acid dissociation energy, ΔG_{diss}, in the first electronically excited state (S_1) compared to the electronic ground state (S_0), caused by different relative energies of the acid–base equilibria of the two electronic states. These are coupled through the (Gibbs free) electronic excitation energy, ΔG_{exci}, of the protonated (ROH) and deprotonated species (RO$^-$), respectively. An asterisk (*) is used for referring to the excited state.

(1947),[100] Petersen (1949),[101] and Förster (1949, 1950),[102–104] who had reported pH-dependent changes in the fluorescence spectra of several dye molecules; including 1,4-naphthylaminosulfonate, acridine, 8-aminopyrene-1,3,6-trisulfonate,‡ as well as 8-hydroxypyrene-1,3,6-trisulfonate§ and 6,8-dihydroxypyrene-1,3-disulfonate,¶ respectively. Recently afterwards, it has also been Förster who introduced the idea of considering a thermodynamic cycle that takes into account the acid–base equilibria for both the electronic ground state and the excited state to rationalize the phenomenon of photoacidity.[102–105] In his memory, this cycle is today referred to as Förster cycle (Fig. 2). This thermodynamic cycle relates ΔpK_a, the difference between the excited-state (pK_a^*) and ground-state (pK_a) acidity, to the difference in the Gibbs free electronic excitation energies (ΔG_{exci}) of the protonated (ROH) and deprotonated (RO$^-$) species, as expressed in eqn (1)

$$\Delta pK_a = pK_a^* - pK_a = \frac{\Delta G_{\mathrm{exci}}(\mathrm{RO}^-) - \Delta G_{\mathrm{exci}}(\mathrm{ROH})}{RT \ln(10)} \quad (1)$$

with the ideal gas constant R and the absolute temperature T.

If the ground-state pK_a is known, eqn (1) can be used to calculate pK_a^* from the electronic transition energies; if the pK_a is unknown, still the ΔpK_a can be determined. Ideally, 0–0 transition energies should be inserted into eqn (1).[106] Owing to its simplicity, the Förster cycle has become the most common route to pK_a^* for both experiments and theory, although also other approaches exist (see Section 7).

---

‡ Initially referred to as 3-aminopyrene-5,8,10-trisulfonate.

§ Initially referred to as 3-hydroxypyrene-5,8,10-trisulfonate.

¶ Initially referred to as 3,5-dihydroxypyrene-8,10-disulfonate.

2.2 Different classes of photoacids

ESPT photoacids are typically hydroxyarene or aminoarene compounds and thus the acidic functional group is either a hydroxy (OH) or an amino (NH$_2$) or ammonium (NH$_3^+$) group. The most common classes of photoacids include naphthols[107–113] (Fig. 3b and c), hydroxyquinolines[79,114–117] (Fig. 3e and f), hydroxycoumarins[118–127] (Fig. 3d), and hydroxypyrenes[61,103,128–131] (Fig. 3g), although also some anilines,[132–134] naphthylamines[99,101,135–137] and aminopyrenes[103,138–144] are known. Phenols (Fig. 3a) also exhibit photoacid character ($\Delta pK_a \sim -6$),[145–149] but their UV absorption (~270 nm) and weak fluorescence make them impractical for applications. Less known photoacids are hydroxyisoquinolines,[150] fluorescein derivatives,[151–153] hydroxybenzoquinolizinium ions,[154,155] and tetracyanohydroquinone.[156] The photoacidity of merocyanine-spiropyran systems both for metastable-state and ESPT photoacids has also been explored in more detail recently.[68,157–163]

The counterparts of photoacids, i.e., photobases, also exist, but have only more recently attracted increased attention in various research fields.[164–179] These photobases are compounds that become more basic in the excited state. To rationalize and quantify photobasicity, one simply has to switch the perspective: a photobase is a species whose conjugate acid becomes less acidic in the electronically excited state compared to the ground state. The term photobase is often used incorrectly for the corresponding base of an excited photoacid, which is in fact exactly the opposite of a photobase since these species are particularly weak excited-state bases.

While the aromatic OH group is typical for many photoacids, a common feature of photobases are N-heterocyclic, aromatic frameworks.[180,181] A peculiarity is the combination of photoacidic and photobasic functional groups within one molecule.[182–187] Here, an ESIPT is possible by contribution of protic solvents, and these systems therefore appear suitable to address the question to which extent water- or proton-wires exist in different solvent compositions.[117,188–195]

3 Spotlight HPTS—the supposably most studied photoacid

The research on photoacids has been largely stimulated by Huppert and co-workers, reaching back to the 1980s when Huppert—at that time under the supervision of Kolodney—had joined the photoacid community.[196,198] After almost 40 years of research, Huppert can be considered one of the leading pioneers in photoacid chemistry. Moreover, he has also catalyzed the huge interest in 8-hydroxypyrene-1,3,6-trisulfonate (HPTS or pyranine), which is one of the first photoacids ever studied.[100–102] To date, HPTS has probably become the photoacid investigated in greatest detail in the literature since its first mention in the 1930s,[199] owing also to its wide applicability, e.g. as an efficient fluorophore and a ground-state pH sensor,[200–203] and to its suitability for use in everyday products like text highlighters and dishwashing detergents. Studying the ESPT of HPTS in water using time-resolved spectroscopy has even been proposed as an educational experiment for students.[204] The
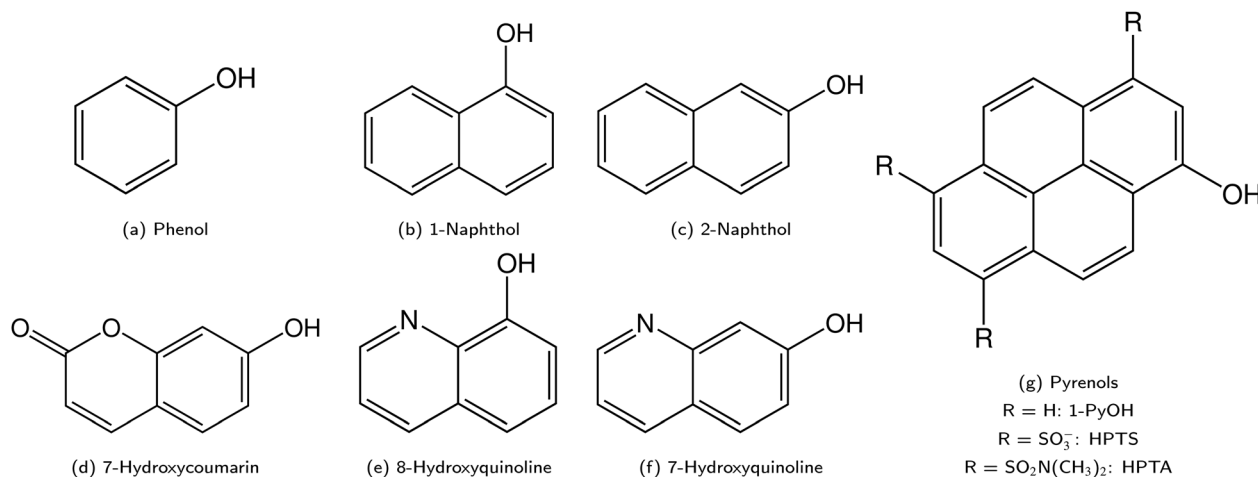
Fig. 3 Overview on the different classes of photoacids. The corresponding naphthylamines and aminopyrenes are obtained by substituting the OH group by an NH_2/NH_3^+ in (b and c) or (g), respectively.

characteristics of the ESPT of HPTS have been deciphered in a vast number of environments and with many different experimental techniques, as well as with theoretical approaches, as highlighted in the following.

3.1 ESPT in dependence on the environment

Aqueous solutions pertain an outstanding role among all studied conditions, and the ESPT to the solvent in bulk water has been analyzed in great detail.[51,52,63,140,205–226] Beyond that, also the ESPT to a co-solute base such as acetate[53,62,221,227–233] or (per)chloroacetate[234–236] could be unveiled, and also the role of co-solvents on the ESPT of HPTS was addressed in solvent mixtures consisting of water and, *e.g.*, methanol[197,237–240] or DMSO.[54,241] Other parameters include the effect of additional salts[198,238,242–245] or the variation of temperature[246,247] and pressure[248] on the ESPT process. Challenging the limits of ESPT, even the ESPT of HPTS in ice and doped ices,[246,249–255] in confined water nanopools of various reverse micelles (with anionic, neutral or cationic surfactants),[256–263] or in Nafion fuel cell membranes[260,264,265] have been explored. This scope also included many biological environments such as the cavity of cyclodextrin,[266–268] other supramolecular assemblies,[269] adsorbing bio-materials (hydrophobic insulin amyloid fibrils and hydrophilic cellulose surfaces; chitin, starch, chitosan),[270–275] hydrogels,[276–278] the presence of proteins,[279] or even living cells.[280–282] In all the experiments listed above, it was observed that ESPT dynamics of HPTS in aqueous environments can be manipulated through the interaction with adjacent molecules. Apart from these studies where water plays a decisive role, studies on ESPT of HPTS in non-aqueous solution are very scarce though, and for instance involve HPTS and acetate in methanol[283] and HPTS in ionic liquids.[284,285] Moreover, due to the three- or four-valent anionic nature, the vast majority of studies on HPTS take place only in actual solutions, in contrast to other photoacids (*e.g.*, naphthols that are also studied in gas-phase solvent clusters[286–289]). One remarkable exception is a photoelectron spectroscopy study that reports a negative

electron binding energy for the acid species of HPTS (generated *via* electrospray), demonstrating the immense reductive potential of such a highly charged anion in the gas phase.[290]

3.2 An arsenal of spectroscopic techniques

Many different spectroscopic techniques have been applied to investigate HPTS and other photoacids, each one with its own advantages and varying accessible information. Changes in the electronic structure upon deprotonation allow spectroscopies in the visible spectral range such as UV/Vis absorption and fluorescence emission to be used for distinguishing the protonated from the deprotonated form. In its simplest form, pH titrations are used for the determination of ground-state pK_a values, and fluorescence read-out, *i.e.* fluorescence excitation spectroscopy, is preferred due to its higher sensitivity.[292] Consequently, pH measurements with few or even single molecules are possible, and nanomolar concentration of samples in the focus of a confocal microscope show stochastic fluorescence fluctuations as a result of continuous cycles of deprotonation and protonation events when only one of the ground-state species is excited by an appropriate laser source.[291] The kinetics of this interconversion in the thermodynamic equilibrium are then accessible by fluorescence correlation spectroscopy when the photostability is high enough.[293] Moreover, since the molecular vibrations are highly specific to intermolecular interactions, mid-infrared (mIR) absorption or Raman scattering spectroscopy can be used to further characterize possible PT intermediates such as ion pairs. In general, time-resolved spectroscopy with high time resolution is unrivaled to obtain information on the dynamics, *i.e.*, the actual kinetics of the ESPT.

To briefly visualize the additional information content, steady-state and time-resolved emission are juxtaposed in Fig. 4 for a super-photoacid. Whereas the steady-state fluorescence spectrum foreshadows that more than one emissive species contributes, the time-resolved data discloses which wavelength is emitted at which moment in time after photoexcitation. Thus, the ESPT and its characteristic time scale can be deduced, while

more detailed analysis can also provide insight into additional transient species when photoacid and base or the ions of the nascent ion pair interact (*vide infra*).

Steady-state UV/Vis absorption and fluorescence emission spectroscopy have been applied since the early days for a qualitative characterization of the ground-state and excited-state equilibria of HPTS in water,[103] but also more recently to its solvatochromism.[295,296] The earliest transient absorption experiments of HPTS in aqueous solution were reported by Förster and Völker (1975)[297] and Lundy-Douglas and Schelly (1976),[298] both using flash photolysis (tens of ns time resolution), followed by laser photolysis experiments by Gutman, Huppert and Pines (1981, 1983).[299,300] In parallel, early time-resolved fluorescence spectroscopy on the ps to ns timescale initially based on streak cameras and later time-correlated single photon counting (TCSPC)—both limited by a rather poor ps time resolution based on today's ultrafast standards—was used to study the slower excited-state dynamics,[197,198,301] which allowed Agmon, Pines, and Huppert in 1986 to establish their well-known two-step model for the ESPT of HPTS to water (*vide infra*).[205–211]

According to the early two-step model for HPTS in water, the excited protonated species (ROH*) of HPTS first transfers its proton to a nearby water molecule under formation of a contact ion pair (CIP) within ~90 ps. Subsequently, this CIP is separated in a diffusive process, yielding the free deprotonated form (RO⁻*) within 100 ps.[206] Noteworthy, in seminal studies published in 1986, it could be unambiguously shown that the emission dynamics of excited HPTS in water proceed in a non-mono-exponential fashion (see Fig. 5), a consequence of geminate recombination within the ion pair consisting of RO⁻* and the generated cation. This process may be considered as a quasi-equilibration, while diffusion eventually facilitates the separation of the ions. Modelling of this reprotonation process of RO⁻* by including a recombination rate and assuming diffusive ion separation allowed a quantitative analysis of the observed dynamics. Furthermore, the discovery of a pronounced recombination contribution could explain why the ion separation is less efficient than expected.[297]

In 1996, Tran-Thi and co-workers applied fs fluorescence up-conversion for the first time to study the ultrafast dynamics of HPTS in water[213] and later (in 2000) complemented the inferences with results from transient UV/Vis absorption.[214] In the same year, ultrafast transient absorption measurements on HPTS were also performed by Huppert *et al.*, but for the bimolecular ESPT of HPTS to acetate.[53] Owing to a much better time resolution compared to the previous TCSPC experiments, the
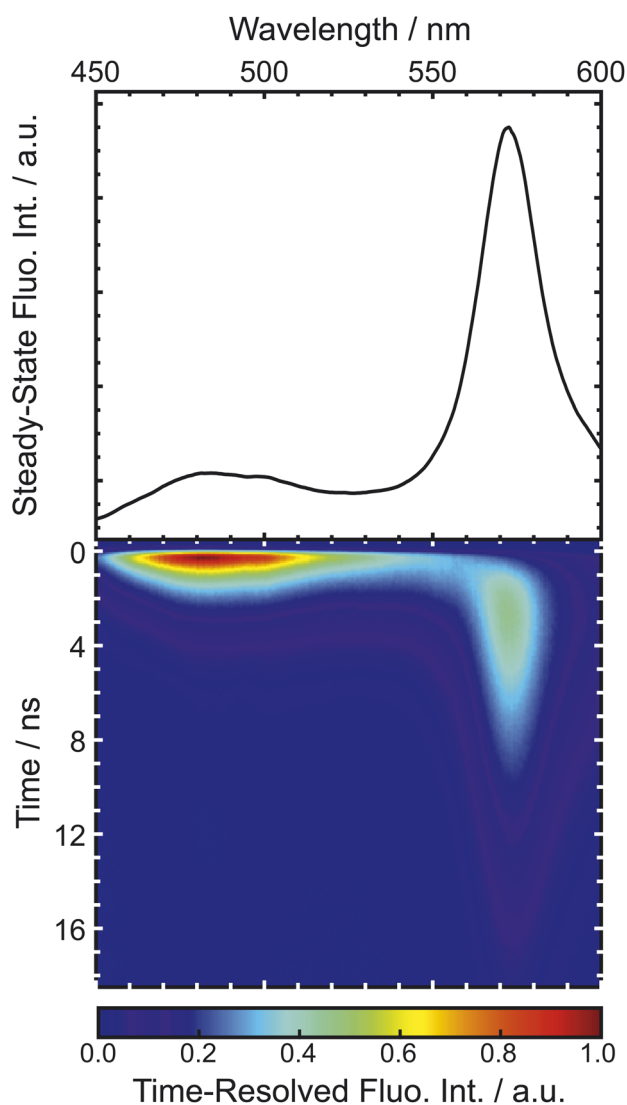

Fig. 4 Emission of super-photoacid **B** (*cf.* Fig. 13d) in an acetone–water mixture (0.55 M of water). The time-resolved fluorescence (bottom panel) resolves that the steady-state fluorescence (top panel) comprises several contributions with different lifetimes. The displayed data is part of the study in ref. 294.
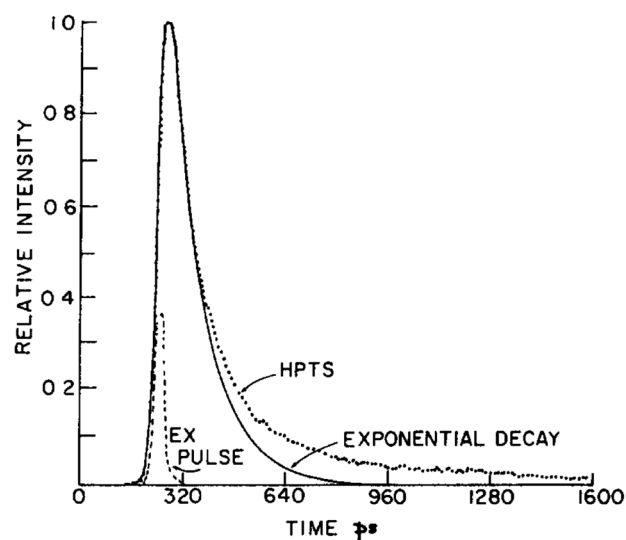

Fig. 5 Fluorescence decay of HPTS in water together with an exponential fit, exemplifying that geminate recombination leads to a tail-like emission behavior of the excited protonated solute. The profile of the 25 ps excitation pulse is shown as well. This figure has been reproduced from ref. 206 with the kind consent of E. Pines and with permission from Elsevier, copyright 1986.

results by Tran-Thi *et al.* revealed the additional involvement of two fast processes in the ESPT kinetics that precede the proton-transfer step, which had been previously unobserved and then started to challenge the two-step model for the ESPT (*vide infra*).[213–216,302]

Particularly in the course of this debate but also as a consequence of further issues on HPTS, ultrafast transient mIR absorption[62,219–221,229–231,234–236,245,303] and fs stimulated Raman scattering[225,226,232,239,304–308] in addition to UV/Vis spectros-copy[52,53,140,213,214,217,223,229,233,309] were established as routine methods, and even the use of less conventional techniques such as photon-echo spectroscopy,[310] magnetic circular dichroism (MCD),[222] Stark spectroscopy,[224] or UV-pump-X-ray-probe spectroscopy has been reported. In the latter study, the electronic structure changes of the proton-donating group of the related photoacid 8-aminopyrene-1,3,6-trisulfonic acid (APTS) upon photo-excitation and the subsequent proton transfer dynamics have been visualized.[311] Moreover, for photoacids under confinement (*vide supra*), time-resolved fluorescence anisot-ropy[256,259,263] together with 2D-NMR spectrosopy[155,312,313] have become powerful tools for probing the interaction with the environment.

A new perspective became recently available through time-resolved THz spectroscopy in combination with advanced calculations that have been applied by Havenith, Head-Gordon and coworkers to directly study the photo-induced solvent response of water in the vicinity of HPTS, the deprotonated form OPTS and the methoxy derivative MPTS.[63] Oscillatory features present in the first ps of the Vis-pump-THz-probe signal could be associated with vibrational energy transfer between solute and adjacent solvent molecules (see Fig. 6). In case of HPTS for which ESPT to the solvent is possible, this transfer of vibrational energy is more efficient and facilitates solvent reorganization, which is a prerequisite for the actual ESPT. Thorough analysis of the data on longer timescales dis-closed a dissipation of the proton into the bulk, reflected in a phonon-like propagation behavior.[314] In this regard, the ESPT dynamics are monitored from a solvent rather than from a solute response.

3.3 Theoretical studies on HPTS

Research groups specialized in theory have continuously put HPTS into the focus of their studies as well, especially in recent years. However, the relatively large size of the HPTS molecule in combination with the fundamental requirement for an accurate description of the electronic excitations hindered the theoret-ical investigations of photoacids in general and HPTS in particular for a long time. Moreover, for HPTS, the three-valent and four-valent anionic character of the protonated and deprotonated species leads to the additional requirement that an adequate description of the solvent needs to be included in the calculations.

This is among the reasons why the early theoretical, and more precisely, quantum-chemical studies rooted in the pho-toacid community (in the early 2000s) have mostly focused on smaller and simpler photoacids as model systems, such as phenol and cyanophenols (using state-specific CASSCF calcu-lations combined with PCM)[302] or cyanonaphthols (using semi-empirical AM1 calculations).[315] Apart from other preliminary calculations, *e.g.*, on hydroxyquinoline–water complexes by Fang *et al.*,[316–318] multi-reference methods (including CASSCF and CASPT2) have been applied more broadly to significantly larger photoacids only in more recent times.[319,320]

The first computational study on HPTS itself has been re-ported not much later by Hynes and co-workers (in 2002),[216] but was still restricted to semi-empirical (CS-INDO) calculations at that time because of relatively high computational costs for a full wavefunction-based treatment using multi-reference methods. In the same year though, Jimenez *et al.* reported a CIS—*i.e.*, the most simple, non-perturbative correlated single-reference method—study on MPTS, the methoxy analogue of HPTS, addressing its vertical electronic transition energies and
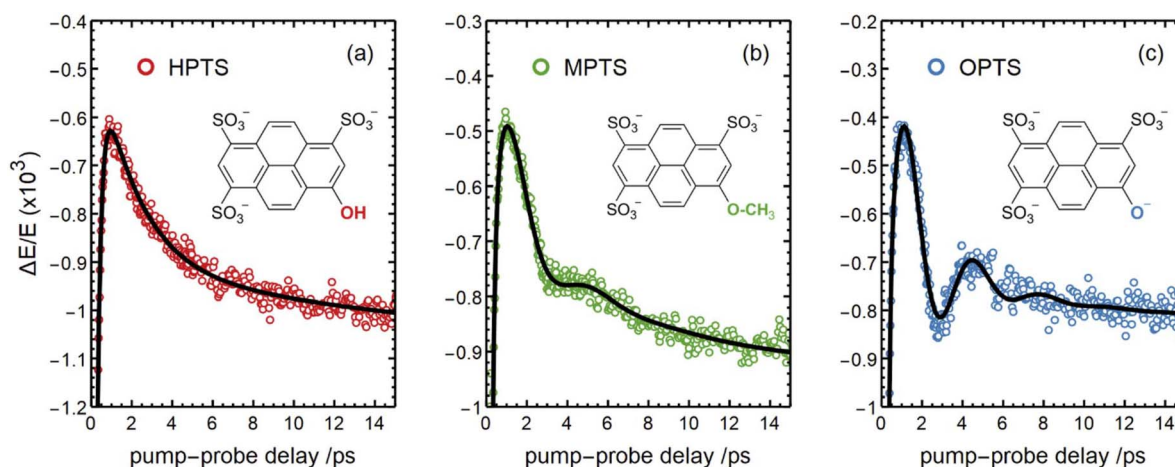

Fig. 6 Transient signals observed *via* Vis-pump-THz-probe spectroscopy applied to a water jet containing solutions of (a) HPTS, (b) MPTS, and (c) OPTS. The oscillatory features originate from vibrational solute–solvent energy transfer, whereas the strong damping in the case of (a) is indicative of a more efficient coupling that paves the way for the subsequent ESPT. This figure has been reproduced from ref. 63 with the kind consent of M. Havenith and with permission from the authors under the terms of CC BY-NC 3.0, copyright 2023.

the vibrational frequencies.[310] About 15 years later, HPTS became the subject of a purely *ab initio* study in (implicit) solution by Cimino *et al.* (in 2016),[321] using TDDFT as a much cheaper method for electronic excitation energies. Similarly, Graef *et al.* studied the lowest-energy transitions of pyrene—the main chromophoric core of HPTS—in vacuum and solution.[322] During that time, TDDFT—often in combination with some variant of the continuum solvation model PCM—has also been applied to many other photoacids[323–341] and particularly also to the prediction of pK_a^* values[342–350] (*vide infra*).

Over the past five years and besides static, quantum-chemical calculations, HPTS has also been investigated theoretically using molecular dynamics simulations, mostly with quantum-mechanics/molecular-mechanics (QM/MM) approaches for the sake of computational efficiency. One of the first examples is the combined experimental–theoretical study on the ESPT of HPTS to acetate by Heo *et al.*, which revealed a coherent wave packet motion of the reactant (acid) and the product (conjugate base) and identified the vibrational modes that actively participate in this coherent proton transfer.[233] The excited-state vibrational dynamics of HPTS have been extensively addressed by Rega and co-workers, *e.g.*, in neat

water[351,352] and in acetate-containing aqueous solution.[353,354] Even the particularly strong so-called super-photoacids (*vide infra*) have been the subject of theoretical studies, *e.g.*, on the ESPT dynamics of QCy9 in water by Raucci *et al.*[355] or the THz and IR signals of NM6HQ+ in water by Petrone *et al.*[356]

Similarly, the ESPT dynamics of HPTS in 1-methyl-imidazole[357] and in water[358] have been recently investigated in a joint experimental–theoretical study by Fayer, Martínez and co-workers. In contrast to the previously mentioned earlier quantum chemical study by Cimino *et al.*, in which no ESPT of HPTS had been observed with up to three water molecules,[321] the excited-state *ab initio* MD simulation by Walker *et al.*[358] scrutinize the ESPT of HPTS in bulk water more thoroughly and indicate the involvement of a strong, more extensive hydrogen-bonded network (*i.e.*, a water wire) between the (photo)acidic OH group and one of the three sulfonate groups, *e.g.*, involving eight water molecules (see Fig. 7). In fact, these results allow for a refinement of the existing experimental knowledge on HPTS by providing a clear molecular picture of the intermediates that are involved in the ESPT. They claim that the intermediate time constant of 2–3 ps that had been commonly assigned to a shared proton between HPTS and proximate water
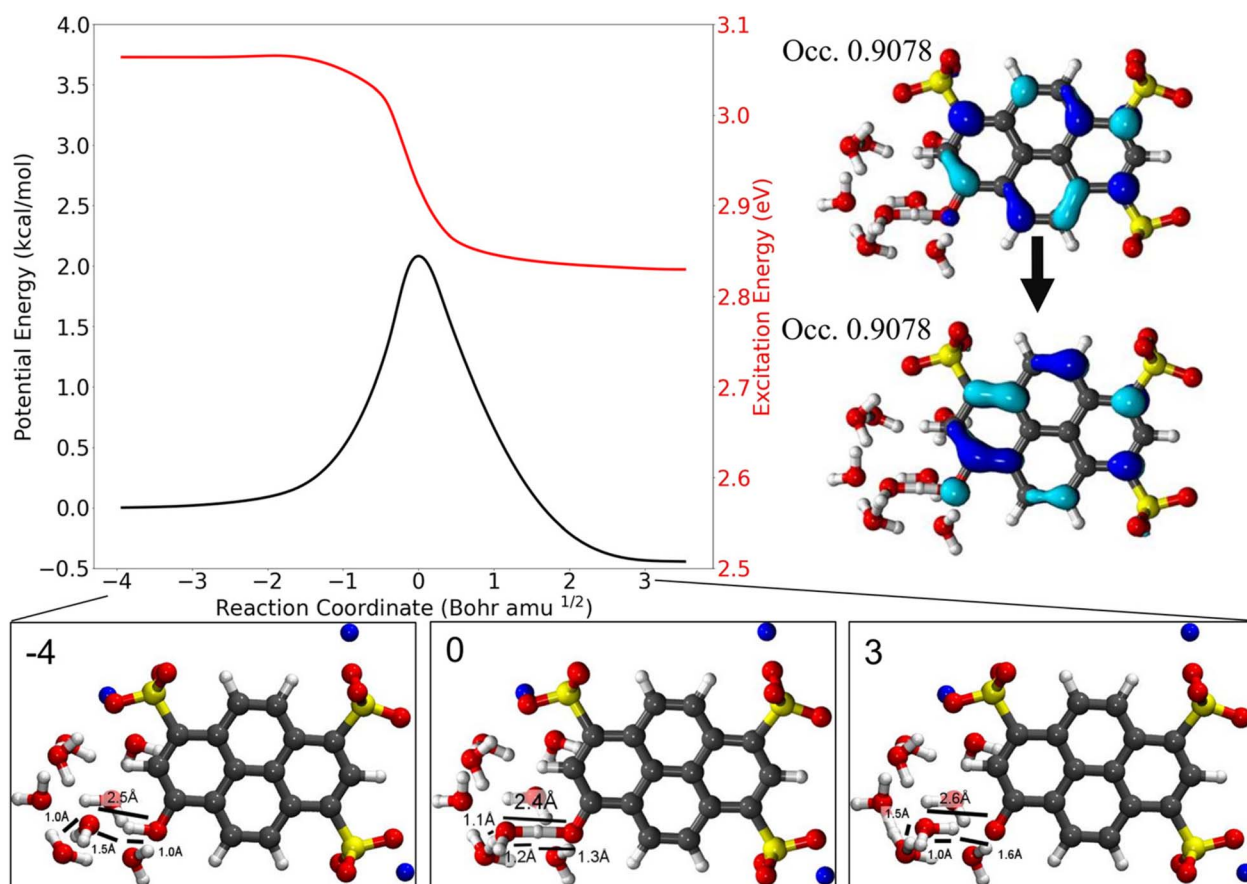

Fig. 7 Scan of the potential energy for the first excited state and the vertical excitation energies along the intrinsic reaction coordinate that corresponds to the deprotonation of HPTS. 8H$_2$O molecules and the implicit solvent model PCM have been used in combination with TDDFT. The change in excitation energy corresponds to 4.1 Å in the collective coordinate that quantifies the location of the proton within the water wire. Structures along the path are shown below, with the natural transition orbitals associated with the transition state geometry shown on the right. This figure has been reproduced from ref. 358 with the kind consent of M. D. Fayer and T. Martínez and with permission from the American Chemical Society, copyright 2021.

molecules[213,214,309] rather reflects the deprotonation of HPTS and the corresponding oscillation of the dissociated proton that first remains mobile within the water wire. Only after that, the proton localizes on one of the water molecules and can then diffuse away from the wire, and not just from a single water molecule coordinating the O⁻ group as assumed in previous interpretations, into the bulk solution on a longer timescale (∼80 ps).

4   Spotlight—naphthols

Naphthols comprise another important class of photoacids with a long-lasting history and a rich background in many research areas. Particularly important are the two parent compounds: 1-naphthol and 2-naphthol (*cf.* Fig. 3b and c). Although naphthols do not belong to the very first photoacids studied—which were in fact naphthyl amines (see Section 2)—, their photo-acidic character has been first reported by Weller in 1952 and 1954.[107,108] Moreover, no research group can be identified who has excelled at studying naphthols in a similar fashion as Huppert and coworkers have for HPTS; rather, the research history of the whole family of naphthols is a collection of many individual contributions. Therefore, this section is less strictly concerned about presenting a complete list, but more about a presentation of exemplary highlights.

Typically, the different naphthol derivatives are functionalized with one or multiple sulfonate groups for solubility reasons. For the 1-naphthols, mono-substituted derivatives with a sulfonate group at the ring positions 2,[359] 3,[360] 4,[361] and 5,[56] 4-chloro[362] and 5-*tert*-butyl[363] and 3,6-disulfonato[364] substitution are reported. For the 2-naphthols, monosulfonation at the 6,[365] 7,[366] or 8 (ref. 55) position and disulfonation at the 6,8 (ref. 367) and 3,6 (ref. 301) positions are typical. Even a dihydroxynaphthalene[368] and dimers of 2-naphthol[369,370] were recently described. In this regard, it is worth noting that 2,2′-dihydroxy-1,1′-naphthaldehyde diazine (pigment yellow 101) can be considered as a bisnaphthol with rich photochemistry beyond ESPT.[371] We will not make a particular distinction with respect to the substituents in the following, with the exception of electron-withdrawing groups such as cyano groups, to which a later section is dedicated (*cf.* Section 5).

4.1   Research highlights

Subsequent to the initial work by Weller,[107,108] important earlier contributions (*i.e.*, here prior to 1990) to the research on naphthols and the fundamental understanding of their properties as photoacids were made by Trieff and Sundheim (1965),[49] Suzuki and Baba (1967),[372] Kuz'min and co-workers (1977–1980),[93,373–375] Gutman, Huppert, and co-workers (1979–1981),[197,301,376] Schulman *et al.* (1979),[110] Harris and Selinger (1980),[111] Tobita, Tsutsumi and Shizuka (1980–1983),[112,377–379] Robinson and co-workers,[359,380–382] and Webb *et al.* (1986).[113] In more recent times (*i.e.*, after 1990), the ESPT of naphthols in gas-phase clusters has emerged as one particular research area, as extensively, but not exclusively,[383–388] studied by Knochenmuss and co-workers.[286,287,389–395] Owing to the neutral nature of

the naphthol (in contrast to the anionic HPTS), techniques such as mass spectrometry, multi-photon ionization (MPI), time-resolved photo ionization (TRPI), or laser-induced fluorescence (LIF) (*cf.* ref. 287), could be applied. Even some QM/MM studies have been reported under these conditions, namely for 1-naphthol in liquid-cooled jets.[396] Pines and co-workers have also made detailed and influential contributions on naphthols, *e.g.*, on the self-quenching of 1-naphthol,[397] the intrinsic proton transfer rate in photoacid–carboxylate pairs,[228] the hydrogen-bonding interactions,[398] and the role of diffusion-assisted recombination as well as isotope and temperature effects.[399–401] Recently, Pines *et al.* have addressed the role of the sulfonate groups in mono- and di-substituted naphthols as competing protonation sites.[402]

The role of geminate recombination[364,403,404] and solvatochromism[405,406] was elucidated for naphthols as well by Huppert and coworkers, who intensified their efforts with the advent of naphthol-based super-photoacids which have enhanced photoacidic behavior (see Section 5.2.1). This includes studies on the ESPT of naphthols in neat solvents,[407–410] its pressure dependence[365,366] and modified ESPT characteristics that arise in binary solvent mixtures, *e.g.*, H_2O/D_2O,[411] methanol–water,[56,57,412] or acetonitrile–water.[413] Other interesting environments that have been studied using naphthols include ethanol–water,[414]   *n*-propanol–water,[415,416]   DMSO–water mixtures,[417]   ESPT to urea,[418]   super-critical water,[419] micelles,[420–425]   polymer–surfactant   aggregates,[426]   ionic liquids,[427] and high-temperature and high-pressure methanol.[428] Theoretical studies have been reported as well.[324] Nibbering and co-workers have employed a 2-naphthol derivative for the real-time observation of carbonic acid formation in aqueous solution.[429] Interestingly, about 10 years later, Pines *et al.* have followed the same approach to study carbonic acid, and additionally the physiologically relevant lactic and pyruvic acids, but using a stripped-off version of HPTS (namely, 6-hydroxypyrene-1-sulfonate).[430] The Nibbering and Pines groups independently obtained the same pK_a value for carbonic acid. Beyond, Cox and Bakker have used naphthol sulfonates to study the deuteron transfer dynamics through short-living water wires.[431]

4.2   Differences in the electronic structure

4.2.1   Introduction to Platt's ^1L_a and ^1L_b states of aromatic molecules.
Perhaps the largest implication from the research on naphthol photoacids is the rationalization that the character of the lowest excited singlet state, S_1, affects the photoacidity and that this character can change with the substituents and/or with the solvent. This aspect has been extensively discussed by the Pines group who labeled it the ^1L_a–^1L_b paradigm.[39,432] Hereby, ^1L_a and ^1L_b refer to Platt's notation for the two lowest lying electronically excited singlet states with $\pi \rightarrow \pi^*$ character of aromatic molecules.[433] Platt originally derived these based on general considerations for cata-condensed hydrocarbons,‖

‖ *E.g.*, see ref. 434 for a definition of the different condensation types for polycyclic aromatic compounds.
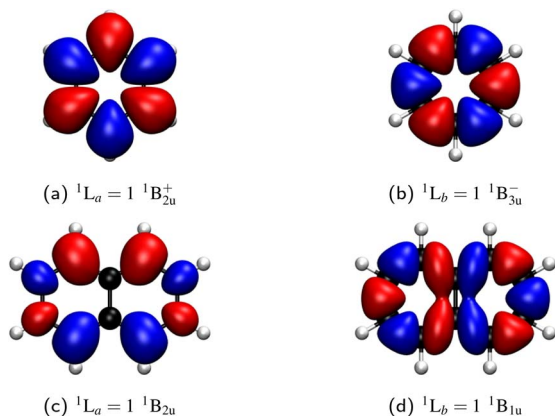
(a) $^1L_a = 1\ ^1B_{2u}^+$

(b) $^1L_b = 1\ ^1B_{3u}^-$

(c) $^1L_a = 1\ ^1B_{2u}$

(d) $^1L_b = 1\ ^1B_{1u}$

Fig. 8 Classification of the two lowest-lying excited singlet states of benzene (D_{6h} point group) and naphthalene (D_{2h} point group), as ^1L_a (a and c) and ^1L_b (b and d), respectively, based on the distribution of effective charges according to Platt. Visualization of the transition density with contours in red and blue referring to opposite signs.

(a) Benzene   (b) Naphthalene   (c) Pyrene

Fig. 9 Orientation of the molecular axes a (in blue) and b (in red) according to Platt's notation for the examples benzene (a), naphthalene (b), and pyrene (c).

usually referred to as the perimeter model.[435] As initially introduced by Platt, the indices a and b describe different distributions of effective charges (*i.e.*, the transition density) that are caused by the electronic redistribution upon excitation from the ground state, S_0, into the ^1L_a or ^1L_b excited state: a indicates effective charges located at the atoms along the perimeter, while b refers to a location at the bonds (*cf.* Fig. 8). In this context, these two indices can be also associated with the orientation of the nodal planes of the molecular orbitals that make up the wavefunction, with the nodes being located at the bonds (^1L_a) or atoms (^1L_b), respectively.

Although not part of Platt's original discussion, a fundamental consequence of this definition is that a and b each also determine an intramolecular axis that directly reflects the orientation of the corresponding transition dipole moment (TDM), *i.e.*, the polarization, for the transitions from S_0 into the ^1L_a and ^1L_b states, respectively. Due to the different orientation and magnitude of their TDMs, these two states depend differently on substituents or the solvent.[433,436] The brighter ^1L_a state is said to have a higher charge-transfer (CT) character (*i.e.*, to be more polar), while the darker ^1L_b state is more covalent in nature. Therefore, the ^1L_a state is assumed to be stabilized more strongly compared to the ^1L_b state by polar substituents. In an extreme, a level inversion between these states can also occur.

For linear polycyclic aromatic hydrocarbons (PAHs) including naphthalene and the acenes (*e.g.*, anthracene), the a axis, which is aligned with the TDM of the strong $S_0 \rightarrow {}^1L_a$ transition, can be identified as the shorter axis, while the b axis, which is aligned with the TDM of the weak (quasi-forbidden) $S_0 \rightarrow {}^1L_b$ transition, is the longer axis, with both axes being perpendicular to each other (*cf.* Fig. 9b). However, this assignment of the a and b axes as the short and long intramolecular axes does not hold generally and depends on the specific compound under study. For example and in contrast to the acenes, the a axis is identified as the longer axis according to the orientation of the TDM in the simple benzene (*cf.* Fig. 9a) and some non-linear PAHs like pyrene (*cf.* Fig. 9c), allowing for two
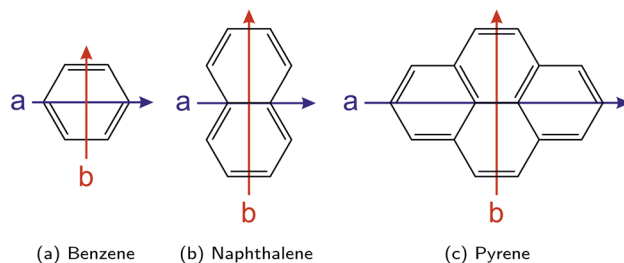
important observations: first, in all of these examples, the a axis turns out to be the one passing through ring carbon atoms, while the b axis is the one cutting carbon–carbon bonds. Second, the character and the symmetry of the ^1L_a and ^1L_b states is preserved among these compounds.

Let us briefly compare Platt's a and b axes with the geometrical orientation of these molecules as typically used in physical and theoretical chemistry. Importantly, due to their relation to electronic states, Platt's a and b axes must not be mistaken for the principal axes of inertia carrying the same labels, which is an occasional misconception in the literature and potential source of confusion. According to Mulliken's recommendation for the notation of spectra of polyatomic molecules, for planar molecules with D_{2h} symmetry, the x axis is chosen perpendicular to the molecular plane, while the z axis should be chosen passing through the largest number of atoms or, if ambiguous, dissecting the largest number of bonds.[437] Hence, for both the selected examples of linear (*i.e.*, naphthalene and the acenes) and non-linear (*i.e.*, pyrene) PAHs with D_{2h} symmetry discussed here, it is the z axis that corresponds to the b axis and the y axis that corresponds to the a axis. With this choice of the axes, ^1L_a and ^1L_b have B_{2u} and B_{1u} symmetry, respectively[438,439] (note that sometimes the z axis is chosen perpendicular to the molecular plane, then the symmetry species would be B_{2u} and B_{3u}).[440,441]

4.2.2 Natural transition orbitals for the analysis of electronic transitions. In the case of the linear and non-linear PAHs mentioned here (*i.e.*, naphthalene, acenes, and pyrene), ^1L_a is described in a molecular orbital (MO) picture by an almost pure HOMO $\rightarrow$ LUMO transition, while ^1L_b is a 50 : 50 mixture of the HOMO $\rightarrow$ LUMO+1 and HOMO−1 $\rightarrow$ LUMO transitions. A perfect example is the simple naphthalene, as illustrated by the natural transition orbitals (NTOs) for the electronic transitions from the ground state (S_0) to the two lowest-lying excited states (S_1, S_2), which can be either ^1L_a, ^1L_b, or a mixture (Fig. 10).

Originating from a singular value decomposition of the transition density matrix, NTOs provide a more compact representation of single excitations compared to the canonical MO basis, becoming particularly powerful when many MOs contribute to a given transition. Thereby, the NTOs allow to visualize and rationalize the changes in the electronic distribution taking place upon excitation. NTOs as the (left and right) singular vectors always come in pairs with a so-called occupied (or hole; *i.e.*, left after excitation) and virtual (or particle; *i.e.* the

excited electron) part, representing the probability distribution of the electron prior and after the transition, respectively. Moreover, the corresponding singular values determine weights describing how strongly each NTO pair contributes to a given transition.

In the case of naphthalene, the NTO analysis verifies that the $S_0 \to {}^1L_a$ transition is dominated by a single NTO pair whose—based on an additional comparison that is not shown here—occupied and virtual parts resemble the HOMO and LUMO,

respectively. Similarly, the two NTO pairs that contribute equally (ca. 50%) to the $S_0 \to {}^1L_b$ transition can be identified with the HOMO and LUMO+1 as well as the HOMO−1 and LUMO based on the occupied and virtual parts of the first and second NTO pairs, respectively. However, it needs to be emphasized here that this correlation of ${}^1L_a$ and ${}^1L_b$ with the frontier orbitals is specific to a given molecular class only and can hence be different for other PAHs (e.g., for different ring
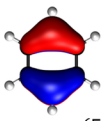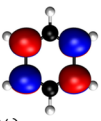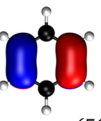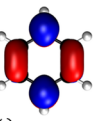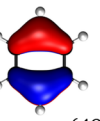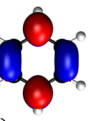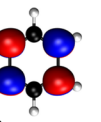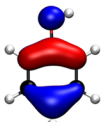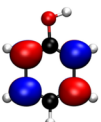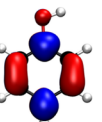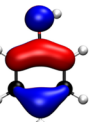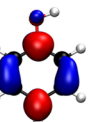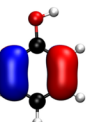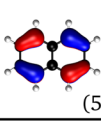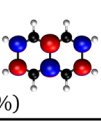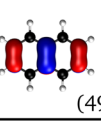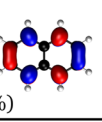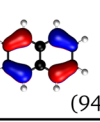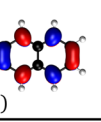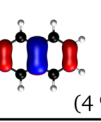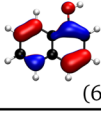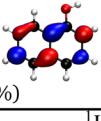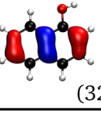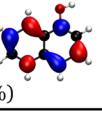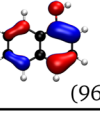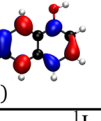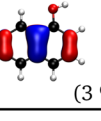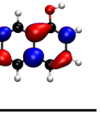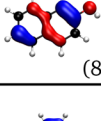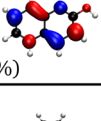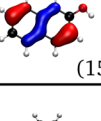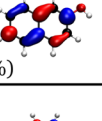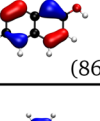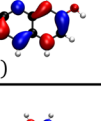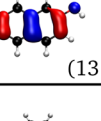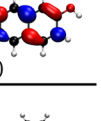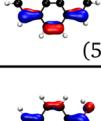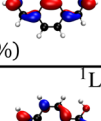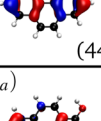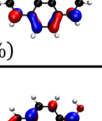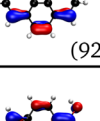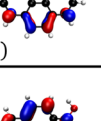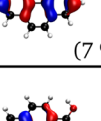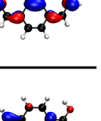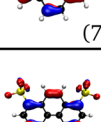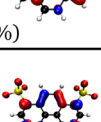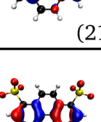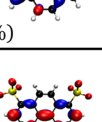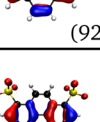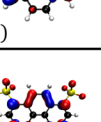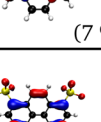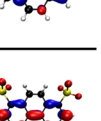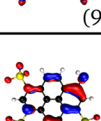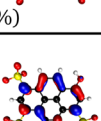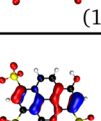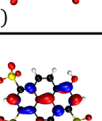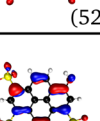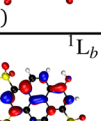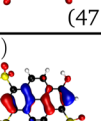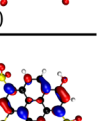
Compound	S$_1$ State				S$_2$ State			
	NTO Pair 1		NTO Pair 2		NTO Pair 1		NTO Pair 2	
	Occ.	Vir.	Occ.	Vir.	Occ.	Vir.	Occ.	Vir.
Benzene	${}^1L_b$ (50 %)		(50 %)		${}^1L_a$ (49 %)		(49 %)	
Phenol	${}^1L_b$ (78 %)		(22 %)		${}^1L_a$ (80 %)		(18 %)	
Naphthalene	${}^1L_b$ (50 %)		(49 %)		${}^1L_a$ (94 %)		(4 %)	
1-Naphthol	${}^1L_b$ (67 %)		(32 %)		${}^1L_a$ (96 %)		(3 %)	
2-Naphthol	${}^1L_b + {}^1L_a$ (83 %)		(15 %)		${}^1L_a + {}^1L_b$ (86 %)		(13 %)	
Pyrene	${}^1L_b$ (55 %)		(44 %)		${}^1L_a$ (92 %)		(7 %)	
1-Pyrenol	${}^1L_b(+{}^1L_a)$ (77 %)		(21 %)		${}^1L_a$ (92 %)		(7 %)	
1,3,6,8-Pyrenetetra-sulfonate (4sPy)	${}^1L_a$ (98 %)		(1 %)		${}^1L_b$ (52 %)		(47 %)	
HPTS	${}^1L_a$ (96 %)		(3 %)		${}^1L_b(+{}^1L_a)$ (76 %)		(22 %)	

Fig. 10 Analysis of the two lowest-lying electronically excited states and assignment of the ${}^1L_a$ and ${}^1L_b$ character for prototypical compounds. For each state, the two dominant natural transition orbital (NTO) pairs together with their weights (in parentheses) are given. The electronic transitions are calculated in the gas phase with ADC(2)/aug-cc-pVDZ at MP2/cc-pVDZ geometries, except for the charged 4sPy and HPTS that refer to implicit solution (water) using COSMO-ADC(2) energies at COSMO-MP2 geometries.

sizes or condensation types), but particularly if substituents are introduced to the aromatic rings.

The NTOs also allow for a direct assignment of ^1L_a and ^1L_b based on pure considerations of charge polarization according to Platt's fundamental definition (*vide supra*). For this, the product of the occupied and virtual parts of the dominant NTOs needs to be considered and analyzed with respect to the location of effective charges and nodes (*e.g.*, see Fig. 11 for naphthalene). Since all NTO pairs for a given transition have the same symmetry, it is furthermore sufficient to consider only a specific pair, *e.g.*, one that appears easiest to interpret. For example, it is quite simple to see that the product of the occupied and virtual parts of the second NTO pair for the $S_0 \rightarrow S_1$ transition of naphthalene (Fig. 11b) mainly consists of $\pi\pi^*$ contributions from the two outmost left and right neighboring C atoms (*i.e.*, C_2–C_3 and C_6–C_7). The coefficients at the other C atoms basically vanish in the product due to the presence of vertical nodal planes in either NTO part. The presence of effective charges located at the bonds is indicate for an ^1L_b and the opposite phase between the coefficients at the terminal C atoms indicates that this transition is polarized along the longer, horizontal axis that becomes assigned as the b axis. In analogy, the product of the occupied and virtual parts of the second NTO pair for the $S_0 \rightarrow S_2$ transition (Fig. 11d) dissects into pure contributions with coefficients at the atoms, indicative for ^1L_a, with a polarization along the shorter, vertical axis, thus labelled a. Despite their dominant weight, the NTO pairs that are shown in the first column of Fig. 10 might be somewhat more difficult to interpret with respect to the charge polarization since their products are harder to imagine (*cf.* Fig. 11a and c). However, we have observed the following rule of thumb that allows for an even faster assignment of the polarization axes: For naphthalene, but also for the other PAH examples in Fig. 10, if there is a common nodal plane (through the center) present in both occupied and virtual parts of a given NTO pair, the nodal plane contains the a or b axis, respectively. For example, for the ^1L_b state one can see that the b axis is the common nodal plane in NTO pair 1, while it is the a axis for ^1L_a as seen in NTO pair 1.

4.2.3 Electronic structure of photoacids

4.2.3.1 Phenol. Although extensively used in the past to describe the electronic structure of various hydroxyarene photoacids, Platt's assignment of the ^1L_a and ^1L_b states is strictly valid only for a limited number of unsubstituted arenes, mainly because (i) (polar) substituents can enhance mixing between the two states and (ii) the perimeter model itself is no longer suitable for larger ring systems (*e.g.*, pyrene). However, care must be

taken when trying to quantify this state mixing, *e.g.*, by comparing the weights of the NTOs. For example, already phenol as the simplest hydroxyarene (see Fig. 10) demonstrates that the orbital transitions involving the HOMO contribute much stronger for both ^1L_a and ^1L_b, as judged based on higher NTO weights compared to the parent compound benzene. In particular, the character of the contributions to these transitions and the orientation of the TDMs remain mostly unaltered for phenol, as can be seen by the almost identical NTOs, excluding any state mixing between ^1L_a and ^1L_b. Thus, the higher weights for the NTOs involving the HOMO just indicate that these transition become HOMO-dominant in the case of phenol, in line with a lower HOMO energy due to the participation of the O atom from the OH group. It should be also noted here that these orbital considerations differ even more strongly from the PAHs in case of the deprotonated species of the photoacids (*e.g.*, phenolate) since the HOMO is dominated even more by the O atom due to the negative charge. However, a detailed discussion of the electronic structure of these corresponding bases is not part of this review.

4.2.3.2 Naphthols. The classical examples to look at in the context of photoacids are 1-naphthol (1N) and 2-naphthol (2N). 1N, despite having an energetically lower ^1L_b state, is considered an ^1L_a photoacid, while 2N, also with a lower ^1L_b state, is regarded an ^1L_b photoacid (*cf.* Fig. 10). Thus, this classification as ^1L_a or ^1L_b photoacids is not simply based on the energetic order of these states, but also considers which of them is relevant for the photoacidity, *i.e.*, the accessibility in terms of the brightness of these states. For both 1N and 2N, the introduction of the OH group as a substituent breaks the initial D_{2h} symmetry of the parent naphthalene, reducing it to C_s. As an important consequence, both ^1L_a and ^1L_b have the same symmetry (A') in the C_s point group, enabling a mixing of these two states. For 1N that is closer to the unsubstituted naphthalene, the lower-lying ^1L_b state is less bright, rendering the brighter ^1L_a the relevant state, while for 2N, which apparently deviates more strongly from naphthalene, the ^1L_b state is much brighter due significant ^1L_a–^1L_b state mixing.

The two compounds 1N and 2N differ remarkably in their photoacidic behavior. Both photoacids show almost the same pK_a values in the ground state (9.3 for 1N, 9.6 for 2N) in water, but 1N (−1.0) is much more acidic in its ^1L_a state, compared to 2N (3.3) in its ^1L_b state.[432] Unveiling the reasons behind this puzzling observation has lead to a debate in the literature. Initially, gas-phase experiments in solvent clusters by Knochenmuss and co-workers[287,390,396] as well as theoretical studies

(a) S₁ (¹Lᵦ): NTO-1   (b) S₁ (¹Lᵦ): NTO-2   (c) S₂ (¹Lₐ): NTO-1   (d) S₂ (¹Lₐ): NTO-2
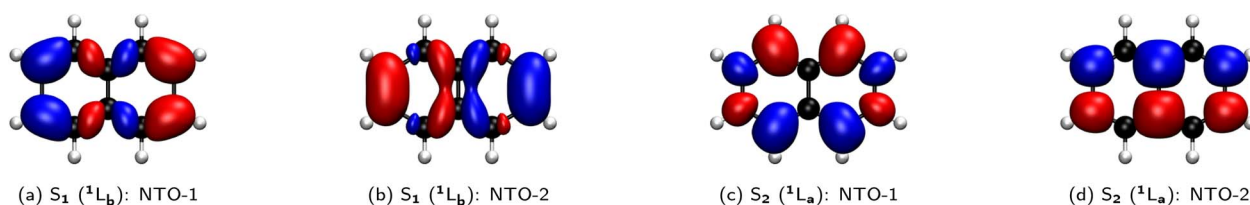
Fig. 11 Visualization of the product of the occupied and virtual parts of the first (NTO-1) and second (NTO-2) dominant NTO pairs for the transition into the first (S_1, ^1L_b; a and b) and second (S_2, ^1L_a; c and d) excited state of naphthalene, respectively.

by Tran-Thi, Hynes, and co-workers[214–216] have largely shaped the view that the polar ^1L_a state, although higher in energy in less polar environments, should be the relevant state for photoacidity in more polar solvents, whereas the less-polar, energetically lower ^1L_b state dominates in less polar solvents. Hence, a so-called level inversion in polar solvents has been suggested as an additional mechanism.[442] Later, Pines has emphasized that the electronic structure of 2N is in fact much more congested than sometimes assumed, meaning that both the ^1L_a and the ^1L_b state need to be considered.[39,432] Indications for this are also observed here (see Fig. 10) as pure ^1L_a character is neither observed for 1N nor for 2N, with particularly strong mixing for 2N. Moreover, to explain the overall increased photoacidity of 1N over 2N, Pines suggested to take the effects on both species into consideration, the naphthol (acid) and naphtholate anion (base), thereby inferring a stronger stabilization on the base side.[39] More recently, Nibbering, Chergui and co-workers have performed time-resolved fluorescence and mIR spectroscopy experiments that compare 1N and 2N in chloroform (as an unpolar solvent) and DMSO (as a polar solvent), demonstrating that the solvent changes the character of the heavily mixed electronic states in the case of 1N (see Fig. 12).[443] For 2N, the fractional ^1L_a character remains low ($\sim$10%) and constant over time after excitation (in accordance with a higher ^1L_b character for 2N, *cf.* Fig. 10), while, for 1N, this fraction also remains constant ($\sim$20%) in the less polar chloroform, but increases within 0.5 ps from $\sim$20% to $\sim$40% in the more polar DMSO.

4.2.3.3 Pyrenols. Similar attempts have also been made to rationalize the photoacidity of HPTS in terms of its electronic structure,[140,214–216,220,222,223] but the experimental and theoretical evidence is not fully conclusive and hence a strict assignment of these two states might not even be possible (*vide supra*), which sometimes is empirically described by heavy ^1L_a–^1L_b mixing. Although Platt's notation does not strictly apply to pyrene that as a peri-condensed hydrocarbon lacks cata-condensation, its electronically excited states can still be nicely characterized as ^1L_a and ^1L_b. For example, the calculations on pyrene presented here (Fig. 10) show that S_1 has roughly equal contributions from two NTO pairs with a transition dipole moment aligned along the b axis, indicative for ^1L_b character, while S_2 is dominated by a single NTO pair with a TDM aligned along the a axis, characteristic for ^1L_a. However, as for the naphthols, symmetry breaking *via* substitution introduces state mixing. Interestingly, the effect from OH substitution is rather small as the character and relative order of S_1 and S_2 remain mostly the same (*i.e.*, moving from pyrene to 1-pyrenol). Quadruple substitution with sulfonate groups does not affect the character since the symmetry is maintained, but alters the energetic order shifting ^1L_a below ^1L_b (*i.e.*, moving from pyrene to 4sPy), as judged based on NTO analysis. Similar as the changes from pyrene to 1-pyrenol, substitution of one of the four sulfonates by an OH group (*i.e.*, moving from 4sPy to HPTS) does again break the symmetry, causing distortion of the NTOs, but also maintains the energetic order. However, while the first excited state (S_1) in HPTS has still dominantly ^1L_a character, the second excited state (S_2) reveals a significant ^1L_a–^1L_b mixing. Using the difference between the NTO weights (or their deviation from 50%) as
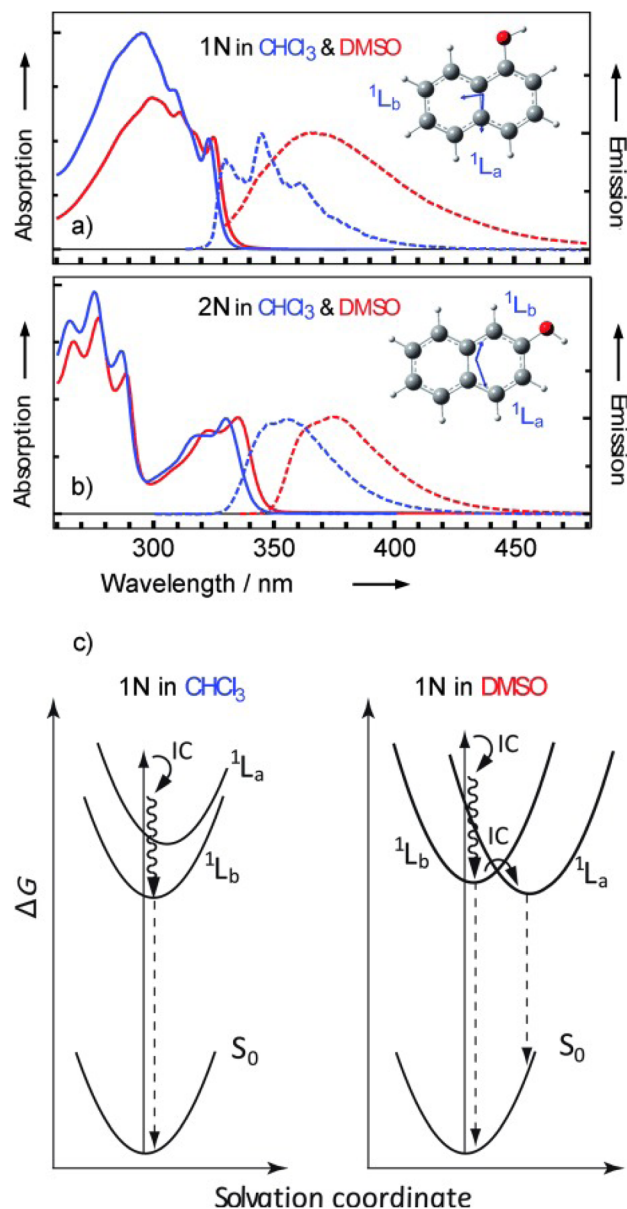
Fig. 12 Normalized static optical absorption (solid lines) and emission (dashed lines) of: (a) 1N and (b) 2N. Insets: molecular structures and transition dipole moments (blue arrows) of the ^1L_a and ^1L_b transitions of 1N and 2N, predicted by TDDFT for the molecules in gas phase. (c) Scheme of the dynamics of 1N after photoexcitation. This figure has been reproduced from ref. 443 with the kind consent from E. T. J. Nibbering and M. Chergui and with permission from Wiley-VCH, copyright 2013.

a rough estimate, the degree of mixing appears similar for HPTS (76%, 22%) as for 1-pyrenol (77%, 21%), and thus somewhat larger than for 1-naphthol (67%, 32%), but considerably less than for 2-naphthol (83%, 15%).

5 Spotlight—super-photoacids

5.1 Initial naphthol derivatives

Despite this wealth in photoacid research, HPTS and most other early photoacids, especially naphthols,[55–57,363,364,431] are mainly

restricted to perform an ESPT in aqueous solutions due to limited acid strength, *i.e.*, too large pK_a^* values. To overcome this, *i.e.*, to enhance the photoacidity by lowering the pK_a^* value, Tolbert and Haubrich (in 1990) had the idea to substitute 2-naphthol with electron-withdrawing cyano (CN) groups at different ring positions.[444] The CN group was chosen as a compromise between strength and stability since the commonly used sulfonate (SO_3^-) group is only a weak electron acceptor, whereas the nitro (NO_2) group is one of the strongest electron acceptors, but nitro-substituted chromophores are typically photo-labile and tend to weakly fluoresce.[445] Owing to the drastically enhanced photoacidity for some of these cyano-naphthols, particularly with the CN at the 5 or 7 position (shifting the pK_a^* to −1.2 and −1.3, respectively), Tolbert and Haubrich also introduced the term super-photoacids, from then on a general term for photoacids with a negative pK_a^* value.

Driven by the enhancement in photoacidity, the ESPT of such super-photoacids is strongly accelerated, leading to an ultrafast deprotonation in water and also rendering the ESPT possible in non-aqueous solution (*vide infra*). For example, as one of the first super-photoacids, the above-mentioned compound 5-cyano-2-naphthol (5CN2, Fig. 13a) has been thoroughly studied with respect to its ESPT in many different solvents including water,[408] alcohols,[409] DMSO,[60] solvent mixtures[400,404,412] and gas-phase solvent clusters[286] as well as to its solvatochromism in a variety of organic solvents.[406,409]

5.2 The race toward strongest photoacids

5.2.1 Naphthols. The initial discovery of super-photoacids triggered a competition for designing increasingly strong (super-)photoacids in order to (i) further accelerate the ESPT and push the kinetics toward the solvent-controlled kinetic regime and (ii) move to less proton-accepting solvents. Fig. 13 and 14 give an overview on a selection of the resulting super-photoacids that have been reported. After the seminal work by Tolbert and Haubrich, the next generation of super-photoacids first included simply further functionalized 2-naphthols, making use of the increased effect of multiple substituents, utilizing either two cyano groups[97,446] or a newly per-fluoroalkylsulfonyl group[410] (Fig. 13a). Among these, 5,8-dicyano-2-naphthol (DCN2, Fig. 13a; $pK_a^* = -4.5$[446]) has become most thoroughly studied, *e.g.*, regarding the ESPT in water[446] and various alcohols,[407,447,448] under high pressures,[366,419,428,449–452] or even in ionic liquids.[427] Although 2-naphthols are weaker photoacids compared to 1-naphthols (*vide supra*), almost exclusively 2-naphthol derivatives (with multiple cyano groups) are known as super-photoacids, which is related to weak fluorescence and facile deactivation of cyano-1-naphthols *via* proton quenching.[113]

5.2.2 Hydroxyquinolines. Hydroxyquinolines (Fig. 13b) pose another interesting compound class. These compounds possess dual photoacid–photobase character though, which leads to more complicated kinetics involving tautomerization reactions.[79,114,117,316–318,453] Therefore, Kim and Topp revived the original idea by Bardez *et al.*[115] of blocking the photobasic nitrogen site of hydroxyquinolines *via* methylation in order to
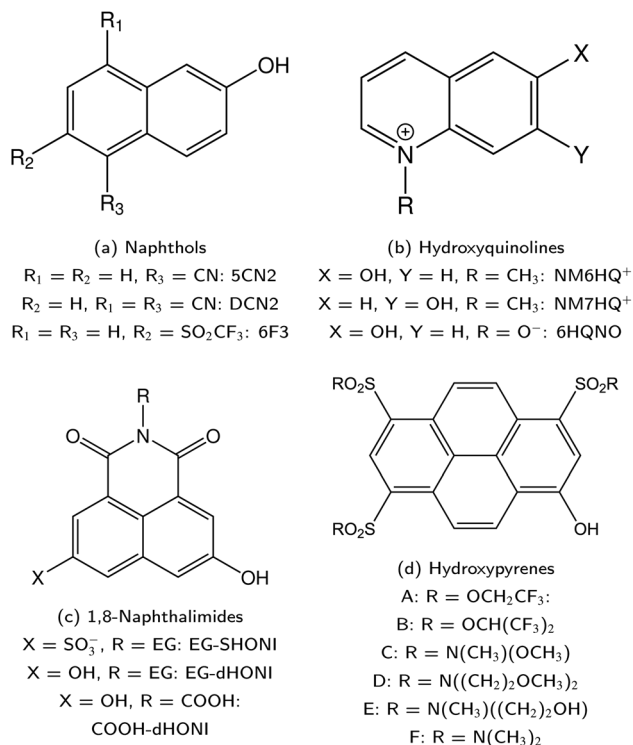
Fig. 13 A selection of super-photoacids I. Naphthol (a), hydroxyquinoline (b), 1,8-naphthalimide (c), and hydroxypyrene (d) derivatives. [Abbreviation: ethylene glycol residue (EG = $CH_2CH_2OCH_2CH_2OH$)].

switch off the photobase character and make use of the largely enhanced photoacid character of the corresponding hydroxyquinolinium cation.[116] Later, Solntsev *et al.* have tested *N*-oxidation as an alternative to *N*-methylation, giving access to a new class of hydroxyquinoline-*N*-oxide photoacids.[454] However, while the photoacidity, in comparison to the parent compound, was successfully enhanced and also the tautomerization disabled, a lack of photo-stability was introduced due to an unwanted, yet efficient non-reversible side-reaction, which made them rather impractical for many purposes.

Upon the hydroxyquinolines, NM6HQ$^+$ ($pK_a^* \sim -7$)[455] has been studied experimentally in water and in various alcohols by Popov and colleagues,[455,456] and the related (non-*N*-methylated) 6HQ as well as NM6HQ$^+$ in the same solvents and additionally in water–acetonitrile mixtures by Pérez Lustres *et al.*[457–459] Moreover, the Kwon group has studied ESPT of NM7HQ$^+$ ($pK_a^* = -2.3$[460]) in hydrogen-bonded complexes with methanol, ethanol, DMSO, and *N*-methylbenzamide in the solvent acetonitrile.[460–465] Similarly, the group has employed the photoacids 7HQ and NM7HQ$^+$ in solutions of diols with varying chain length to study the role of hydrogen-bond bridging on the ESPT.[194,466] Very recently, Choi *et al.* have presented a new method for determining the equilibrium constant for the ground-state hydrogen-bond formation *via* time-resolved instead of steady-state spectroscopy, which is superior to the traditional determination in cases when the addition of the HB acceptor (base) impacts the bulk polarity of the solution, as for NM7HQ$^+$ and DMSO in acetonitrile.[464]
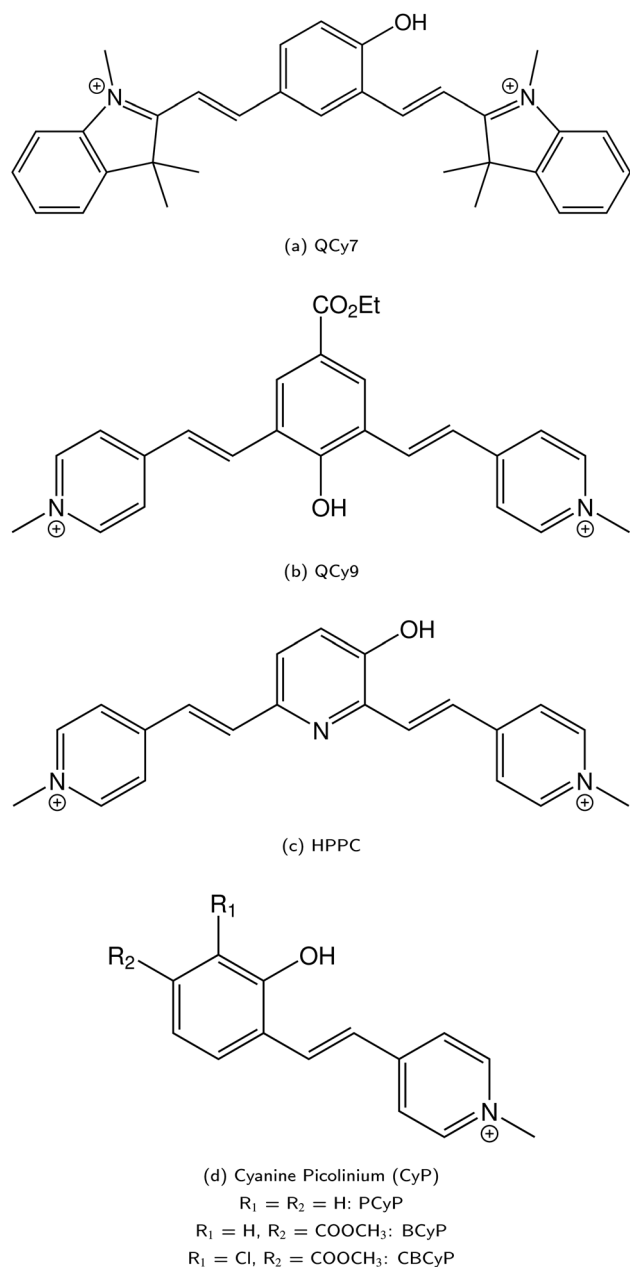
Fig. 14 A selection of super-photoacids II. Quinone cyanine dyes: QCy7 (a), QCy9 (b), HPPC (c), and CyP (d).

5.2.3 Quinone cyanines. The subsequent design of super-photoacids by Huppert and co-workers has followed the direction of cyanine fluorochrome dyes (see Fig. 14), originally known from near-infrared (NIR) imaging due to their pronounced NIR emission.[467,468] Important examples, with weak fluorescence of the deprotonated species, are the quinone cyanines QCy7 (Fig. 14a, $pK_a^* = -6.5$)[469] and QCy9 (Fig. 14b, $pK_a^* = -8.5$).[470] Both are able to readily perform an ESPT in liquid[469–471] or even solid[472,473] H_2O (or D_2O) as well as in typical alcohols such as methanol and ethanol,[58] and also in ethanol–trifluoroethanol solvent mixtures in the case of QCy9.[474] Due to its immense (photo-)acidity, the ESPT rate of QCy9, which continues to be the strongest photoacid among the

hydroxyaromatics to date, reaches a value of $k_{PT} \sim 10^{13}$ s^{-1} (i.e., a lifetime of 100 fs) that is identical in water, methanol, and ethanol, indicating ESPT kinetics beyond the solvent-controlled regime.[58] Even more recently, Huppert and co-workers have continued to fine-tune the properties of these dyes and reported newly synthesized

- 3-hydroxypyridine-dipicolinium cyanine (HPPC, Fig. 14c; $pK_a^* \sim -6$),[475]
- phenol cyanine picolinium (PCyP, Fig. 14d; $pK_a^* \sim -1$),[476]
- chloro benzoate cyanine picolinium (CBCyP, Fig. 14d; $pK_a^* \sim -6$),[59,477] and
- phenol benzoate cyanine picolinium (BCyP, Fig. 14d; $pK_a^* \sim -7$)[478]

salt super-photoacids. Apart from the common solvents for ESPT (i.e., water, methanol, and ethanol), CBCyP is one of the very few photoacids that has also been studied in acetonitrile–water mixtures.[413]

5.3 Naphthalimides of Brouwer & Kumpulainen

As highlighted above, the design of new super-photoacids mainly pursued the route of functionalizing already known weaker photoacids or promising candidates (e.g., fluorescent dyes) with electron-withdrawing groups in order to shift the pK_a^* into the negative regime. This strategy also applies to the super-photoacidic HPTS derivatives developed by Jung and co-workers,[61] to which the subsequent section has been dedicated. However, as the final example here, the super-photoacids based on 1,8-naphthalimide introduced by Kumpulainen et al. are presented.

Substituted 1,8-naphthalimides (NI) had been known as fluorescent probes and sensors for quite some time[479–481] and even the excited-state ion-pair formation of 3- and 4-hydroxy-N-methyl-1,8-naphthalimides in organic solvents had been studied via fluorescence.[482–484] However, due to the missing data for aqueous solutions in combination with the promising properties of these compounds, Kumpulainen, Brouwer, et al. have developed three new NI-based super-photoacids (see Fig. 13c) with pK_a^* values ranging from -1.2 to -1.9.[485] These compounds differ only in the number of OH groups and in the substituent at the N atom of the NI framework. EG-SHONI ($pK_a^* = -1.9$) contains an ethylene glycol (EG) moiety at the N, one OH (HO) group in the first aromatic ring and a sulfonate (S) group in the second ring. In contrast, this sulfonate group is replaced by another OH group in EG-dHONI ($pK_a^* = -1.2$), having two (dual) OH groups in total. Lastly, COOH-dHONI ($pK_a^* = -1.4$) is similar to EG-dHONI, but the ethylene glycol is replaced by a carboxy (COOH) group. All three compounds exhibit deprotonation upon excitation in alcohols and in DMSO.[485] EG-dHONI has been subject to more detailed kinetic studies in water, which revealed that ESPT follows a two-step model involving a short-range proton transfer under formation of a contact ion pair and its diffusive separation.[485] Moreover, the complex formation and the ESPT of other dHONI photoacids and different organic bases in acetonitrile and benzonitrile solution has been studied, strongly indicating a three-step model for the ESPT in these environments

involving hydrogen-bonded complexes and a solvent-separated ion pair as additional intermediates.[486] Later, EG-SHONI has been studied more detailed using a combination of fluorescence up-conversion, transient UV/Vis absorption, and transient mIR absorption to decipher the ultrafast ESPT in DMSO, revealing not only a reversibility of the initial PT step that yields the contact ion pair, but also a breakdown of the (two-step) Eigen–Weller model—despite excellent agreement with the experimental data—due to a solvent control *via* solvent relaxation.[487,488]

5.4 Pyrene derivatives in the new millennium

5.4.1 Previous HPTS derivatives. The fundamental importance of HPTS for the field of photoacids, but also its effective restriction to aqueous solutions as a major drawback has been outlined in the previous sections. Moreover, even before the concept of functionalization with electron-withdrawing groups for the design of new (super-) photoacids was systematically applied, some HPTS derivatives were already known. The most common examples include 8-hydroxy-N,N,N',N',N'',N''-hexamethylpyrene-1,3,6-trisulfonamide (HPTA),[129,223,264,489] in which all three sulfonate groups of HPTS are converted into sulfonamides of dimethylamine, and 8-aminopyrene-1,3,6-trisulfonic acid (APTS),[39,140,223] in which the OH group of HPTS is replaced by an ammonium (NH_3^+) group (see Fig. 3g). Due to this positive charge in the (photo)acidic group, APTS ($pK_a^* \approx -7$)[224,489] is frequently referred to in the literature as a cationic photoacid and HPTS as a neutral photoacid, despite their net negative charges in solution.[140] In contrast, HPTA is a truly non-charged photoacid and exhibits a slightly higher excited-state acidity ($pK_a^* = -0.8$)[140] compared to the parent compound HPTS ($pK_a^* = 1.4$).[207]

5.4.2 Design of new pyrene-based photoacids. This enhancement in the photoacidity of HPTA over HPTS along the removal of the negative charges as putative source for the weak photostability (see the ESI of ref. 490) with the aim of improving the properties of HPTS for biological applications motivated Jung and co-workers to design a new class of non-charged HPTS derivatives (see Fig. 13d). They introduced electron-withdrawing perfluoroalkyl ester (**A–B**)—similar to the substituents used to enhance the photoacidity of 2-naphthol (*vide supra*)—and amide (**C–E**) moieties to the sulfonate groups of HPTS and obtained highly photostable photoacids with bright visible fluorescence for biological applications (note that compound **F** is identical to HPTA).[61] Overall, the substitution does not significantly alter the pK_a drop upon excitation (~7 units), but allows to downshift the pK_a^* by up to 5 units by changing the ground-state pK_a, yielding a set of photoacids with pK_a^* between −0.8 and −3.9. Owing to the larger effect of the fluorinated esters, compounds **A** and **B** are stronger photoacids compared to **C–F**, while **B** is the strongest ($pK_a^* = -3.9$) of this class. The N atom of the amide group(s) in compound **C** is directly attached to a methoxy (OCH_3) group, which makes **C** slightly more acidic compared to photoacids **D–F**. However, compounds **D** and **E**, which turned out to have similar strengths as the previously reported **F** (HPTA), were actually (successfully) designed to

improve the water solubility compared to **F**, whereas **C** shows a high permeability through biological membranes. Aiming at even stronger photoacids that are capable of performing an ESPT in even more exotic environments, Maus *et al.* recently synthesized an APTS-based analogue of compound **A**, which is strong enough ($pK_a^* = -9.9$) to perform ESPT in concentrated sulfuric acid (H_2SO_4), hence pointing to the development of magic photoacids.[491] Here, the actual proton acceptor is bisulfate (HSO_4^-). Further attempts to generate even stronger photoacids by electrophilic substitution of diazapyrene[492] failed so far.[493] Unrelated to the Jung group, Lennox *et al.* reported an even newer pyrene-based photoacid, *i.e.*, N,N,N',N',N'',N''-hexaethyl-8-hydroxypyrene-1,3,6-trisulfonamide (^{Et}HPTA), derived from HPTS by conversion of the sulfonate into diethyl sulfonamide groups, with a pK_a drop of *ca.* −11 (in acetonitrile) and exhibiting a long-lived (80 μs) triplet state.[131] Besides, Hu *et al.* developed 2-(benzothiazol-2-yl)pyren-1-ol (P3-NS), a new hydroxypyrene derivative bearing benzothiazole, as a fluorescent sensor for nitroaromatic compounds (*e.g.*, picric acid) that undergoes ESIPT in nonpolar or weakly polar solvents.[494]

5.4.3 Previous experimental work. The solvatochromism in a broad range of 29 solvents[495] and the ESPT kinetics (on the ps–ns timescale) in DMSO[61] have been studied for the full set of these new photoacids (**A–E**). In addition, for the strongest photoacid **B** of this class, namely tris(1,1,1,3,3,3-hexafluoropropan-2-yl)-8-hydroxypyrene-1,3,6-trisulfonate, as well as for compound **E**, the ESPT has been studied more thoroughly in water, methanol, and ethanol using ultrafast time-resolved fluorescence spectroscopy (sub-ps timescale), demonstrating that geminate recombination is not crucial in these cases and that multi-exponential fits describe the kinetics sufficiently well.[496] For photoacid **B**, ESPT rate constants, k_{PT}, of 3×10^{11} s^{-1} (water), 8×10^9 s^{-1} (methanol), and 5×10^9 s^{-1} (ethanol) have been reported.[496] For comparison, in the aprotic solvent DMSO,[61] the ESPT rate constant further drops to a value of 1.25×10^9 s^{-1}. Moreover, the recombination kinetics of photoacids **A–C** have been addressed using photon anti-bunching experiments, revealing the involvement of hydrogen-bonded ion pairs (HBIPs) as intermediates, at least in the ground state.[497,498]

Whereas most standard photoacids cannot transfer their proton to DMSO, the super-photoacid **B** shows indications to do so even in the aprotic, weakly basic solvent acetone.[61] Acetone appears to be a solvent that has not been the subject of any ESPT study until recently. In particular, impurities of water are known to interfere with the ESPT in such aprotic environments, *e.g.*, as known for 6-hydroxyquinolinium in acetonitrile–water mixtures.[458] In order to address the ESPT of photoacid **B** in acetone, we recently first performed a systematic study on the ESPT in acetone–water mixtures,[294] prior to the experiments in neat acetone.[499] These studies revealed that the ESPT in acetone–water mixtures follows a three-step Eigen–Weller model (see Section 6.2) with a reaction complex (CPX) between the photoacid and water, formed either already in the ground state or at least in the first step after excitation, and a hydrogen-bonded ion pair (HBIP) as central intermediates. Only the CPX can effectively perform an ESPT, passing through the HBIP, and

finally yielding the free RO⁻* species if sufficient water molecules are present. Overall, the effective ESPT rate constant in acetone takes a value of 0.25×10^9 s⁻¹, approaching the fluorescence lifetime and being slower compared to all other studied solvents (*vide supra*). Experiments with the strongest available ammonium-based photoacids in acetone in order to observe, *e.g.*, keto–enol tautomerism by time-resolved IR spectroscopy failed as the mandatory ground-state protonation of the aminopyrene derivative initiated polymerization of acetone.[493]

While association constants could be determined from the changes in the UV/Vis absorption spectra, more detailed spectroscopic information on these intermediates was not directly accessible. Similarly, the study in neat acetone did not fully answer the question regarding the actual proton acceptor, keeping the possibility of ESPT to acetone still not fully settled. To fill this gap, complementary theoretical studies on the thermodynamics, *i.e.*, the pK_a^* value in DMSO[500] and acetone[501] have been performed as well. These further support that the experimentally observed peak progression in the UV/Vis absorption spectra of photoacid **B** upon addition of water can only be explained based on specific intermolecular interactions, as well as that **B** remains the strongest photoacid among **A–F** even in acetone (with p$K_a^* \sim 5$).[501]

6 Variations of the ESPT kinetics with photoacid strength and solvent

6.1 Separating different timescales

ESPT reactions are the outcome of numerous consecutive elementary processes that in total cover a wide range of timescales, from the sub-fs to the ns regime, comprising:[48,502]

- electronic redistribution upon excitation (sub-fs),
- hydrogen-bond rearrangement near the (photo)acidic functional group (fs),
- proton dissociation and proton solvation (ps), and
- geminate recombination and excited-state decay (ns).

Huppert and colleagues proposed a classification of the photoacids into four regimes:[503]

(I) p$K_a^* \gtrsim 0$ (Weak photoacids): relatively slow ESPT ($k_{PT} \sim 10^{10}$ s⁻¹), efficient only in water; limited by covalent interactions within the proton-transferring complex; *e.g.*, HPTS.

(II) $-4 \leq$ p$K_a^* \leq 0$ (Typical super-photoacids): faster ESPT in water, also more efficient in many protic solvents; *e.g.*, HPTS derivatives (HPTA, **A–E**).

(III) $-6 \leq$ p$K_a^* \leq -4$ (Strong super-photoacids): rapid ESPT under solvent control in water, efficient in aprotic solvents; limited by solvent re-orientation; *e.g.*, NM6HQ⁺.

(IV) p$K_a^* < -7$ (Strongest super-photoacids): ultrafast ESPT beyond solvent control in water, methanol, and ethanol ($k_{PT} \approx 10^{13}$ s⁻¹); limited by donor–acceptor distance within complex; *e.g.*, QCy7.

When moving from regime I to IV, the photoacid strength and ESPT rate increase, *i.e.* the capability to transfer protons to the solvent grows. In a nutshell, this classification reflects the competition between the ESPT rate constant, which is

determined by the pK_a^* of a given photoacid and the solvent, and the radiative decay rate. Only if the photoacid is sufficiently strong, the ESPT is fast enough to happen within the typical fluorescence lifetime of a few ns. This distinction also highlights that the exact mechanism of the ESPT depends on the photoacid strength.

6.2 Multi-step models for ESPT in water

The Förster cycle (*cf.* Fig. 2) marks the simplest starting point for any description of the ESPT process, involving only the protonated species (ROH*) and the fully separated ion pair (FIP) consisting of the deprotonated species (RO⁻*) in the excited state and the dissociated proton (attached to some proton acceptor). However, since this one-step model was proposed based on a purely thermodynamic view that does not necessarily correspond to any mechanism, it often constitutes a drastic oversimplification. Instead, owing to the pioneering work of Eigen[4,504,505] and Weller,[107–109] a multi-step model for acid dissociation (in water) has been established that involves multiple proton-transfer intermediates in a step-wise dissociation. With respect to photoacids, the Eigen–Weller model has become particularly popular due to the work by Huppert and co-workers who have extensively applied it to the ESPT kinetics of HPTS[205–212,237] and other weak (anionic) photoacids (*e.g.*, naphthol sulfonates)[364,400,404,409,412] in aqueous solution. Consisting of only two steps in the early description, this model has been extended over the years to a total of four steps, *i.e.*, involving five species, in its most general formulation (see Fig. 15).

According to the early two-step model for HPTS in water, the ROH* species first transfers its proton to a nearby water molecule under formation of a (hydrogen-bonded) contact ion pair (CIP or HBIP) within 90 ps.[205,206] Only in a second step, this CIP is separated in a diffusive process, yielding the free RO⁻*. It is important to note here that diffusion plays a central role in the special case of HPTS. Due to its quadruple negative charge, geminate recombination of RO⁻* and the dissociated proton is largely enhanced by the coulomb attraction, giving rise to non-exponential (de-)population kinetics (Fig. 5) for ROH* and RO⁻*, manifesting in a characteristic long-time tail with a $t^{-3/2}$ power-law asymptote.[211,212] Thus, a mathematical treatment of the ESPT kinetics requires a (numerical) solution to the Debye–Smoluchowski equation (DSE).[207–210] However, for most strong neutral or even cationic photoacids, solving the DSE is not necessary as diffusion has only a minor effect.[58,456,470] Particularly, in the case of cationic photoacids, the lack of the negative charge in the corresponding base leads to the formation of a so-
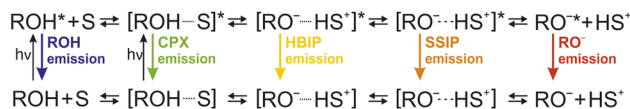
Fig. 15 Four-step Eigen–Weller model. Five reactive species are considered: the free photoacid (ROH, blue), the reaction complex (CPX, green), the hydrogen-bonded ion pair (HBIP, yellow), the solvent-separated ion pair (SSIP, orange), and the free anion (RO⁻, red) [or fully separated ion pair (FIP), red].

called Eigen complex instead of a HBIP, which is held together by dipole–dipole rather than coulomb interactions.[465,506]

Later, the rise of ultrafast time-resolved measurements revealed additional contributions to the ESPT of HPTS in water on the timescale of ∼300 fs and ∼3 ps, preceding the actual proton-transfer step, which challenged the existing two-step model.[213–216] While the first (fastest) contribution was originally assigned by Tran-Thi et al. to solvation dynamics of an initial locally excited (LE) state and has been widely accepted,[214] the interpretation of the second (intermediate) contribution became heavily debated. Interpretations are multifold and range from a conversion of an initial LE state into another electronic state (Tran-Thi),[216] a reorganization of the surrounding water molecules to form a water wire (Bakker),[231] a slow charge redistribution prior to the PT step (Spry/Fayer),[140,223,224] the formation of a solvent-separated ion pair (Huppert),[217,218] the hydration of the proton during deprotonation (Fang),[226] and vibrational energy transfer into the first hydration shell (Havenith).[63] In particular, the assignment to a solvent-separated ion pair (SSIP) as an additional intermediate between the CIP and the FIP by Huppert and co-workers lead to an expansion of their two-step into a three-step Eigen–Weller model[217,218] (compare Fig. 15). Moreover, in light of the new knowledge on HPTS during 30 years of research and specifically a discrepancy regarding recent results by Lawler and Fayer[259] for HPTS in water, Simkovitch et al. have recently presented a retrospective on their analysis.[51,52] By repeating the experiments using newer equipment with better time resolution, they reaffirmed their previous reports regarding the $t^{-3/2}$ power-law behavior, but they adopt the interpretation by Spry and Fayer for the 3 ps contribution as a slow charge rearrangement.

6.3 ESPT in non-aqueous solution

Several characteristics of the ESPT change when moving from aqueous to non-aqueous solutions. For example, in contrast to the most protic solvent, water, excited ion pairs such as the HBIP and SSIP are no longer short-lived in alcohols[458,488,496] and even longer-lived in aprotic solvents,[458,485–488] owing to lower proton conductivities (as argued by Kumpulainen et al.[486]). Moreover, diffusion-assisted geminate recombination usually has a negligible effect in aprotic solvents and thus the DSE does not need be considered, as demonstrated by Agmon and co-workers who discussed a (general) kinetic transition in reversible excited state reactions as a function of the excited-state lifetimes of the involved species.[60,403,507–509] Besides, it has been argued that the solvent has a decisive effect on the order of the two lowest-lying electronic states, which can change when moving from aqueous to non-aqueous solutions.[220,443,510] However, the reduced proton-acceptor ability in the case of protic or polar-aprotic solvents (e.g., DMSO) raises in parallel the need for complex formation prior to the ESPT. Therefore, if the photoacid and the proton acceptor are not in direct proximity prior to excitation, the (diffusive) formation of an encounter complex will typically constitute the first step, which requires another expansion of the kinetic model into a four-step Eigen–Weller model[458,486] (Fig. 15). In the extreme, further

restraining proton dissociation by changing to even less polar solvents (e.g., acetonitrile) finally completely prevents the ESPT unless a strong base is present for this complexation.[460,486] Very recently, Lee et al. have demonstrated that the ESPT of the cationic photoacid NM7HQ+ (cf. Section 5.2.2) to DMSO in acetonitrile solution involves an Eigen complex and a Zundel-type ion, $[(DMSO)_2 \cdot H]^+$, for the solvated proton species.[465] The importance of the transient Eigen complex as a short-lived, rarely observed ESPT intermediate has been recently highlighted in ref. 495. Similarly, also in aqueous solution this demand for pre-coordination with a base is reflected in the formation of water wires during (or prior to) the ESPT in water-co-solvent mixtures.[56,57,413]

If a hydrogen-bonded pre-assembly between the photoacid and the proton-accepting base is present in aprotic solvents which themselves are bad proton acceptors, it is possible to isolate the characteristic emission spectra of the different species of the Eigen–Weller model in an elegant way. This was exemplarily shown for a complex of compound **A** (see Fig. 13d) and tri-n-octylphosphine oxide (TOPO), for which a deconvolution of the fluorescence spectrum into four contributing species could be realized in a systematic study using aprotic solvents with strongly varying polarity.[511] It could be shown for a sample in acetonitrile that 7% of the integrated emission originate from ROH and RO− each, 39% from CPX, and 47% from HBIP (Fig. 16); whereas, no distinction between an SSIP as another potential intermediate and the FIP was possible. The formation of HBIP was proven by another change of the static dipole moment in the order of 3 debye. Time-resolved studies further revealed that the emission signals do not all occur simultaneously, but also not purely sequentially, as an equilibrium between CPX and HBIP is established faster than the excited-
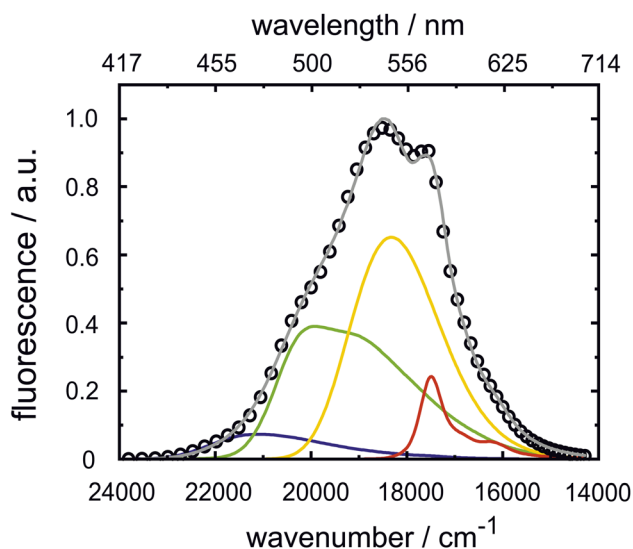
Fig. 16 Emission spectrum (dots) from a sample in which a complex between compound **A** and TOPO is present (solvent acetonitrile, 400 nm excitation). The spectrum is comprised of contributions from non-complexed ROH, a hydrogen-bonded complex CPX, a hydrogen-bonded ion pair HBIP, and the anionic species after the ion pair has separated. The displayed data is part of the study in ref. 511.

state lifetime.[512] The subsequent irreversible dissociation of the HBIP takes place on the nanosecond timescale.

6.4 Theories for the kinetics of elementary proton-transfer reactions

In the preceding sections of this review, ESPT to solvent was described as a sequential process with several steps. However, once SSIP is formed, no influence of the proton in aprotic solvents or only little influence in protic solvents on the electronic properties of the remaining base molecule (the former photoacid in its excited state) is expected.[235] Therefore, differences in the ESPT kinetics of photoacids are assumed to be dominated by the initial proton-transfer step, that is the formation of HBIP from CPX, and, to a lower extent, by the subsequent transition from HBIP to SSIP. Kinetics models for the proton-transfer step were developed already in the past century and have been assessed elsewhere,[88,503] and isotope effects turned out as worthwhile tools to verify the different models.[513–516]

Shortly, these theories rely on intersecting harmonic electronic potentials in the diabatic regime (Marcus theory) which split up in the adiabatic limit, resulting in the well-accepted one dimensional double-well potential of proton transfer reactions.[517,518] Both general approaches predict a correlation between the thermodynamic free energy of the reaction and the rate constant for the proton hopping along the reaction coordinate (free-energy correlation).[513,519] Maximum rate constants are found in the range of 10^{12} to 10^{13} s^{-1},[235,496,503] and the interpretation of this maximum value depends on the investigated system: solvent relaxation dynamics[359,520] or the frequency of the intermolecular vibration of the donor and acceptor heavy atoms framing the hydrogen-transfer coordinate were held responsible for this limit.[503] Irrespective of the accuracy of these interpretations, these findings revealed that analyses based on the reaction proceeding solely along a hydrogen-bond coordinate are an oversimplification and that taking into account additional contributions might be necessary.[521] Modifications still in terms of an one-dimensional model are accomplished by considering an activation term, the work function, which does not contribute to the overall reaction energy but comprises geometric changes facilitating the proton transfer.[50] This correction term for the simplified Marcus theory can become even larger than the intrinsic barrier of the proton transfer.[522] Alternatively, further coordinates spanning potential energy surfaces for the proton transfer reaction are developed, which allow for considering tunneling as well.[514,515]

A peculiarity of Marcus theory is that it predicts a decreasing proton transfer rate constant for very large exergonicities, whereas, models in the adiabatic regime like the semi-empirical bond-energy bond-order (BEBO) model level off. So far, it is still debated whether multidimensional configurations, required to promote proton transfer, are compatible with this so-called inverted Marcus regime.[522,523] First studies in this direction have been reported,[518] and magic photoacids might be appropriate to provide additional insight into this highly topical facet of ESPT.

7 Quantification of excited-state acidity

7.1 The molecular origin of photoacidity

The most fundamental origin of photoacidity can be found in the electronic charge redistribution upon excitation (cf. Fig. 17). As commonly explained, photoacidity is caused by an intramolecular charge transfer (ICT) in the excited state of the ROH species from the O atom in the OH group to the aromatic ring, more precisely the distal ring in the case of condensed aromatics.[94,113] In terms of molecular orbitals, this ICT corresponds to a transition of an electron from the non-bonding MO (NBMO) localized at the O atom into the lowest unoccupied MO (LUMO) that does not or less extend over the O atom (cf. Saway et al.[7]). Accordingly, the decreased electronic charge density at the OH group enhances its acidity. However, despite its plausibility, this explanation is incomplete since it does not take into account the corresponding base RO$^-$, as pointed out by Agmon.[48] As for the ground-state, (photo)acidity is the mutual outcome of both a destabilization of ROH and a stabilization of RO$^-$. If no charge transfer was found for RO$^-$, the proposed ICT of ROH would actually lead to an increased ROH–RO$^-$ energy gap that would make the excited-state deprotonation less favored. Thus, an even larger ICT with the same character must occur for the base, which is indeed confirmed by experiments, e.g. in solvatochromism[295,296,405,406,524] or Stark spectroscopy.[223] Therefore, photoacidity can be exemplified as the net effect of an excess RO$^-$ stabilization.

Another possibility to rationalize this phenomenon is in terms of Hückel's (anti)aromaticity,[525] as originally proposed by Agmon[48,315] and recently reviewed by Wen[526] and Yan et al.[527] Aromatic molecules experience an energetic stabilization due to a beneficial electronic configuration, whereas molecules that would be classified as antiaromatic are energetically destabilized leading to structural perturbations, e.g., non-planarity or bond length alternation, in order to avoid the antiaromatic structure.[528] For both excited triplet and singlet states, it has been shown that the situation changes and Hückel aromatics become less aromatic, i.e., more antiaromatic, and vice versa antiaromatics become more aromatic.[529–531] Prototypic hydroxyarene photoacids such as phenols or naphthols are aromatic in their protonated form. However, after deprotonation the negative charge is

(a) Acid   (b) Base
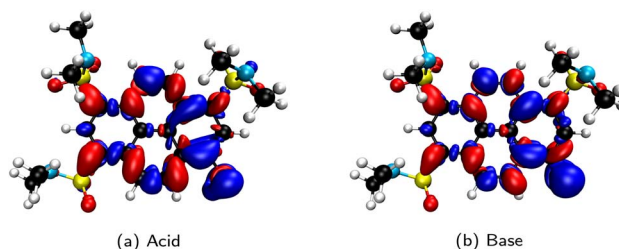
Fig. 17 Differences in the electron density between the first excited state S_1 and the ground state S_0 for the acid (a) and corresponding base (b) species of photoacid **F** (cf. Fig. 14d). Densities calculated with ADC(2)/aug-cc-pVDZ at optimized MP2/cc-pVDZ geometries and plotted at isosurface values of $\pm 5 \times 10^{-4}$ (−: blue; +: red). The displayed data is part of the study in ref. 500.

stabilized by delocalizing it in the conjugated π system at the expense of including an additional electron pair in the conjugation and lowering its aromatic character. Due to the reversal of aromaticity and antiaromaticity in the S_1 state, the protonated species is less aromatic in the excited state (S_1) and hence becomes destabilized compared the ground state (S_0). Even more important, in the excited state, the deprotonated species increases in aromaticity corresponding to a stabilization in accordance with the strong ICT. These differences in the aromatic character of the acid and the base and between S_1 and S_0 typically lead to larger Stokes shifts for the acid compared to the base and correspondingly stronger structural changes for the acid.[302,315]

7.2 Different ways to determine pK_a^*

7.2.1 Approaches based on the Förster cycle. The Förster cycle[102–104] has been established as the most frequent route to pK_a^* in both experimental and theoretical investigations.[532] It has been critically reviewed many times, *e.g.*, by Pines *et al.*[39,432] and Grabowski *et al.*[105,533] From an experimental perspective, UV/Vis absorption and fluorescence emission spectroscopy are typically used to determine the band maximum positions for the first electronic transition of the two species and then the average absorption–emission energy is used in eqn (1), as an approximation to the true 0–0 transition energy.[47,105] This implicitly assumes that the shape of the potential energy

surfaces in both electronic states are similar (*i.e.*, the harmonic force constants are alike), allowing the vibrational contributions to the vibronic 0–0 transition and the differences between absorption and fluorescence emission to effectively cancel out in the average.[534] However, the main problem arises from the use of the fluorescence energies in the first place since full equilibration is not generally given in the excited state, depending on the lifetime, which can cause pK_a^* to be effectively treated as a non-equilibrium quantity. Moreover, the Förster cycle requires knowledge on pK_a, which is usually straightforward in aqueous solution, but becomes more difficult in non-aqueous solution (*vide supra*). Alternatively, pK_a^* can also be determined experimentally by use of fluorescence titration,[535,536] which identifies pK_a^* as the inflection point in the plot of the fluorescence intensity ratio $I(\text{ROH})/(I(\text{ROH}) + I(\text{RO}^-))$ against pH, or by direct kinetic measurements of the excited-state proton dissociation and recombination rate constants[48] (see Fig. 18); both with their own limitations. Fluorescence titration is virtually limited to aqueous solutions due to the requirement of having a defined pH, which becomes non-trivial in non-aqueous solutions where no unified pH has yet been established.[538–541] The direct kinetic method is in principle most accurate, but such measurements are technically more demanding and also the (missing) reversibility of the ESPT process can become an issue again.[542] Therefore, the Förster
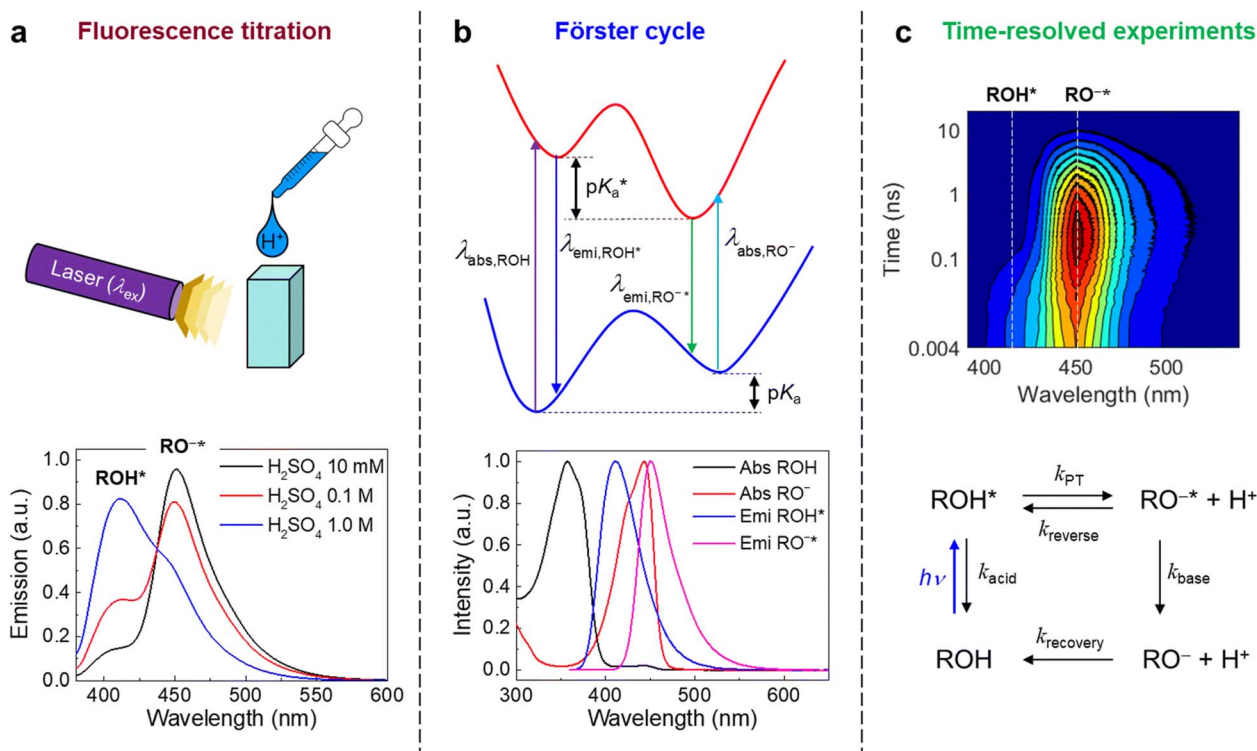
Fig. 18 Three main experimental methods for determining the excited-state acidity, pK_a^*, using coumarin 183 as an example: (a) fluorescence titration that measures the fluorescence spectra of the excited ROH* and RO$^-$* species at varying pH; (b) the Förster cycle that shifts the ground-state pK_a by the change in acidity ΔpK_a^* determined from electronic transition (*i.e.*, absorption and/or emission) energies; (c) time-resolved experiments that measure the transient signals of the excited species after electronic excitation, allowing for determination of the rate constants involved in the ESPT based on kinetic models. This figure has been reproduced from ref. 537 with the kind consent from S. Park and with permission from the Royal Society of Chemistry, copyright 2022.

cycle continues to be the standard route for experimental pK_a^* determination. Recently, Bhide *et al.* have reported a method for the experimental quantification of acidity for weak photoacids—*i.e.*, when the ESPT is slow—using steady-state photoluminescence spectroscopy and a driving-force-dependent kinetic theory.[543]

7.2.2 (Other) theoretical approaches. In contrast, theoretical approaches (*vide infra*) do not necessarily rely on the Förster cycle, but can use any target thermodynamic cycle of interest instead, including direct (also referred to as Born–Haber cycle) or indirect approaches that avoid dealing with the ground state equilibrium[342,346,347] (see Fig. 19). However, each thermodynamic cycle comes at a certain prize and has its own advantages and disadvantages.[545–548] Direct approaches (*cf.* Fig. 19a) basically shift the requirement for the ground-state pK_a to requiring knowledge on the total Gibbs free energy in solution of the proton $(G_{\text{soln.}}(\text{H}^+))$ and its Gibbs free energy of solvation $(\delta G_{\text{solv.}}(\text{H}^+))$. While the former can be calculated using statistical thermodynamics,[549] determining the latter is cumbersome theoretically and is usually taken from experiments.[547] Moreover, $\delta G_{\text{solv.}}(\text{H}^+)$ is nowadays known in water with a high certainty, *i.e.*, a value of (-264.6 ± 0.2) kcal mol^{-1} with an agreement between most recent experimental and theoretical values,[550–552] but only known in a few other solvents.[553,554] For these non-aqueous solvents, $\delta G_{\text{solv.}}(\text{H}^+)$ is thus either implicitly assumed or explicitly assigned, *e.g.*, by determination from experimental pK_a *via* regression.[555–560] In contrast, indirect cycles (*cf.* Fig. 19b) depend on the reliable knowledge of the pK_a of a reference compound. To keep a certain proximity with the experimental results for comparison reasons, also theoretical work frequently uses the Förster cycle.[342–347] This highlights two aspects: first, particular attention needs to be paid to the precise determination method of pK_a^* when comparing experimental and theoretical pK_a^*, and second, pK_a^* will often not be a pure equilibrium quantity.

(a) Direct (or absolute) Born-Haber cycle

(b) Indirect proton-exchange cycle

Fig. 19 Different thermodynamic cycles for the calculation of (ground-state) pK_a values. The direct cycle (a) and the proton-exchange cycle (b) as an example of an indirect cycle. These cycles can be equally applied to electronically excited states for the prediction of pK_a^*. This figure is based on ref. 544.

7.3 Existing theoretical studies on pK_a^*

7.3.1 Early quantum chemical studies. To date, the set of computational studies in the literature on photoacids in general and theoretical approaches to pK_a^* in particular is still very sparse. Early calculations by Gao *et al.* used a QM/MM formalism—treating the solute at the Complete Active Space Self Consistent Field (CASSCF) and multi-reference second-order perturbation theory (CASPT2) levels and the solvent classically—to determine the ΔpK_a of phenol in water.[561] Later, Granucci *et al.* also applied CASSCF and CASPT2, but in combination with the Polarizable Continuum Model (PCM)[562] for implicit solvation to study the excited-state acidity of phenol and cyanophenols in the gas phase and in water.[302] The use of such high-level multi-reference (MR) methods is generally restricted to smaller molecules due to the size of the active space. This is the reason why larger systems such as pyrenols[216] or anthocyanins,[563] but even naphthols[315] could only be studied within semi-empirical frameworks for some time. In line with this, Szczepanik *et al.* also discussed the effect of the cyano (CN) group on pK_a and pK_a^* in phenol, naphthol, biphenyl, and aniline derivatives using AM1 and single excitation CI (SECI).[532,564] In addition, also some molecular simulation studies on pK_a^*, *e.g.*, on pyrimidine in aqueous solution by Gao *et al.* (using semi-empirical AM1 for the electronic structure)[565] or the biologically relevant phytochromobilin chromophore by Borg *et al.* (using TDDFT in combination with IEF-PCM for the electronic excitations; tested against CIS, CIS(D), SAC-CI, and CASSCF)[566,567] have been reported.

7.3.2 Studies using density functional theory (DFT). Although electronic excitation energies could be calculated using MR methods (*e.g.*, MRCI, CASSCF, CASPT2) already decades earlier, it was not before the rise of time-dependent density functional theory (TDDFT) that electronically excited states became accessible much cheaper and in a more easy-to-use fashion in quantum chemistry (*e.g.*, see ref. 568 for an overview on DFT methods for excited states). TDDFT was particularly important for the application of calculating electronic excitation energies to larger systems and/or to the optimization of excited-state geometries (since these are much more expensive than a single-point energy calculation) as well as for the combination with solvent models (since this is technically more demanding for multi-reference methods).[569–571] Jacquemin *et al.* have described a computational protocol for the theoretical prediction of pK_a^* for coumarins that is purely based on TDDFT in combination with PCM.[342] This approach has been further extended by Houari *et al.* to the classes of naphthols and cyanonaphthols by critically comparing the results for the Förster cycle and the direct (Born–Haber) cycle as well as for the linear response (LR) and state-specific (SS) variants of PCM.[346] Later, Houari *et al.* have applied their improved protocol for pK_a^* prediction based on TDDFT and (SS)-PCM again to the coumarins, while also addressing the effect of explicit solvent (water) in the first solvation shell of these photoacids.[328] Recently, Aquino and co-workers have used TDDFT in combination with PCM or the Conductor-Like Screening Model (COSMO) to study the photoacidity of two different
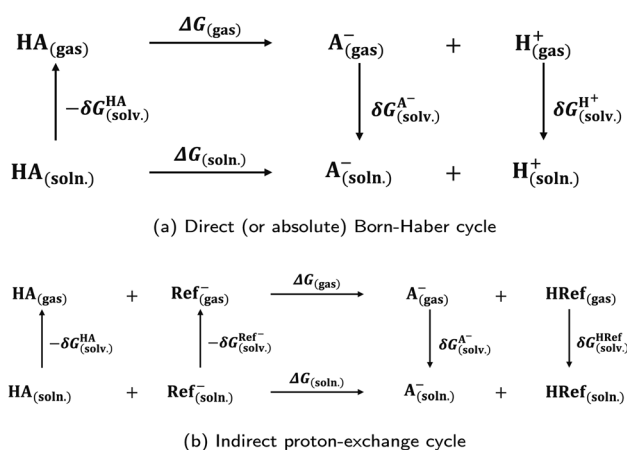
hydroxyflavylium cations.[348,350] Moreover, Joung et al. have used (TD)DFT as a reference for evaluating different experimental methods for the determination of pK_a^*, revealing the usage of optical bandgaps that are defined by the absorption and emission edges as transition energies in the Förster cycle to be most reliable.

7.3.3 Limitations of (TD)DFT.

In general, TDDFT has become extremely popular for the study of photoacids, as examples of typical (organic) fluorescent dye molecules,[572,573] also apart from pK_a^*, e.g., regarding the reaction mechanism of the ESPT (kinetics) mechanism,[68,191,321,325–330,332,335,574–576] spectral characterization and insights into the origin of photoacidity through the electronic structure,[322,331,334,336,471,577] or as the method of choice for treating the electronic excitations in numerous QM/MM molecular dynamics (MD) studies (see Section 3).[193,351–355,357,358,578–580] TDDFT has been also applied to study the proton transfer within the biologically relevant green fluorescent proteins.[27,28] Only a few AIMD studies using MR methods instead of TDDFT have been reported.[581–583] While the use of TDDFT for electronic excitation energies is for sure not an issue on its own—TDDFT has established as a rich field that continuously develops and validates new methods—,[584–586] standard DFT methods can still not be said to be fully generally reliable.[587,588] Prominent examples of such failures for TDDFT include charge-transfer or Rydberg excitations, and these have been addressed in the literature, e.g., by using range-separated functionals such as CAM-B3-LYP.[589] However, TDDFT sometimes gives wrong shapes for the potential energy surfaces of the excited states[590] and suffers from relatively low accuracies for vertical excitations (± 0.3 eV).[591] In an extreme case, TDDFT can even predict a wrong order of the electronic states under certain circumstances. Recently, Acharya et al. have demonstrated that TDDFT fails to predict the correct order of the ^1L_a and ^1L_b states of the photoacids 1- and 2-naphthol by comparison with Equation-Of-Motion Coupled Cluster Singles and Doubles (EOM-CCSD) (all calculations using C-PCM) and with experimental results.[592] Similar observations had been previously made by Grimme and Parac,[593] who assigned this imbalanced description of the two states with TDDFT to an underestimation of the interaction of the ionic components in the corresponding ^1L_a-state wave functions with current standard functionals, and by Prlj et al.,[594] who extended the scope of this issue to a set of fused heteroaromatics and demonstrated that the ^1L_b state is highly sensitive to correlation effects, while the ^1L_a state suffers from the same drawbacks as charge transfer excitations.

7.3.4 Studies using wavefunction theory (WFT).

These limitations may motivate to refrain from using (TD)DFT for the description of the electronic excitations of photoacids. Instead, the wavefunction theory (WFT) methods algebraic diagrammatic construction scheme through second order (ADC(2)) and approximate coupled cluster singles and doubles method (CC2), which are known to be more accurate (± 0.2 eV) and more robust,[591] appear a better choice. Although WFT, e.g., CASSCF and CASPT2 have already been used for predicting pK_a^* (vide supra), ADC(2) and CC2 are much more applicable in a black-

box fashion with respect to the computational costs compared to aforementioned multi-reference methods.

Until recently, the only study that had used ADC(2) in the calculations of the excitation energies for (photoacid) pK_a^* has been the work by Wang et al. on the photoacidity of cationic hydroxypyranoanthocyanines.[349] However, in the actual computation of pK_a^* values, they restrict themselves to B3-LYP TDDFT instead of ADC(2) despite—or due to—a close similarity between the results for these two methods. Related studies by the same groups (i.e., Aquino, Quina, and co-workers) on similar pyranoanthocyanines[337,338] or other hydroxyflavylium cations[339,340] also use ADC(2) in combination with COSMO for describing the electronically excited states, but do not explore pK_a^* values. Recently, Khodia et al. have also used ADC(2) in a combined experimental–computational study on the ESIPT of a pyridylbenzimidazole photoacid within a water complex.[595] Still, to the best of our knowledge, there had still been basically no approach to pK_a^* beyond TDDFT that actually uses accurate, but easy-to-apply WFT methods like ADC(2) or CC2. This gap regarding WFT studies on photoacid pK_a^* values has recently been addressed by Hättig and co-workers.

Ghiami-Shomami and Hättig performed extensive benchmark calculations of Förster-cycle-based pK_a^* values of 12 photoacids (phenols, naphthols, and hydroxycoumarins) and 8 photobases (quinolines and acridine) in water,[596] covering a broad variety of methods for describing the electronic transitions (including 8 simple up to state-of-the-art DFT functionals, ADC(2), and CC2) and obtaining the corresponding ground-state pK_a values with COSMO-RS[597–599] at the DFT BP86 level. Their results indicate that such a simple protocol based on an implicit solvent model and vertical excitation energies is in general not sufficient to predict pK_a^* values with an accuracy comparable with that achieved by the above mentioned protocols for the ground state pK_a values. Following the same approach, Sülzner and Hättig have studied the pK_a^* values of the hydroxypyrene derivatives discussed in Section 5.4 in the aprotic solvents DMSO[500] and acetone[501] using ADC(2) and CC2 in combination with COSMO. Prior to pK_a^* prediction in acetone, the study in DMSO first assessed the performance of the selected computational methods for the full set of photoacids **A–F** (cf. Fig. 13d) by validation against experimental data.[500] Additionally, with COSMO-RS as the underlying method for the ground-state pK_a values in this computational protocol, the (previously missing) corresponding linear free-energy relationship parameters for pK_a prediction in acetone also needed to be determined.[600] Overall, the results on these photoacids in DMSO and acetone (cf. Fig. 20) show that whenever the photoacidic OH group can form hydrogen bonds either with solvent molecules or by self-association, the errors of a purely implicit solvation model limit the accuracy of the calculations. However, and in line with the previous results by Ghiami-Shomami and Hättig, the second-order methods ADC(2) and CC2 significantly outperform TDDFT for the prediction of ΔpK_a, i.e., the only contribution to pK_a^* including the excitation energies according to this protocol. For reliable calculations of the absolute pK_a^*, but also in general for the description of excited-state proton-transfer reactions in solution, a more accurate approach
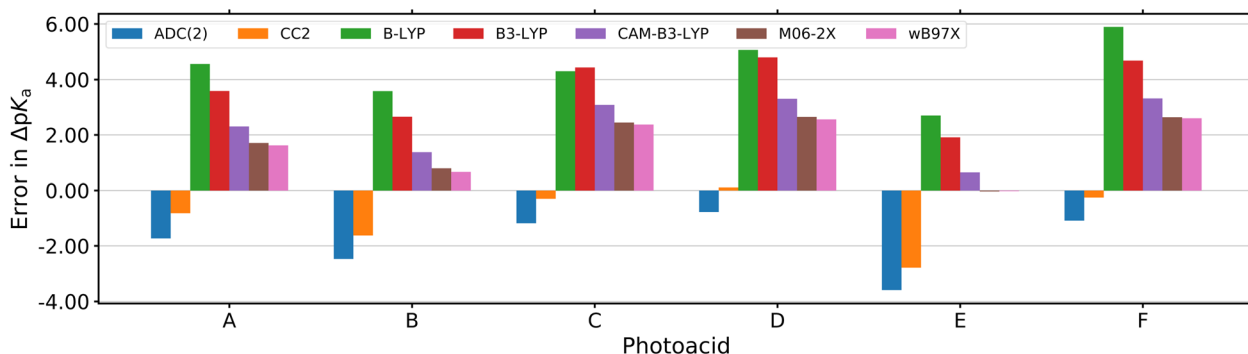
Fig. 20 Comparison of the prediction error in Förster–cycle ΔpK_a values (*cf.* eqn (1)) of Jung's super-photoacids **A–F** (*cf.* Fig. 13d) in the aprotic solvent acetone for different quantum-chemical methods with respect to the experiment. In total, the wavefunction-based methods ADC(2) and CC2 perform much better compared to TDDFT. The slightly worse performance for photoacids **A** and **B** is attributed to the higher need for explicit solvent interactions that are missing with an implicit solvent model. The distinct deviations for **E** are due to intermolecular hydrogen bonding between two photoacid molecules. The displayed data is part of the study in ref. 501.

seems required, with MD simulations comprising explicit solvent being among the desiderata for future studies.

8 Conclusion and outlook

8.1 The theoretical future of photoacids

Among the theoretical studies presented and discussed here, we would like to conclude with some highlights that are particularly interesting to us. First, the ability to obtain direct insights into the electronic structure of photoacids *via* quantum-chemical calculations remains a fundamental advantage from the theoretical perspective, as the character of the excited states is known to play a role for the photoacidity.[39,432] This is not only important for the comparison of calculated with experimental spectra, but can, *vice versa*, even help with the interpretation of experimental data. Platt's notation for the two lowest-lying excited states, ^1L_a and ^1L_b, although being conceptually very useful, quickly reaches its limit, *e.g.*, for highly-substituted systems whose broken symmetry can introduce mixing between these two states. Such a mixing already occurs for the naphthols[443] and attempts to assign the ^1L_a and ^1L_b states of HPTS have led to an apparently unresolved debate.[214,216–218,220,223,224,226,230] Although new high-level calculations on HPTS could contribute to resolving this debate, forcing such an assignment of ^1L_a and ^1L_b might not be meaningful due the potential limitations of that model when exceeding its intended range of molecules. Second, even outside the picture of Platt's ^1L_a and ^1L_b states, an accurate description of the electronically excited states is important. In this regard, a general gap of WFT studies can be made out in the literature since most studies use (TD)DFT, which can be potentially problematic since the order of the these two low-lying states is sensitive to the amount of exact exchange in the DFT functional.[593] Particularly, the purpose of a theoretical study might be to actually predict the order of these states, requiring extra caution from the user in these cases.

An improved protocol for the prediction of ΔpK_a, *i.e.*, the acidity change upon excitation, still remains a future goal. Easy-to-use protocols developed so far typically rely on cheap

methods like TDDFT combined with an implicit solvent model.[342,346,347] Methodologically, not only a reliable and accurate electronic structure method (*e.g.*, coupled cluster theory instead of TDDFT), but also a proper solvation treatment are required for this. While preceding studies have shown that the implicit solvent model COSMO in combination with ADC(2) or CC2 can yield reasonably good accuracy in the prediction of Förster-cycle-based ΔpK_a values in the aprotic solvents DMSO and acetone,[500,501] implicit solvation is not sufficient in the protic solvent water.[501,596] Improving the description of solvation must not directly lead to incorporating lots of explicit solvent molecules and running an MD simulation, but could also first try to use a more accurate model within these two extremes of implicit and fully explicit solvation [*e.g.*, the embedded cluster reference interaction site model (EC-RISM)].[601,602] However, when aiming at best compatibility between theory and experiments, such MD simulations in solution will eventually become inevitable since, even apart from solvent effects, the vertical approximation has already been identified as the (other) main limitation (*cf.* acetone and DMSO).[500,501] In contrast to static calculations (often on isolated molecules in vacuum), these MD simulations are capable of explicitly accounting for the vibrational contributions to the vibronic transitions (*e.g.*, *via* an ensemble average), as further discussed in the following.

On the one hand, the sampling for generating representative solvent configurations around the photoacid as the solute is best performed using *ab initio* MD (AIMD) instead of classical MD techniques to avoid a systematic bias on the electronic excitation energies through the geometries as affected by the underlying method for calculating the energy gradients. While such AIMD simulations are practically restricted to DFT as the electronic structure method for the time propagation, a different (higher-level) method could be used for calculating the vertical excitation energies at selected snapshots taken from the trajectory (*e.g.*, see references in ref. 603). On the other hand, the comparison of theoretical and experimental ΔpK_a values will also involve the fluorescence because an average of the absorption and emission band maxima is typically used in

the experiments as an approximation to the 0–0 transition energies. This makes things even worse since already a ground-state AIMD simulation can be a demanding task for photoacid molecules of the size of HPTS with explicit solvent, but an equivalent description of fluorescence requires capturing the excited-state dynamics. Due to the higher computational demands compared to the ground state, such MD simulations for the excited state are basically restricted to TDDFT as a cheap method, with the potential disadvantages discussed earlier (see Section 7.3.3).

Mentioning excited-state dynamics brings us to our final highlight from a theoretical perspective: The allegate dream of simulating the full ESPT process of a photoacid in solution. Technically, this still requires an AIMD simulation for sampling excited-state dynamics, again with the associated requirements and limitations discussed above. If level crossing is involved, *e.g.*, an inversion of the ^1L_a and ^1L_b states that is frequently discussed for the naphthols (*cf.* ref. 39 and 432 and references therein), surface-hopping techniques,** (*e.g.*, Tully's fewest switches surface hopping, FSSH)[605] are needed to account for transitions between the excited states. Important examples of such surface-hopping AIMD studies on photoacids, which are still quite rare in general, include the work on the ESIPT of 2-phenylphenol[582] and 4-(2′-hydroxyphenyl)pyridine[583] by Cui, Thiel, and co-workers; and that on salicylidene methylamine Schiff-base photoswitches[606] by Barbatti and co-workers. Importantly, in these non-adiabatic excited-state dynamics studies, the choice of initial points has been generally found a rather important topic in theoretical-computational studies, from spectrum simulation to solute–solvent configuration.[607–610] Moreover, a fundamental problem arises from the different timescales of the ESPT process itself (*cf.* Section 6.1). Since such AIMD simulations in the excited state are typically restricted to a few tens or hundreds of ps, only the initial processes contributing to the ESPT might be observable apart from ultrafast solvation dynamics; including (1) the possible conversion from a locally excited (LE) state into a charge-transfer (CT) state (*i.e.*, $^1L_a/^1L_b$ conversion) of the ROH* species prior to the proton transfer (PT) and (2) the PT event itself yielding a contact ion pair (CIP) as the first intermediate. The subsequent separation of the CIP into free ions, with other hydrogen-bonded species as additional intermediates in terms of a multi-step Eigen–Weller model are out of reach for excited-state AIMD. However, it can be argued that the separation of the CIP is less unique—and hence less interesting—for photoacids as this resembles the normal dissociation of ionic species in solution that is characteristic for a given solvent. Among the few AIMD studies on photoacids in the literature, the two recent ones on the excited-state and ESPT of HPTS in 1-methyl-imidazole (by Thomaz *et al.*)[357] and water (by Walker *et al.*)[358] appear impressive examples to us, demonstrating how the technical frontiers are evolving.

8.2 Established and future-oriented applications of photoacids

Among all photoacids, HPTS is certainly the most widely used and commercially available fluorescence marker due to its strong visible fluorescence. Some applications rely on its multiple negative charges,[611] a property which is, however, not specific and other fluorophores might be equally useful, *e.g.*, for the delivery of electrons upon photoexcitation.[612,613] Its usefulness as paradigmatic†† pH indicator was noticed already many decades ago (see references in ref. 203), but an application to cellular systems is limited by the restricted permeation through biological interfaces due to the high number of charges. Therefore, removal of these by substitution drastically accelerates the uptake,[61] and similar synthetic modifications enable the incorporation into nanoparticles making them pH-sensitive.[615] Also the related ESIPT photoacids,[616] metastable-state photoacids,[617,618] and photo-acid generators[619] have proven successful for controlling (intracellular) pH. The advantage of photoacids over other pH-sensitive fluorophores is the possible ratiometric readout turning these pH-indicators more robust against concentration variations.[620] One might argue here that the intensity ratio is obtained by exciting both the neutral and deprotonated state. Such a readout consequently calls for two excitation light sources which is less beneficial than those systems where the intensity ratio results from two detection channels.[291] Fluorescence titrations of photoacids can make use of this experimental approach if the kinetics of de- and reprotonation are faster than the excited-state lifetime.[621]

Truly dual-emissive conditions are met in the ESPT reaction itself, and several groups have pointed out that a minimum number of water molecules is necessary for ESPT in otherwise spectroscopically silent solvents or environments (see also the discussion in ref. 97).[286,294,622] Such a strategy has been exploited to assess the water content in acetonitrile,[623] or even in solid phases like metal–organic frameworks,[624] silica materials and phosphate matrices.[615,625] Likewise, hydrogen isotopes can be distinguished in protic solvents due to the kinetic isotope effect when the rate constant for the overall ESPT is in same range as the time constant for fluorescence emission.[491,626]

Another well-known way to make use of the dual-emissive properties is to inhibit the ESPT reaction by chemical substitution of the proton. A variety of substrates for enzyme reactions with low substrate specificity has been realized in the past.[200,201,627] Removal of the negative charges allows for visualizing enzymatic reactions in the cellular environment as exemplified in the classification of the most abundant brain tumor meningioma by its phosphatase activity.[628] Even the activity of two enzymes, independently from each other, can be probed by four emission colors in a confocal microscope: color tuning is achieved by playing with the electron-withdrawing capability of one substituent.[184] As previous work has demonstrated the high photostability and large fluorescence quantum

---

** *E.g.*, see ref. 604 for a recent perspective on the use of surface hopping modeling for describing charge (including proton) and energy transfer by Barbatti and co-workers.

†† See ref. 614 for an example of real-time monitoring of the photo-induced pH jump using a diamagnetic pH indicator consisting of a mestable-state photoacid and an EPR spin probe.

yields of these pyrene-based new millennium dyes,[61] transfer of this dual-emissive readout to single-molecule microscopy enabled to track individual, Pd-induced deprotection reactions. This example of single-molecule chemistry can be operated in a fluorogenic approach or by simultaneously recording trajectories of substrate and product fluorescence.[629,630]

ESPT is often exploited for mechanistic studies of proton transfer in general and may complement findings by other spectroscopies. Therefore, ESPT is studied in solid materials[625] as well as in unconventional liquids like concentrated sulfuric acid,[491] liquid crystals,[631] or ionic liquids.[285,427] Among these, the luminescent ionic liquid with HPTS as anion is worth being highlighted;[632] we are curious about the properties of cationic photoacids with weakly coordinating counter anions once they are available. Studies of ESPT on material surfaces or membranes are focused on characterizing proton diffusion with geometrical restrictions.[633,634] The generation of protons on the surface of photocatalytically active nanoparticles even allows for manipulating their motion due to a change of the charge.[635] More generally, owing to their property as light-controlled proton sources, photoacids can be used in photo-catalysis (see ref. 7 for a recent review), e.g., as initiators for polymerization,[636,637] esterification,[638] acetalization,[639,640] glycosylation,[641] olefin hydroarylation,[313] indane synthesis,[642] and self-propulsion of oil droplets;[636] as photosensitizers (e.g., for singlet oxygen generation),[643] or, for photoswitching enzyme activity.[644] Other, more technically oriented applications of the photoinduced generation of protons aim at the release of CO_2 from captured CO_2 (as HCO_3^-)[645–647] or the build-up of a pH gradient for a photo-electrochemical cell.[648–650] The performance of these devices, however, is facilitated when the deprotonated state lasts longer, which explains the preference yet for metastable-state photoacids. Another electrochemical application of ESPT is light-controlled proton conduction.[651,652] As free protons require additional water molecules for stabilization, ionization of photoacids buried in polymeric structures is supposed to lead to larger structures, and an application as carrier for therapeutics which release the cargo by a light stimulus on demand is foreseen.[653–658] On the other hand, proton release in free solution apparently leads to a volume shrinkage.[659] In conclusion, the swelling behaviour of photoacids in polymers is more complicated.[163]

Further research areas will be addressed once more regioselective substitution of pyrene-based photoacids or even stronger photoacids than those reported before are available: specific modifications on the pyrene core[430,502] appear challenging according to our experience.

8.3 Open questions—new aspects to be explored by excited-state proton transfer

While some of the latter described applications certainly deserve further development for generating technologically relevant devices, we focus here on fundamental aspects of proton transfer reactions. Although the proton transfer is one of the best investigated reactions, not all aspects of this elementary reaction are known. For example, we wonder how the proton jumps away from the HBIP to the next intermediate of the reaction chain depicted in Fig. 15 and which molecular rearrangement or solvent properties assist this process. Is tunneling playing a significant role in ESPT?[626,660] Actually, few low-temperature studies of ESPT in protic solvents are known and point into that direction.[253,254,456,472,661]

ESPT is a paradigmatic charge transfer reaction including the transfer of a mass particle (compared to electron transfer), and findings about it may have impact for other chemical reactions.[662,663] Even the important questions of chirality can be addressed.[369,664] However, some peculiarities may be met due to the low mass (compared to the transfer of other atoms), and one may look for further evidence of the inverted Marcus-regime in proton transfer reactions.[518]

Finally, we emphasize that ESPT is one of the few adiabatic photochemical reactions—if not the only one useful. The adiabatic character becomes superior to the other well-studied charge transfer reaction, i.e., the electron transfer, when light emission is mandatory for detection like in single-molecule fluorescence spectroscopy. ESPT is quasi-reversible and can be monitored multiple times due to the ground-state reprotonation, in contrast to irreversible reactions. Hence, we expect to detect even intermediates and to characterize the influence of the environment on the different reaction steps which makes this kind of reaction unique. So far, single-molecule ESPT experiments in solution have been performed,[497,498] but the transfer to individual molecules, e.g., the continuous observation of ESPT in solid DMSO, broke down yet. Our current interpretation is that infrequent formation of FIP, but still too frequent for single-molecule studies, leads to an intermittent disappearance of the photoacid state until the proton accidently is recaptured by the left negative charge. Other combinations of quantum-optical phenomena with photochemistry include different strengths of light-matter coupling,[654,665,666] and we attempt to realize different logical gates for the generation of photons by means of photoacids.[184]

Data availability

No primary research results, software or code have been included as part of this review.

Author contributions

Niklas Sülzner: conceptualization, methodology, validation, investigation, visualization, writing – original draft. Gregor Jung: conceptualization, supervision, resources, funding acquisition, writing – review & editing. Patrick Nuernberger: conceptualization, visualization, supervision, project administration, resources, funding acquisition, writing – review & editing.

Conflicts of interest

There are no conflicts to declare.

Acknowledgements

References

1 P.-T. Chou and K. M. Solntsev, *J. Phys. Chem. B*, 2015, **119**, 2089.

2 H. Kagel, M. Frohme and J. Glökler, *J. Cell. Biotechnol.*, 2018, **4**, 23–30.

3 S. Hammes-Schiffer, *J. Phys. Chem. B*, 2021, **125**, 3725–3726.

4 M. Eigen, *Angew Chem. Int. Ed. Engl.*, 1964, **3**, 1–19.

5 H. Hattori and Y. Ono, *Metal Oxides in Heterogeneous Catalysis*, Elsevier, 2018, pp. 133–209.

6 P. Wan and D. Shukla, *Chem. Rev.*, 1993, **93**, 571–584.

7 J. Saway, Z. M. Salem and J. J. Badillo, *Synthesis*, 2021, **53**, 489–497.

8 M. Shabani, H. Younesi, M. Pontié, A. Rahimpour, M. Rahimnejad and A. A. Zinatizadeh, *J. Cleaner Prod.*, 2020, **264**, 121446.

9 M. Petukh, S. Stefl and E. Alexov, *Curr. Pharm. Des.*, 2013, **19**, 4182–4190.

10 G. S. Longo, N. A. Pérez-Chávez and I. Szleifer, *Curr. Opin. Colloid Interface Sci.*, 2019, **41**, 27–39.

11 P. Neupane, S. Bhuju, N. Thapa and H. K. Bhattarai, *Biomol. Concepts*, 2019, **10**, 1–10.

12 A. J. Kirby, *eLS*, John Wiley & Sons, Ltd, 2010.

13 I. Ghosh, S. Khan, G. Banerjee, A. Dziarski, D. J. Vinyard, R. J. Debus and G. W. Brudvig, *J. Phys. Chem. B*, 2019, **123**, 8195–8202.

14 M. Chattoraj, B. A. King, G. U. Bublitz and S. G. Boxer, *Proc. Natl. Acad. Sci.*, 1996, **93**, 8362–8367.

15 H. Lossau, A. Kummer, R. Heinecke, F. Pöllinger-Dammer, C. Kompa, G. Bieser, T. Jonsson, C. M. Silva, M. M. Yang, D. C. Youvan and M. E. Michel-Beyerle, *Chem. Phys.*, 1996, **213**, 1–16.

16 P. Leiderman, R. Gepshtein, I. Tsimberov and D. Huppert, *J. Phys. Chem. B*, 2008, **112**, 1232–1239.

17 P. Leiderman, D. Huppert, S. J. Remington, L. M. Tolbert and K. M. Solntsev, *Chem. Phys. Lett.*, 2008, **455**, 303–306.

18 K. M. Solntsev, O. Poizat, J. Dong, J. Rehault, Y. Lou, C. Burda and L. M. Tolbert, *J. Phys. Chem. B*, 2008, **112**, 2700–2711.

19 J. N. Henderson, M. F. Osborn, N. Koon, R. Gepshtein, D. Huppert and S. J. Remington, *J. Am. Chem. Soc.*, 2009, **131**, 13212–13213.

20 S. P. Laptenok, J. Conyard, P. C. Bulman Page, Y. Chan, M. You, S. R. Jaffrey and S. R. Meech, *Chem. Sci.*, 2016, **7**, 5747–5752.

21 C. Chen, L. Zhu, M. S. Baranov, L. Tang, N. S. Baleeva, A. Y. Smirnov, I. V. Yampolsky, K. M. Solntsev and C. Fang, *J. Phys. Chem. B*, 2019, **123**, 3804–3821.

22 Z. Wang, Y. Zhang, C. Chen, R. Zhu, J. Jiang, T.-C. Weng, Q. Ji, Y. Huang, C. Fang and W. Liu, *Angew. Chem., Int. Ed.*, 2023, **62**, e202212209.

23 J. J. v. Thor and P. M. Champion, *Annu. Rev. Phys. Chem.*, 2023, **74**, 123–144.

24 A. Acharya, A. M. Bogdanov, B. L. Grigorenko, K. B. Bravaya, A. V. Nemukhin, K. A. Lukyanov and A. I. Krylov, *Chem. Rev.*, 2017, **117**, 758–795.

25 V. Helms and W. Gu, *Fluorescent Proteins I: From Understanding to Design*, Springer, Berlin, Heidelberg, 2012, pp. 171–181.

26 G. Jung, *Fluorescent Analogues of Biomolecular Building Blocks: Design and Applications*, John Wiley & Sons, Ltd, 2016, pp. 55–90.

27 G. Donati, A. Petrone, P. Caruso and N. Rega, *Chem. Sci.*, 2018, **9**, 1126–1135.

28 A. Petrone, P. Cimino, G. Donati, H. P. Hratchian, M. J. Frisch and N. Rega, *J. Chem. Theory Comput.*, 2016, **12**, 4925–4933.

29 Y. Erez and D. Huppert, *J. Phys. Chem. A*, 2010, **114**, 8075–8082.

30 I. Presiado, Y. Erez and D. Huppert, *J. Phys. Chem. A*, 2010, **114**, 13337–13346.

31 I. Presiado, Y. Erez and D. Huppert, *J. Phys. Chem. A*, 2010, **114**, 9471–9479.

32 Y. Erez, I. Presiado, R. Gepshtein and D. Huppert, *J. Phys. Chem. A*, 2011, **115**, 1617–1626.

33 I. Presiado, R. Gepshtein, Y. Erez and D. Huppert, *J. Phys. Chem. A*, 2011, **115**, 7591–7601.

34 J. Kuchlyan, D. Banik, A. Roy, N. Kundu and N. Sarkar, *J. Phys. Chem. B*, 2014, **118**, 13946–13953.

35 J. Kuchlyan, D. Banik, N. Kundu, S. Ghosh, C. Banerjee and N. Sarkar, *J. Phys. Chem. B*, 2014, **118**, 3401–3408.

36 J. J. Snellenburg, S. P. Laptenok, R. J. DeSa, P. Naumov and K. M. Solntsev, *J. Am. Chem. Soc.*, 2016, **138**, 16252–16258.

37 V. O. Silva, A. A. Freitas, A. L. Maçanita and F. H. Quina, *J. Phys. Org. Chem.*, 2016, **29**, 594–599.

38 F. H. Quina, P. F. Moreira, C. Vautier-Giongo, D. Rettori, R. F. Rodrigues, A. A. Freitas, P. F. Silva and A. L. Maçanita, *Pure Appl. Chem.*, 2009, **81**, 1687–1694.

39 D. Pines and E. Pines, *Hydrogen-Transfer Reactions*, John Wiley & Sons, Ltd, 2006, pp. 377–415.

40 *Proton-Transfer Reactions*, ed. E. Caldin and V. Gold, Springer US, Boston, MA, 1975.

41 J. Reijenga, A. van Hoof, A. van Loon and B. Teunissen, *Anal. Chem. Insights*, 2013, **8**, ACIS12304.

42 B. Pathare, V. Tambe and V. P. Patil, *Int. J. Pharm. Pharm. Sci.*, 2014, **6**, 26–34.

43 L. Barcza and Á. Buvári-Barcza, *J. Chem. Educ.*, 2003, **80**, 822.

44 A. Buvári-Barcza and L. Barcza, *Die Pharmazie*, 2005, **60**, 243–246.

45 K. S. Alongi and G. C. Shields, *Annual Reports in Computational Chemistry*, Elsevier, 2010, vol. 6, pp. 113–138.

46 P. G. Seybold and G. C. Shields, *Wiley Interdiscip. Rev.: Comput. Mol. Sci.*, 2015, **5**, 290–297.

47 J. F. Ireland and P. A. H. Wyatt, *Advances in Physical Organic Chemistry*, Academic Press, 1976, vol. 12, pp. 131–221.

48 N. Agmon, *J. Phys. Chem. A*, 2005, **109**, 13–35.

49 N. M. Trieff and B. R. Sundheim, *J. Phys. Chem.*, 1965, **69**, 2044–2059.

50 L. G. Arnaut and S. J. Formosinho, *J. Photochem. Photobiol., A*, 1993, **75**, 1–20.

51 R. Simkovitch, D. Pines, N. Agmon, E. Pines and D. Huppert, *J. Phys. Chem. B*, 2016, **120**, 12615–12632.

52 R. Simkovitch, G. G. Rozenman and D. Huppert, *J. Photochem. Photobiol., A*, 2017, **344**, 15–27.

53 L. Genosar, B. Cohen and D. Huppert, *J. Phys. Chem. A*, 2000, **104**, 6689–6698.

54 A. A. Awasthi and P. K. Singh, *ChemPhysChem*, 2018, **19**, 198–207.

55 O. Gajst, O. Green, L. Pinto da Silva, J. C. G. Esteves da Silva, D. Shabat and D. Huppert, *J. Phys. Chem. A*, 2018, **122**, 8126–8135.

56 O. Gajst, L. Pinto da Silva, J. C. G. Esteves da Silva and D. Huppert, *J. Phys. Chem. A*, 2018, **122**, 4704–4716.

57 O. Gajst, L. Pinto da Silva, J. C. G. Esteves da Silva and D. Huppert, *J. Phys. Chem. A*, 2019, **123**, 48–58.

58 R. Simkovitch, S. Shomer, R. Gepshtein, M. E. Roth, D. Shabat and D. Huppert, *J. Photochem. Photobiol., A*, 2014, **277**, 90–101.

59 O. Gajst, O. Green, R. Simkovitch, D. Shabat and D. Huppert, *J. Photochem. Photobiol., A*, 2018, **353**, 546–556.

60 I. V. Gopich, K. M. Solntsev and N. Agmon, *J. Chem. Phys.*, 1999, **110**, 2164–2174.

61 B. Finkler, C. Spies, M. Vester, F. Walte, K. Omlor, I. Riemann, M. Zimmer, F. Stracke, M. Gerhards and G. Jung, *Photochem. Photobiol. Sci.*, 2014, **13**, 548.

62 M. Rini, B.-Z. Magnes, E. Pines and E. T. J. Nibbering, *Science*, 2003, **301**, 349–352.

63 C. Hoberg, J. J. Talbot, J. Shee, T. Ockelmann, D. D. Mahanta, F. Novelli, M. Head-Gordon and M. Havenith, *Chem. Sci.*, 2023, **14**, 4048–4058.

64 Z. Shi, P. Peng, D. Strohecker and Y. Liao, *J. Am. Chem. Soc.*, 2011, **133**, 14699–14703.

65 L. A. Tatum, J. T. Foy and I. Aprahamian, *J. Am. Chem. Soc.*, 2014, **136**, 17438–17441.

66 Y. Liao, *Acc. Chem. Res.*, 2017, **50**, 1956–1964.

67 Y. Liao, *Phys. Chem. Chem. Phys.*, 2022, **24**, 4116–4124.

68 Y.-Z. Ma, U. I. Premadasa, V. S. Bryantsev, A. R. Miles, I. N. Ivanov, A. Elgattar, Y. Liao and B. Doughty, *Phys. Chem. Chem. Phys.*, 2024, **26**, 4062–4070.

69 M. Shirai and M. Tsunooka, *Bull. Chem. Soc. Jpn.*, 1998, **71**, 2483–2507.

70 C. J. Martin, G. Rapenne, T. Nakashima and T. Kawai, *J. Photochem. Photobiol., C*, 2018, **34**, 41–51.

71 N. Zivic, P. K. Kuroishi, F. Dumur, D. Gigmes, A. P. Dove and H. Sardon, *Angew. Chem., Int. Ed.*, 2019, **58**, 10410–10422.

72 N. A. Kuznetsova, G. V. Malkov and B. G. Gribov, *Russ. Chem. Rev.*, 2020, **89**, 173.

73 T. Kumpulainen, B. Lang, A. Rosspeintner and E. Vauthey, *Chem. Rev.*, 2017, **117**, 10826–10939.

74 R. I. Cukier and D. G. Nocera, *Annu. Rev. Phys. Chem.*, 1998, **49**, 337–369.

75 S. Hammes-Schiffer and A. V. Soudackov, *J. Phys. Chem. B*, 2008, **112**, 14108–14123.

76 D. R. Weinberg, C. J. Gagliardi, J. F. Hull, C. F. Murphy, C. A. Kent, B. C. Westlake, A. Paul, D. H. Ess, D. G. McCafferty and T. J. Meyer, *Chem. Rev.*, 2012, **112**, 4016–4093.

77 N. Berg, S. Bergwinkl, P. Nuernberger, D. Horinek and R. M. Gschwind, *J. Am. Chem. Soc.*, 2021, **143**, 724–735.

78 D. G. Nocera, *J. Am. Chem. Soc.*, 2022, **144**, 1069–1081.

79 S.-I. Lee and D.-J. Jang, *J. Phys. Chem.*, 1995, **99**, 7537–7541.

80 G. Jackson and G. Porter, *Proc. R. Soc. London, Ser. A*, 1997, **260**, 13–30.

81 K. Park, K. J. Shin and H. Kim, *J. Chem. Phys.*, 2009, **131**, 154105.

82 S. Goia, M. A. P. Turner, J. M. Woolley, M. D. Horbury, A. J. Borrill, J. J. Tully, S. J. Cobb, M. Staniforth, N. D. M. Hine, A. Burriss, J. V. Macpherson, B. R. Robinson and V. G. Stavros, *Chem. Sci.*, 2022, **13**, 486–496.

83 X. Pan, T. Han, J. Long, B. Xie, Y. Du, Y. Zhao, X. Zheng and J. Xue, *Phys. Chem. Chem. Phys.*, 2022, **24**, 18427–18434.

84 X. Pan, J. Long, Y. Du, X. Zheng and J. Xue, *Chin. J. Chem. Phys.*, 2023, **36**, 50–56.

85 J. D. Henrich, S. Suchyta and B. Kohler, *J. Phys. Chem. B*, 2015, **119**, 2737–2748.

86 E. G. Hohenstein, *J. Am. Chem. Soc.*, 2016, **138**, 1868–1876.

87 N. Iibuchi, T. Eto, M. Aoyagi, R. Kurinami, H. Sakai, T. Hasobe, D. Takahashi and K. Toshima, *Org. Biomol. Chem.*, 2020, **18**, 851–855.

88 S. J. Formosinho and L. G. Arnaut, *J. Photochem. Photobiol., A*, 1993, **75**, 21–48.

89 V. I. Tomin, A. P. Demchenko and P.-T. Chou, *J. Photochem. Photobiol., C*, 2015, **22**, 1–18.

90 R. K. Venkatraman and A. J. Orr-Ewing, *Acc. Chem. Res.*, 2021, **54**, 4383–4394.

91 E. Vander Donckt, *Progress in Reaction Kinetics*, Pergamon Press, Oxford, 1st edn, 1970, ch. 5, vol. 5, pp. 273–299.

92 S. G. Schulman, *Modern Fluorescence Spectroscopy*, Plenum Pres, New York, 1st edn, 1976, ch. 6, vol. 2, pp. 239–275.

93 I. Y. Martynov, A. B. Demyashkevich, B. M. Uzhinov and M. G. Kuz'min, *Russ. Chem. Rev.*, 1977, **46**, 1.

94 H. Shizuka, *Acc. Chem. Res.*, 1985, **18**, 141–147.

95 E. M. Kosower and D. Huppert, *Annu. Rev. Phys. Chem.*, 1986, **37**, 127–156.

96 E. Pines and D. Pines, *Ultrafast Hydrogen Bonding Dynamics and Proton Transfer Prosesses in the Condensed Phase*, Springer Netherlands, Dordrecht, 2002, pp. 155–184.

97 L. M. Tolbert and K. M. Solntsev, *Acc. Chem. Res.*, 2002, **35**, 19–27.

98 E. Pines, *Patai's Chemistry of Functional Groups*, John Wiley & Sons, Ltd, 2009.

99 K. Weber, *Z. Phys. Chem.*, 1932, **15B**, 18–44.

100 A. Terenin and A. Kariakin, *Nature*, 1947, **159**, 881–882.

101 S. Petersen, *Angew. Chem.*, 1949, **61**, 17–19.

102 T. Förster, *Naturwissenschaften*, 1949, **36**, 186–187.

103 T. Förster, *Z. Elektrochem. Angew. Phys. Chem.*, 1950, **54**, 42–46.

104 T. Förster, *Z. Elektrochem. Angew. Phys. Chem.*, 1950, **54**, 531–535.

105 Z. R. Grabowski and A. Grabowska, *Z. Phys. Chem.*, 1976, **101**, 197–208.

106 W. H. Mulder, *J. Photochem. Photobiol., A*, 2003, **161**, 21–25.

107 A. Weller and Z. Elektrochem, *Ber. Bunsenges. Phys. Chem.*, 1952, **56**, 662–668.

108 A. Weller and Z. Elektrochem, *Ber. Bunsenges. Phys. Chem.*, 1954, **58**, 849–853.

109 A. Weller, *Z. Phys. Chem.*, 1958, **17**, 224–245.

110 S. G. Schulman, L. S. Rosenberg and W. R. Vincent, *J. Am. Chem. Soc.*, 1979, **101**, 139–142.

111 C. M. Harris and B. K. Selinger, *J. Phys. Chem.*, 1980, **84**, 1366–1371.

112 K. Tsutsumi and H. Shizuka, *Z. Phys. Chem.*, 1980, **122**, 129–142.

113 S. P. Webb, L. A. Philips, S. W. Yeh, L. M. Tolbert and J. H. Clark, *J. Phys. Chem.*, 1986, **90**, 5154–5164.

114 T. Nakagawa, S. Kohtani and M. Itoh, *J. Am. Chem. Soc.*, 1995, **117**, 7952–7957.

115 E. Bardez, I. Devol, B. Larrey and B. Valeur, *J. Phys. Chem. B*, 1997, **101**, 7786–7793.

116 T. G. Kim and M. R. Topp, *J. Phys. Chem. A*, 2004, **108**, 10060–10065.

117 M. Ekimova, F. Hoffmann, G. Bekçioğlu-Neff, A. Rafferty, O. Kornilov, E. T. J. Nibbering and D. Sebastiani, *J. Am. Chem. Soc.*, 2019, **141**, 14581–14592.

118 D. W. Fink and W. R. Koehler, *Anal. Chem.*, 1970, **42**, 990–993.

119 G. J. Yakatan, R. J. Juneau and S. G. Schulman, *Anal. Chem.*, 1972, **44**, 1044–1046.

120 S. G. Schulman and L. S. Rosenberg, *J. Phys. Chem.*, 1979, **83**, 447–451.

121 R. Simkovitch and D. Huppert, *J. Phys. Chem. B*, 2015, **119**, 14683–14696.

122 J. Sérgio Seixas de Melo and A. L. Maçanita, *J. Phys. Chem. B*, 2015, **119**, 2604–2610.

123 R. Simkovitch, L. Pinto da Silva, J. C. G. Esteves da Silva and D. Huppert, *J. Phys. Chem. B*, 2016, **120**, 10297–10310.

124 R. Simkovitch and D. Huppert, *J. Phys. Chem. B*, 2017, **121**, 129–142.

125 J. F. Joung, S. Kim and S. Park, *J. Phys. Chem. B*, 2015, **119**, 15509–15515.

126 J. F. Joung, S. Kim and S. Park, *Phys. Chem. Chem. Phys.*, 2017, **19**, 25509–25517.

127 J. F. Joung, S. Kim and S. Park, *J. Phys. Chem. B*, 2018, **122**, 5087–5093.

128 B. H. Milosavljevic and J. K. Thomas, *Photochem. Photobiol. Sci.*, 2002, **1**, 100–104.

129 E. Pines, D. Pines, Y.-Z. Ma and G. R. Fleming, *ChemPhysChem*, 2004, **5**, 1315–1327.

130 M. Lukeman, M.-D. Burns and P. Wan, *Can. J. Chem.*, 2011, **89**, 433–440.

131 J. Christian Lennox, E. O. Danilov and J. L. Dempsey, *Phys. Chem. Chem. Phys.*, 2019, **21**, 16353–16358.

132 S. Shiobara, S. Tajima and S. Tobita, *Chem. Phys. Lett.*, 2003, **380**, 673–680.

133 J. Oshima, S. Shiobara, H. Naoumi, S. Kaneko, T. Yoshihara, A. K. Mishra and S. Tobita, *J. Phys. Chem. A*, 2006, **110**, 4629–4637.

134 J. Oshima, T. Yoshihara and S. Tobita, *Chem. Phys. Lett.*, 2006, **423**, 306–311.

135 K. Tsutsumi and H. Shizuka, *Chem. Phys. Lett.*, 1977, **52**, 485–488.

136 A. A. El-Rayyes, H. P. Perzanowski, S. A. I. Barri and U. K. A. Klein, *J. Phys. Chem. A*, 2001, **105**, 10169–10175.

137 A.-R. Al-Betar, A. El-Rayyes and U. K. A. Klein, *J. Fluoresc.*, 2005, **15**, 689–696.

138 H. Shizuka, K. Tsutsumi, H. Takeuchi and I. Tanaka, *Chem. Phys.*, 1981, **59**, 183–190.

139 E. Pines and G. R. Fleming, *J. Phys. Chem.*, 1991, **95**, 10448–10457.

140 D. B. Spry and M. D. Fayer, *J. Chem. Phys.*, 2008, **128**, 084508.

141 P. Daublain, A. K. Thazhathveetil, Q. Wang, A. Trifonov, T. Fiebig and F. D. Lewis, *J. Am. Chem. Soc.*, 2009, **131**, 16790–16797.

142 C.-H. Ho, B. R. Clark, M. R. Guerin, B. D. Barkenbus, T. K. Rao and J. L. Epler, *Mutat. Res., Environ. Mutagen. Relat. Subj.*, 1981, **85**, 335–345.

143 N. Acar and Ö. Koçak, *Turkish J. Chem.*, 2002, **26**, 201–211.

144 H. Örücü and N. Acar, *J. Mol. Struct.*, 2018, **1174**, 43–51.

145 E. L. Wehry and L. B. Rogers, *J. Am. Chem. Soc.*, 1965, **87**, 4234–4238.

146 I. Avigal, J. Feitelson and M. Ottolenghi, *J. Chem. Phys.*, 1969, **50**, 2614–2617.

147 S. G. Schulman, W. R. Vincent and W. J. M. Underberg, *J. Phys. Chem.*, 1981, **85**, 4068–4071.

148 J. Steadman and J. A. Syage, *J. Chem. Phys.*, 1990, **92**, 4630–4632.

149 J. A. Syage and J. Steadman, *J. Chem. Phys.*, 1991, **95**, 2497–2510.

150 R. F. Salikov, A. Y. Belyy, K. P. Trainov, J. A. Velmiskina, M. G. Medvedev, V. M. Korshunov, I. V. Taydakov, D. N. Platonov and Y. V. Tomilov, *J. Photochem. Photobiol., A*, 2022, **427**, 113808.

151 J. Yguerabide, E. Talavera, J. M. Alvarez and B. Quintero, *Photochem. Photobiol.*, 1994, **60**, 435–441.

152 A. Orte, E. M. Talavera, A. L. Maçanita, J. C. Orte and J. M. Alvarez-Pez, *J. Phys. Chem. A*, 2005, **109**, 8705–8718.

153 D. Surzhikova, M. Gerasimova, V. Tretyakova, A. Plotnikov and E. Slyusareva, *J. Photochem. Photobiol., A*, 2021, **413**, 113233.

154 H. Ihmels and K. Schäfer, *Photochem. Photobiol. Sci.*, 2009, **8**, 309–311.

155 K. Schäfer, H. Ihmels, C. Bohne, K. P. Valente and A. Granzhan, *J. Org. Chem.*, 2016, **81**, 10942–10954.

156 M. Zahid, G. Grampp, A. Mansha, I. A. Bhatti and S. Asim, *J. Fluoresc.*, 2013, **23**, 829–837.

157 Y. Luo, C. Wang, P. Peng, M. Hossain, T. Jiang, W. Fu, Y. Liao and M. Su, *J. Mater. Chem. B*, 2013, **1**, 997–1001.

158 T. Halbritter, C. Kaiser, J. Wachtveitl and A. Heckel, *J. Org. Chem.*, 2017, **82**, 8040–8047.

159 C. Kaiser, T. Halbritter, A. Heckel and J. Wachtveitl, *Chem.–A Eur. J.*, 2021, **27**, 9160–9173.

160 C. R. Aldaz, T. E. Wiley, N. A. Miller, N. Abeyrathna, Y. Liao, P. M. Zimmerman and R. J. Sension, *J. Phys. Chem. B*, 2021, **125**, 4120–4131.

161 V. J. Périllat, C. Berton and C. Pezzato, *Mater. Today Chem.*, 2022, **25**, 100918.

162 C. Berton and C. Pezzato, *Eur. J. Org Chem.*, 2023, **26**, e202300070.

163 A. Zika, M. Agarwal, W. Zika, D. M. Guldi, R. Schweins and F. Gröhn, *Nanoscale*, 2024, **16**, 923–940.

164 V. L. Shapovalov, A. B. Demyashkevich and M. G. Kuz'min, *J. Appl. Spectrosc.*, 1980, **33**, 1362–1366.

165 B. Zelent, J. M. Vanderkooi, R. G. Coleman, I. Gryczynski and Z. Gryczynski, *Biophys. J.*, 2006, **91**, 3864–3871.

166 N. V. Nucci, B. Zelent and J. M. Vanderkooi, *J. Fluoresc.*, 2008, **18**, 41–49.

167 B. Zelent, J. M. Vanderkooi, N. V. Nucci, I. Gryczynski and Z. Gryczynski, *J. Fluoresc.*, 2009, **19**, 21–31.

168 E. W. Driscoll, J. R. Hunt and J. M. Dawlaty, *J. Phys. Chem. Lett.*, 2016, **7**, 2093–2099.

169 E. W. Driscoll, J. R. Hunt and J. M. Dawlaty, *J. Phys. Chem. A*, 2017, **121**, 7099–7107.

170 J. R. Hunt and J. M. Dawlaty, *J. Phys. Chem. A*, 2018, **122**, 7931–7940.

171 W. Sheng, M. Nairat, P. D. Pawlaczyk, E. Mroczka, B. Farris, E. Pines, J. H. Geiger, B. Borhan and M. Dantus, *Angew. Chem., Int. Ed.*, 2018, **57**, 14742–14746.

172 J. Lahiri, M. Moemeni, J. Kline, B. Borhan, I. Magoulas, S. H. Yuwono, P. Piecuch, J. E. Jackson, M. Dantus and G. J. Blanchard, *J. Phys. Chem. B*, 2019, **123**, 8448–8456.

173 S. Roy, S. Ardo and F. Furche, *J. Phys. Chem. A*, 2019, **123**, 6645–6651.

174 J. F. Joung, J. Lee, J. Hwang, K. Choi and S. Park, *New J. Chem.*, 2020, **44**, 668–673.

175 M. Sittig, J. C. Tom, J. K. Elter, F. H. Schacher and B. Dietzek, *Chem.–A Eur. J.*, 2021, **27**, 1072–1079.

176 M. J. Voegtle and J. M. Dawlaty, *J. Am. Chem. Soc.*, 2022, **144**, 8178–8184.

177 R. Mathew, P. Verma, A. Barak and Y. Adithya Lakshmanna, *J. Phys. Chem. A*, 2023, **127**, 7419–7428.

178 B. Antalicz, J. Versluis and H. J. Bakker, *J. Am. Chem. Soc.*, 2023, **145**, 6682–6690.

179 J. R. Hunt, J. Hecht, C. Goolsby, J. Hagihara, M. Loza and S. del Pozo, *J. Phys. Chem. A*, 2024, **128**(30), 6199–6207.

180 S. F. Alamudun, K. Tanovitz, A. Fajardo, K. Johnson, A. Pham, T. Jamshidi Araghi and A. S. Petit, *J. Phys. Chem. A*, 2020, **124**, 2537–2546.

181 S. F. Alamudun, K. Tanovitz, L. Espinosa, A. Fajardo, J. Galvan and A. S. Petit, *J. Phys. Chem. A*, 2021, **125**, 13–24.

182 J. Ditkovich, T. Mukra, D. Pines, D. Huppert and E. Pines, *J. Phys. Chem. B*, 2015, **119**, 2690–2701.

183 J. Ditkovich, D. Pines and E. Pines, *Phys. Chem. Chem. Phys.*, 2016, **18**, 16106–16115.

184 B. Finkler, I. Riemann, M. Vester, A. Grüter, F. Stracke and G. Jung, *Photochem. Photobiol. Sci.*, 2016, **15**, 1544–1557.

185 R. Hilal and S. G. Aziz, *Mol. Simul.*, 2019, **45**, 165–177.

186 T. Stoerkler, T. Pariat, A. D. Laurent, D. Jacquemin, G. Ulrich and J. Massue, *Molecules*, 2022, **27**, 2443.

187 K. U. Jagushte, N. Sadhukhan, H. P. Upadhyaya and S. Dutta Choudhury, *J. Phys. Chem. B*, 2023, **127**, 9788–9801.

188 Q.-S. Li, W.-H. Fang and J.-G. Yu, *J. Phys. Chem. A*, 2005, **109**, 3983–3990.

189 W. Qin, A. Vozza and A. M. Brouwer, *J. Phys. Chem. C*, 2009, **113**, 11790–11795.

190 Y. Wang, H. Yin, Y. Shi, M. Jin and D. Ding, *New J. Chem.*, 2014, **38**, 4458–4464.

191 Y. Cui, H. Zhao, J. Zhao, P. Li, P. Song and L. Xia, *New J. Chem.*, 2015, **39**, 9910–9917.

192 G. Bekçioğlu, C. Allolio, M. Ekimova, E. T. J. Nibbering and D. Sebastiani, *Phys. Chem. Chem. Phys.*, 2014, **16**, 13047–13051.

193 G. Bekçioğlu, C. Allolio and D. Sebastiani, *J. Phys. Chem. B*, 2015, **119**, 4053–4060.

194 Y.-J. Kim and O.-H. Kwon, *Phys. Chem. Chem. Phys.*, 2016, **18**, 32826–32839.

195 Y.-H. Liu, S.-M. Wang, C. Zhu and S. H. Lin, *New J. Chem.*, 2017, **41**, 8437–8442.

196 O.-H. Kwon, Y.-S. Lee, B. K. Yoo and D.-J. Jang, *Angew. Chem., Int. Ed.*, 2006, **45**, 415–419.

197 D. Huppert and E. Kolodney, *Chem. Phys.*, 1981, **63**, 401–410.

198 D. Huppert, E. Kolodney, M. Gutman and E. Nachliel, *J. Am. Chem. Soc.*, 1982, **104**, 6949–6953.

199 E. Tietze and O. Bayer, *Adv. Cycloaddit.*, 1939, **540**, 189–210.

200 O. S. Wolfbeis, E. Fürlinger, H. Kroneis and H. Marsoner, *Fresenius Z. Anal. Chem.*, 1983, **314**, 119–124.

201 O. S. Wolfbeis and E. Koller, *Anal. Biochem.*, 1983, **129**, 365–370.

202 Y. Avnir and Y. Barenholz, *Anal. Biochem.*, 2005, **347**, 34–41.

203 R. Nandi and N. Amdursky, *Acc. Chem. Res.*, 2022, **55**, 2728–2739.

204 P. Changenet, T. Gustavsson and I. Lampre, *J. Chem. Educ.*, 2020, **97**, 4482–4489.

205 E. Pines and D. Huppert, *J. Chem. Phys.*, 1986, **84**, 3576–3577.

206 E. Pines and D. Huppert, *Chem. Phys. Lett.*, 1986, **126**, 88–91.

207 N. Agmon, E. Pines and D. Huppert, *J. Chem. Phys.*, 1988, **88**, 5631–5638.

208 N. Agmon, *J. Chem. Phys.*, 1988, **88**, 5639–5642.

209 N. Agmon, *J. Chem. Phys.*, 1988, **89**, 1524–1528.

210 E. Pines, D. Huppert and N. Agmon, *J. Chem. Phys.*, 1988, **88**, 5620–5630.

211 D. Huppert, E. Pines and N. Agmon, *J. Opt. Soc. Am. B*, 1990, **7**, 1545–1550.

212 D. Huppert, S. Y. Goldberg, A. Masad and N. Agmon, *Phys. Rev. Lett.*, 1992, **68**, 3932–3935.

213 C. Prayer, T. Gustavsson and T.-H. Tran-Thi, *AIP Conf. Proc.*, 1996, **364**, 333–339.

214 T. H. Tran-Thi, T. Gustavsson, C. Prayer, S. Pommeret and J. T. Hynes, *Chem. Phys. Lett.*, 2000, **329**, 421–430.

215 J. T. Hynes, T.-H. Tran-Thi and G. Granucci, *J. Photochem. Photobiol., A*, 2002, **154**, 3–11.

216 T.-H. Tran-Thi, C. Prayer, P. Millié, P. Uznanski and J. T. Hynes, *J. Phys. Chem. A*, 2002, **106**, 2244–2255.

217 P. Leiderman, L. Genosar and D. Huppert, *J. Phys. Chem. A*, 2005, **109**, 5965–5977.

218 R. Gepshtein, P. Leiderman, L. Genosar and D. Huppert, *J. Phys. Chem. A*, 2005, **109**, 9674–9684.

219 O. F. Mohammed, D. Pines, J. Dreyer, E. Pines and E. T. J. Nibbering, *Science*, 2005, **310**, 83–86.

220 O. F. Mohammed, J. Dreyer, B.-Z. Magnes, E. Pines and E. T. J. Nibbering, *ChemPhysChem*, 2005, **6**, 625–636.

221 B. J. Siwick and H. J. Bakker, *J. Am. Chem. Soc.*, 2007, **129**, 13412–13420.

222 D. B. Spry, A. Goun, C. B. Bell and M. D. Fayer, *J. Chem. Phys.*, 2006, **125**, 144514.

223 D. B. Spry and M. D. Fayer, *J. Chem. Phys.*, 2007, **127**, 204501.

224 L. N. Silverman, D. B. Spry, S. G. Boxer and M. D. Fayer, *J. Phys. Chem. A*, 2008, **112**, 10244–10249.

225 F. Han, W. Liu and C. Fang, *Chem. Phys.*, 2013, **422**, 204–219.

226 W. Liu, Y. Wang, L. Tang, B. G. Oscar, L. Zhu and C. Fang, *Chem. Sci.*, 2016, **7**, 5484–5494.

227 S. Y. Goldberg, E. Pines and D. Huppert, *Chem. Phys. Lett.*, 1992, **192**, 77–81.

228 E. Pines, B.-Z. Magnes, M. J. Lang and G. R. Fleming, *Chem. Phys. Lett.*, 1997, **281**, 413–420.

229 M. Rini, D. Pines, B.-Z. Magnes, E. Pines and E. T. J. Nibbering, *J. Chem. Phys.*, 2004, **121**, 9593–9610.

230 B. J. Siwick, M. J. Cox and H. J. Bakker, *J. Phys. Chem. B*, 2008, **112**, 378–389.

231 M. J. Cox, R. L. A. Timmer, H. J. Bakker, S. Park and N. Agmon, *J. Phys. Chem. A*, 2009, **113**, 6599–6606.

232 W. Liu, F. Han, C. Smith and C. Fang, *J. Phys. Chem. B*, 2012, **116**, 10535–10550.

233 W. Heo, N. Uddin, J. W. Park, Y. M. Rhee, C. H. Choi and T. Joo, *Phys. Chem. Chem. Phys.*, 2017, **19**, 18243–18251.

234 O. F. Mohammed, D. Pines, E. T. J. Nibbering and E. Pines, *Angew. Chem.*, 2007, **119**, 1480–1483.

235 O. F. Mohammed, D. Pines, E. Pines and E. T. J. Nibbering, *Chem. Phys.*, 2007, **341**, 240–257.

236 M. J. Cox and H. J. Bakker, *J. Chem. Phys.*, 2008, **128**, 174501.

237 N. Agmon, D. Huppert, A. Masad and E. Pines, *J. Phys. Chem.*, 1991, **95**, 10407–10413.

238 P. Leiderman, R. Gepshtein, A. Uritski, L. Genosar and D. Huppert, *J. Phys. Chem. A*, 2006, **110**, 5573–5584.

239 B. G. Oscar, W. Liu, N. D. Rozanov and C. Fang, *Phys. Chem. Chem. Phys.*, 2016, **18**, 26151–26160.

240 N. Nandi and K. Sahu, *J. Photochem. Photobiol., A*, 2019, **374**, 138–144.

241 S. G. Schulman, R. N. Kelly and N. J. Gonzalez, *Pure Appl. Chem.*, 1987, **59**, 655–662.

242 E. Pines and D. Huppert, *J. Am. Chem. Soc.*, 1989, **111**, 4096–4097.

243 E. Pines, D. Huppert and N. Agmon, *J. Phys. Chem.*, 1991, **95**, 666–674.

244 N. Agmon, S. Y. Goldberg and D. Huppert, *J. Mol. Liq.*, 1995, **64**, 161–195.

245 M. J. Cox, B. J. Siwick and H. J. Bakker, *ChemPhysChem*, 2009, **10**, 236–244.

246 E. Pines, B. Cohen and D. Huppert, *Isr. J. Chem.*, 1999, **39**, 347–360.

247 P. Leiderman, R. Gepshtein, A. Uritski, L. Genosar and D. Huppert, *J. Phys. Chem. A*, 2006, **110**, 9039–9050.

248 D. H. Huppert, A. Jayaraman, R. G. Maines, D. W. Steyert and P. M. Rentzepis, *J. Chem. Phys.*, 1984, **81**, 5596–5600.

249 E. Pines and D. Huppert, *Chem. Phys. Lett.*, 1985, **116**, 295–301.

250 A. Uritski, P. Leiderman and D. Huppert, *J. Phys. Chem. A*, 2006, **110**, 13686–13695.

251 A. Uritski, P. Leiderman and D. Huppert, *J. Phys. Chem. C*, 2007, **111**, 8856–8865.

252 P. Leiderman, A. Uritski and D. Huppert, *J. Phys. Chem. A*, 2007, **111**, 4998–5007.

253 A. Uritski and D. Huppert, *J. Phys. Chem. A*, 2008, **112**, 4415–4425.

254 A. Uritski, I. Presiado, Y. Erez, R. Gepshtein and D. Huppert, *J. Phys. Chem. C*, 2009, **113**, 17915–17926.

255 R. L. A. Timmer, M. J. Cox and H. J. Bakker, *J. Phys. Chem. A*, 2010, **114**, 2091–2101.

256 K. J. Tielrooij, M. J. Cox and H. J. Bakker, *ChemPhysChem*, 2009, **10**, 245–251.

257 T. Mondal, A. K. Das, D. K. Sasmal and K. Bhattacharyya, *J. Phys. Chem. B*, 2010, **114**, 13136–13142.

258 A. K. Mandal, S. Ghosh, A. K. Das, T. Mondal and K. Bhattacharyya, *ChemPhysChem*, 2013, **14**, 788–796.

259 C. Lawler and M. D. Fayer, *J. Phys. Chem. B*, 2015, **119**, 6024–6034.

260 D. B. Spry, A. Goun, K. Glusac, D. E. Moilanen and M. D. Fayer, *J. Am. Chem. Soc.*, 2007, **129**, 8122–8130.

261 G. Ghosh, R. Ghosh, D. Mukherjee, M. N. Hasan, N. Pan, L. Roy, S. Biswas, R. Das and S. Kumar Pal, *J. Mol. Liq.*, 2024, **407**, 125181.

262 G. Ghosh, D. S. Roy, R. Ghosh, D. Mukherjee, S. Biswas, L. Roy, A. Chattopadhyay, R. Das and S. K. Pal, *ChemPhysChem*, 2024, **25**, e202300635.

263 T. Jang, S. Lee and Y. Pang, *Phys. Chem. Chem. Phys.*, 2024, **26**, 11283–11294.

264 D. B. Spry and M. D. Fayer, *J. Phys. Chem. B*, 2009, **113**, 10210–10221.

265 J. E. Thomaz, C. M. Lawler and M. D. Fayer, *J. Phys. Chem. B*, 2017, **121**, 4544–4553.

266 S. K. Mondal, K. Sahu, P. Sen, D. Roy, S. Ghosh and K. Bhattacharyya, *Chem. Phys. Lett.*, 2005, **412**, 228–234.

267 S. K. Mondal, K. Sahu, S. Ghosh, P. Sen and K. Bhattacharyya, *J. Phys. Chem. A*, 2006, **110**, 13646–13652.

268 R. Gepshtein, P. Leiderman, D. Huppert, E. Project, E. Nachliel and M. Gutman, *J. Phys. Chem. B*, 2006, **110**, 26354–26364.

269 S. Ghosh, S. Dey, U. Mandal, A. Adhikari, S. K. Mondal and K. Bhattacharyya, *J. Phys. Chem. B*, 2007, **111**, 13504–13510.

270 N. Amdursky, R. Simkovitch and D. Huppert, *J. Phys. Chem. B*, 2014, **118**, 13859–13869.

271 R. Chowdhury, A. Saha, A. K. Mandal, B. Jana, S. Ghosh and K. Bhattacharyya, *J. Phys. Chem. B*, 2015, **119**, 2149–2156.

272 R. Simkovitch and D. Huppert, *J. Phys. Chem. A*, 2015, **119**, 641–651.

273 R. Simkovitch and D. Huppert, *J. Phys. Chem. B*, 2015, **119**, 11684–11694.

274 R. Simkovitch and D. Huppert, *J. Phys. Chem. B*, 2015, **119**, 9795–9804.

275 H. Peretz-Soroka, A. Pevzner, G. Davidi, V. Naddaka, M. Kwiat, D. Huppert and F. Patolsky, *Nano Lett.*, 2015, **15**, 4758–4768.

276 N. Amdursky, R. Orbach, E. Gazit and D. Huppert, *J. Phys. Chem. C*, 2009, **113**, 19500–19505.

277 R. Simkovitch, O. Gajst, E. Zelinger, O. Yarden and D. Huppert, *J. Photochem. Photobiol., B*, 2017, **174**, 1–9.

278 S. Chakraborty, S. Nandi, K. Bhattacharyya and S. Mukherjee, *ChemPhysChem*, 2019, **20**, 3221–3227.

279 I. Das, S. Panja and M. Halder, *J. Phys. Chem. B*, 2016, **120**, 7076–7087.

280 S. S. Mojumdar, R. Chowdhury, A. K. Mandal and K. Bhattacharyya, *J. Chem. Phys.*, 2013, **138**, 215102.

281 M. A. Amin, S. Nandi, P. Mondal, T. Mahata, S. Ghosh and K. Bhattacharyya, *Phys. Chem. Chem. Phys.*, 2017, **19**, 12620–12627.

282 S. Nandi, S. Ghosh and K. Bhattacharyya, *J. Phys. Chem. B*, 2018, **122**, 3023–3036.

283 S. K. Mondal, S. Ghosh, K. Sahu, P. Sen and K. Bhattacharyya, *J. Chem. Sci.*, 2007, **119**, 71–76.

284 S. Sen Mojumdar, T. Mondal, A. K. Das, S. Dey and K. Bhattacharyya, *J. Chem. Phys.*, 2010, **132**, 194505.

285 S. Maiti, S. Mitra, C. A. Johnson, K. C. Gronborg, S. Garrett-Roe and P. M. Donaldson, *J. Phys. Chem. Lett.*, 2022, **13**, 8104–8110.

286 R. Knochenmuss, K. M. Solntsev and L. M. Tolbert, *J. Phys. Chem. A*, 2001, **105**, 6393–6401.

287 R. Knochenmuss and I. Fischer, *Int. J. Mass Spectrom.*, 2002, **220**, 343–357.

288 A. J. Fleisher, P. J. Morgan and D. W. Pratt, *J. Chem. Phys.*, 2009, **131**, 211101.

289 A. Melnichuk and R. J. Bartlett, *J. Chem. Phys.*, 2011, **134**, 244303.

290 J. Yang, X.-P. Xing, X.-B. Wang, L.-S. Wang, A. P. Sergeeva and A. I. Boldyrev, *J. Chem. Phys.*, 2008, **128**, 091102.

291 J. E. Whitaker, R. P. Haugland and F. G. Prendergast, *Anal. Biochem.*, 1991, **194**, 330–344.

292 J. Widengren, B. Terry and R. Rigler, *Chem. Phys.*, 1999, **249**, 259–271.

293 F. H. C. Wong and C. Fradin, *J. Fluoresc.*, 2011, **21**, 299–312.

294 N. Sülzner, B. Geissler, A. Grandjean, G. Jung and P. Nuernberger, *ChemPhotoChem*, 2022, **6**, e202200041.

295 N. Barrash-Shiftan, B. B. Brauer and E. Pines, *J. Phys. Org. Chem.*, 1998, **11**, 743–750.

296 G. Jung, S. Gerharz and A. Schmitt, *Phys. Chem. Chem. Phys.*, 2009, **11**, 1416.

297 T. Förster and S. Völker, *Chem. Phys. Lett.*, 1975, **34**, 1–6.

298 K. Lundy-Douglas and Z. A. Schelly, *Adv. Mol. Relax. Processes*, 1976, **8**, 79–86.

299 M. Gutman, D. Huppert and E. Pines, *J. Am. Chem. Soc.*, 1981, **103**, 3709–3713.

300 E. Pines and D. Huppert, *J. Phys. Chem.*, 1983, **87**, 4471–4478.

301 K. K. Smith, K. J. Kaufmann, D. Huppert and M. Gutman, *Chem. Phys. Lett.*, 1979, **64**, 522–527.

302 G. Granucci, J. T. Hynes, P. Millié and T.-H. Tran-Thi, *J. Am. Chem. Soc.*, 2000, **122**, 12243–12253.

303 J. Shin, C. H. Lim and M. Lim, *Photochem. Photobiol. Sci.*, 2022, **21**, 1419–1431.

304 Y. Wang, W. Liu, L. Tang, B. Oscar, F. Han and C. Fang, *J. Phys. Chem. A*, 2013, **117**, 6024–6042.

305 W. Liu, L. Tang, B. G. Oscar, Y. Wang, C. Chen and C. Fang, *J. Phys. Chem. Lett.*, 2017, **8**, 997–1003.

306 B. G. Oscar, C. Chen, W. Liu, L. Zhu and C. Fang, *J. Phys. Chem. A*, 2017, **121**, 5428–5441.

307 L. Tang, Y. Wang, L. Zhu, C. Lee and C. Fang, *J. Phys. Chem. Lett.*, 2018, **9**, 2311–2319.

308 L. Tang, L. Zhu, Y. Wang and C. Fang, *J. Phys. Chem. Lett.*, 2018, **9**, 4969–4975.

309 D. B. Spry, A. Goun and M. D. Fayer, *J. Phys. Chem. A*, 2007, **111**, 230–237.

310 R. Jimenez, D. A. Case and F. E. Romesberg, *J. Phys. Chem. B*, 2002, **106**, 1090–1103.

311 S. Eckert, M.-O. Winghart, C. Kleine, A. Banerjee, M. Ekimova, J. Ludwig, J. Harich, M. Fondell, R. Mitzner, E. Pines, N. Huse, P. Wernet, M. Odelius and E. T. J. Nibbering, *Angew. Chem., Int. Ed.*, 2022, **61**, e202200709.

312 M. Sedgwick, R. L. Cole, C. D. Rithner, D. C. Crans and N. E. Levinger, *J. Am. Chem. Soc.*, 2012, **134**, 11904–11907.

313 G. Ferrino, M. De Rosa, P. Della Sala, C. Gaeta, C. Talotta, A. Soriente, Z. Cao, B. Maity, L. Cavallo and P. Neri, *Chem.–A Eur. J.*, 2024, **30**, e202303678.

314 T. Ockelmann, C. Hoberg, A. Buchmann, F. Novelli and M. Havenith, *J. Phys. Chem. B*, 2023, **127**, 9560–9565.

315 N. Agmon, W. Rettig and C. Groth, *J. Am. Chem. Soc.*, 2002, **124**, 1089–1096.

316 W.-H. Fang, *J. Am. Chem. Soc.*, 1998, **120**, 7568–7576.

317 W.-H. Fang, *J. Phys. Chem. A*, 1999, **103**, 5567–5573.

318 Q.-S. Li and W.-H. Fang, *Chem. Phys. Lett.*, 2003, **367**, 637–644.

319 B.-b. Xie, C.-x. Li, G.-l. Cui and Q. Fang, *Chin. J. Chem. Phys.*, 2016, **29**, 38–46.

320 X.-F. Tang, P.-K. Jia, Y. Zhao, J. Xue, G. Cui and B.-B. Xie, *Phys. Chem. Chem. Phys.*, 2022, **24**, 20517–20529.

321 P. Cimino, U. Raucci, G. Donati, M. G. Chiariello, M. Schiazza, F. Coppola and N. Rega, *Theor. Chem. Acc.*, 2016, **135**, 117.

322 E. L. Graef and J. B. L. Martins, *J. Mol. Model.*, 2019, **25**, 183.

323 A. Kyrychenko and J. Waluk, *J. Phys. Chem. A*, 2006, **110**, 11958–11967.

324 H. Wang, X. Wang, X. Li and C. Zhang, *J. Mol. Struct.:THEOCHEM*, 2006, **770**, 107–110.

325 M. Savarese, P. A. Netti, C. Adamo, N. Rega and I. Ciofini, *J. Phys. Chem. B*, 2013, **117**, 16165–16173.

326 M. Savarese, P. A. Netti, N. Rega, C. Adamo and I. Ciofini, *Phys. Chem. Chem. Phys.*, 2014, **16**, 8661–8666.

327 A. D. Laurent, Y. Houari, P. H. P. R. Carvalho, B. A. D. Neto and D. Jacquemin, *RSC Adv.*, 2014, **4**, 14189–14192.

328 Y. Houari, S. Chibani, D. Jacquemin and A. D. Laurent, *J. Phys. Chem. B*, 2015, **119**, 2180–2192.

329 U. Raucci, M. Savarese, C. Adamo, I. Ciofini and N. Rega, *J. Phys. Chem. B*, 2015, **119**, 2650–2657.

330 J. Zhao, H. Yao, J. Liu and M. R. Hoffmann, *J. Phys. Chem. A*, 2015, **119**, 681–688.

331 Z. Qu, P. Li, X. Zhang, E. Wang, Y. Wang and P. Zhou, *J. Lumin.*, 2016, **177**, 197–203.

332 M. Savarese, U. Raucci, R. Fukuda, C. Adamo, M. Ehara, N. Rega and I. Ciofini, *J. Comput. Chem.*, 2017, **38**, 1084–1092.

333 D. Yang, J. Zhao, M. Jia and X. Song, *RSC Adv.*, 2017, **7**, 34034–34040.

334 P. Krishnakumar, R. Kar and D. K. Maity, *J. Phys. Chem. A*, 2018, **122**, 929–936.

335 P. Zhou and K. Han, *Acc. Chem. Res.*, 2018, **51**, 1681–1690.

336 A. A. Freitas, K. Shimizu, L. G. Dias and F. H. Quina, *J. Braz. Chem. Soc.*, 2007, **18**, 1537–1546.

337 F. Siddique, C. P. Silva, G. T. M. Silva, H. Lischka, F. H. Quina and A. J. A. Aquino, *Photochem. Photobiol. Sci.*, 2019, **18**, 45–53.

338 C. P. Silva, G. T. M. Silva, T. d. S. Costa, V. M. T. Carneiro, F. Siddique, A. J. A. Aquino, A. A. Freitas, J. A. Clark, E. M. Espinoza, V. I. Vullev and F. H. Quina, *Pure Appl. Chem.*, 2020, **92**, 255–263.

339 J. He, X. Li, G. T. M. Silva, F. H. Quina and A. J. A. Aquino, *J. Braz. Chem. Soc.*, 2019, **30**, 492–498.

340 G. T. M. Silva, C. P. Silva, K. M. Silva, R. M. Pioli, T. S. Costa, V. V. Marto, A. A. Freitas, J. Rozendo, L. M. O. S. Martins, V. F. Cavalcante, L. Sun, A. J. A. Aquino, V. M. T. Carneiro and F. H. Quina, *Photochem*, 2022, **2**, 423–434.

341 T. Udagawa, I. Hattori, Y. Kanematsu, T. Ishimoto and M. Tachikawa, *Int. J. Quantum Chem.*, 2022, **122**, e26962.

342 D. Jacquemin, E. A. Perpète, I. Ciofini and C. Adamo, *J. Phys. Chem. A*, 2008, **112**, 794–796.

343 T. Le Bahers, C. Adamo and I. Ciofini, *J. Phys. Chem. A*, 2010, **114**, 5932–5939.

344 M. S. Baranov, K. A. Lukyanov, A. O. Borissova, J. Shamir, D. Kosenkov, L. V. Slipchenko, L. M. Tolbert, I. V. Yampolsky and K. M. Solntsev, *J. Am. Chem. Soc.*, 2012, **134**, 6025–6032.

345 É. Brémond, M. E. Alberto, N. Russo, G. Ricci, I. Ciofini and C. Adamo, *Phys. Chem. Chem. Phys.*, 2013, **15**, 10019.

346 Y. Houari, D. Jacquemin and A. D. Laurent, *Phys. Chem. Chem. Phys.*, 2013, **15**, 11875.

347 Y. Houari, D. Jacquemin and A. D. Laurent, *Chem. Phys. Lett.*, 2013, **583**, 218–221.

348 A. Aqdas, F. Siddique, R. Nieman, F. H. Quina and A. J. A. Aquino, *Photochem. Photobiol.*, 2019, **95**, 1339–1344.

349 J. Wang, F. Siddique, A. A. Freitas, C. P. Silva, G. T. M. Silva, F. H. Quina, H. Lischka and A. J. A. Aquino, *Theor. Chem. Acc.*, 2020, **139**, 117.

350 J. Cui, F. Siddique, R. Nieman, G. T. M. Silva, F. H. Quina and A. J. A. Aquino, *Theor. Chem. Acc.*, 2021, **140**, 90.

351 M. G. Chiariello and N. Rega, *J. Phys. Chem. A*, 2018, **122**, 2884–2893.

352 M. G. Chiariello, G. Donati and N. Rega, *J. Chem. Theory Comput.*, 2020, **16**, 6007–6013.

353 M. G. Chiariello, U. Raucci, G. Donati and N. Rega, *J. Phys. Chem. A*, 2021, **125**, 3569–3578.

354 M. G. Chiariello, G. Donati, U. Raucci, F. Perrella and N. Rega, *J. Phys. Chem. B*, 2021, **125**, 10273–10281.

355 U. Raucci, M. G. Chiariello and N. Rega, *J. Chem. Theory Comput.*, 2020, **16**, 7033–7043.

356 A. Petrone, G. Donati, P. Caruso and N. Rega, *J. Am. Chem. Soc.*, 2014, **136**, 14866–14874.

357 J. E. Thomaz, A. R. Walker, S. J. Van Wyck, J. Meisner, T. J. Martinez and M. D. Fayer, *J. Phys. Chem. B*, 2020, **124**, 7897–7908.

358 A. R. Walker, B. Wu, J. Meisner, M. D. Fayer and T. J. Martínez, *J. Phys. Chem. B*, 2021, **125**, 12539–12551.

359 G. W. Robinson, *J. Phys. Chem.*, 1991, **95**, 10386–10391.

360 A. Uritski, I. Presiado and D. Huppert, *J. Phys. Chem. C*, 2008, **112**, 11991–12002.

361 A. Uritski, I. Presiado and D. Huppert, *Isr. J. Chem.*, 2009, **49**, 235–249.

362 I. Sarkar, *New J. Chem.*, 2016, **40**, 6666–6674.

363 M. Prémont-Schwarz, T. Barak, D. Pines, E. T. J. Nibbering and E. Pines, *J. Phys. Chem. B*, 2013, **117**, 4594–4603.

364 A. Masad and D. Huppert, *Chem. Phys. Lett.*, 1991, **180**, 409–415.

365 P. Leiderman, L. Genosar, N. Koifman and D. Huppert, *J. Phys. Chem. A*, 2004, **108**, 2559–2566.

366 L. Genosar, P. Leiderman, N. Koifman and D. Huppert, *J. Phys. Chem. A*, 2004, **108**, 1779–1789.

367 E. Pines, D. Pines, O. Gajst and D. Huppert, *J. Chem. Phys.*, 2020, **152**, 074205.

368 G. R. Han, E. Lim, J. Kang, D. Hwang, J. Heo, S. K. Kim and J. W. Lee, *J. Phys. Chem. A*, 2023, **127**, 7884–7891.

369 K. M. Solntsev, E.-A. Bartolo, G. Pan, G. Muller, S. Bommireddy, D. Huppert and L. M. Tolbert, *Isr. J. Chem.*, 2009, **49**, 227–233.

370 M. Sambol, K. Ester, S. Landgraf, B. Mihaljević, M. Cindrić, M. Kralj and N. Basarić, *Photochem. Photobiol. Sci.*, 2019, **18**, 1197–1211.

371 L. Lorenz, J. Plötner, V. V. Matylitsky, A. Dreuw and J. Wachtveitl, *J. Phys. Chem. A*, 2007, **111**, 10891–10898.

372 S. Suzuki and H. Baba, *Bull. Chem. Soc. Jpn.*, 1967, **40**, 2199–2200.

373 I. Y. Martynov, N. K. Zaitsev, I. V. Soboleva, B. M. Uzhinov and M. G. Kuz'min, *J. Appl. Spectrosc.*, 1978, **28**, 732–736.

374 A. B. Demjaschkewitch, N. K. Zaitsev and M. G. Kuzmin, *Chem. Phys. Lett.*, 1978, **55**, 80–83.

375 H. Lemmetyinen, A. B. Demyashkevich and M. G. Kuzmin, *Chem. Phys. Lett.*, 1980, **73**, 98–101.

376 M. Gutman and D. Huppert, *J. Biochem. Biophys. Methods*, 1979, **1**, 9–19.

377 S. Tobita and H. Shizuka, *Chem. Phys. Lett.*, 1980, **75**, 140–144.

378 H. Shizuka and S. Tobita, *J. Am. Chem. Soc.*, 1982, **104**, 6919–6927.

379 H. Shizuka and K. Tsutsumi, *Bull. Chem. Soc. Jpn.*, 1983, **56**, 629–630.

380 J. Lee, G. W. Robinson, S. P. Webb, L. A. Philips and J. H. Clark, *J. Am. Chem. Soc.*, 1986, **108**, 6538–6542.

381 G. W. Robinson, P. J. Thistlethwaite and J. Lee, *J. Phys. Chem.*, 1986, **90**, 4224–4233.

382 G. W. Robinson, J. Lee and M.-P. Bassez, *J. Chem. Soc., Faraday Trans. 2*, 1986, **82**, 2351–2359.

383 O. Cheshnovsky and S. Leutwyler, *J. Chem. Phys.*, 1988, **88**, 4127–4138.

384 J. J. Breen, L. W. Peng, D. M. Willberg, A. Heikal, P. Cong and A. H. Zewail, *J. Chem. Phys.*, 1990, **92**, 805–807.

385 T. C. Swinney and D. F. Kelley, *J. Phys. Chem.*, 1991, **95**, 2430–2434.

386 S. K. Kim, J.-K. Wang and A. H. Zewail, *Chem. Phys. Lett.*, 1994, **228**, 369–378.

387 S. K. Kim, J. J. Breen, D. M. Willberg, L. W. Peng, A. Heikal, J. A. Syage and A. H. Zewail, *J. Phys. Chem.*, 1995, **99**, 7421–7435.

388 Y. Matsumoto, T. Ebata and N. Mikami, *J. Chem. Phys.*, 1998, **109**, 6303–6311.

389 R. Knochenmuss, O. Cheshnovsky and S. Leutwyler, *Chem. Phys. Lett.*, 1988, **144**, 317–323.

390 R. Knochenmuss and S. Leutwyler, *J. Chem. Phys.*, 1989, **91**, 1268–1278.

391 R. Knochenmuss, G. R. Holtom and D. Ray, *Chem. Phys. Lett.*, 1993, **215**, 188–192.

392 R. D. Knochenmuss and D. E. Smith, *J. Chem. Phys.*, 1994, **101**, 7327–7336.

393 R. Knochenmuss, *Chem. Phys. Lett.*, 1998, **293**, 191–196.

394 R. Knochenmuss, *Chem. Phys. Lett.*, 1999, **311**, 439–445.

395 R. Knochenmuss, I. Fischer, D. Lührs and Q. Lin, *Isr. J. Chem.*, 1999, **39**, 221–230.

396 R. Knochenmuss, P. L. Muiño and C. Wickleder, *J. Phys. Chem.*, 1996, **100**, 11218–11227.

397 E. Pines and G. R. Fleming, *Chem. Phys.*, 1994, **183**, 393–402.

398 B.-Z. Magnes, D. Pines, N. Strashnikova and E. Pines, *Solid State Ionics*, 2004, **168**, 225–233.

399 E. Pines, D. Tepper, B.-Z. Magnes, D. Pines and T. Barak, *Ber. Bunsenges. Phys. Chem.*, 1998, **102**, 504–510.

400 E. Pines, D. Pines, T. Barak, B.-Z. Magnes, L. M. Tolbert and J. E. Haubrich, *Ber. Bunsenges. Phys. Chem.*, 1998, **102**, 511–517.

401 E. Pines, B.-Z. Magnes and T. Barak, *J. Phys. Chem. A*, 2001, **105**, 9674–9680.

402 D. Pines, D. Eliovich, D. Aminov, M. Sigalov, D. Huppert and E. Pines, *Spectroscopy and Computation of Hydrogen-Bonded Systems*, John Wiley & Sons, Ltd, 2023, pp. 261–292.

403 I. V. Gopich and N. Agmon, *J. Chem. Phys.*, 1999, **110**, 10433–10444.

404 K. M. Solntsev and N. Agmon, *Chem. Phys. Lett.*, 2000, **320**, 262–268.

405 K. M. Solntsev, D. Huppert and N. Agmon, *J. Phys. Chem. A*, 1998, **102**, 9599–9606.

406 K. M. Solntsev, D. Huppert, L. M. Tolbert and N. Agmon, *J. Am. Chem. Soc.*, 1998, **120**, 7981–7982.

407 I. Carmeli, D. Huppert, L. Tolbert and J. Haubrich, *Chem. Phys. Lett.*, 1996, **260**, 109–114.

408 D. Huppert, L. M. Tolbert and S. Linares-Samaniego, *J. Phys. Chem. A*, 1997, **101**, 4602–4605.

409 K. M. Solntsev, D. Huppert and N. Agmon, *J. Phys. Chem. A*, 1999, **103**, 6984–6997.

410 C. Clower, K. M. Solntsev, J. Kowalik, L. M. Tolbert and D. Huppert, *J. Phys. Chem. A*, 2002, **106**, 3114–3122.

411 O. Gajst, G. G. Rozenman and D. Huppert, *J. Phys. Chem. A*, 2018, **122**, 209–216.

412 K. M. Solntsev, D. Huppert, N. Agmon and L. M. Tolbert, *J. Phys. Chem. A*, 2000, **104**, 4658–4669.

413 O. Gajst, L. Pinto da Silva, J. C. G. Esteves da Silva and D. Huppert, *J. Phys. Chem. A*, 2018, **122**, 6166–6175.

414 M. Than Htun, A. Suwaiyan and U. K. A. Klein, *Chem. Phys. Lett.*, 1995, **243**, 506–511.

415 M. Than Htun, A. Suwaiyan and U. K. A. Klein, *Chem. Phys. Lett.*, 1995, **243**, 512–518.

416 M. T. Htun, *Chem. Phys. Lett.*, 2011, **510**, 73–77.

417 R. Yang and S. G. Schulman, *Talanta*, 2003, **60**, 535–542.

418 M. Than Htun, *Chem. Phys. Lett.*, 2000, **328**, 437–445.

419 I. Kobayashi, M. Terazima and Y. Kimura, *J. Phys. Chem. B*, 2012, **116**, 1043–1052.

420 S. Abou-Al Einin, A. K. Zaitsev, N. K. Zaitsev and M. G. Kuzmin, *J. Photochem. Photobiol., A*, 1988, **41**, 365–373.

421 Y. V. Il'ichev, A. B. Demyashkevich and M. G. Kuzmin, *J. Phys. Chem.*, 1991, **95**, 3438–3444.

422 Y. V. Il'ichev, A. B. Demyashkevich, M. G. Kuzmin and H. Lemmetyinen, *J. Photochem. Photobiol., A*, 1993, **74**, 51–63.

423 K. M. Solntsev, Y. V. Il'ichev, A. B. Demyashkevich and M. G. Kuzmin, *J. Photochem. Photobiol., A*, 1994, **78**, 39–48.

424 K. M. Solntsev, S. A. Al.Ainain, Y. V. Il'ichev and M. G. Kuzmin, *J. Phys. Chem. A*, 2004, **108**, 8212–8222.

425 D. Mandal, S. K. Pal and K. Bhattacharyya, *J. Phys. Chem. A*, 1998, **102**, 9710–9714.

426 P. Dutta, A. Halder, S. Mukherjee, P. Sen, S. Sen and K. Bhattacharyya, *Langmuir*, 2002, **18**, 7867–7871.

427 K. Fujii, Y. Yasaka, M. Ueno, Y. Koyanagi, S. Kasuga, Y. Matano and Y. Kimura, *J. Phys. Chem. B*, 2017, **121**, 6042–6049.

428 K. Fujii, M. Aramaki and Y. Kimura, *J. Phys. Chem. B*, 2018, **122**, 12363–12374.

429 K. Adamczyk, M. Prémont-Schwarz, D. Pines, E. Pines and E. T. J. Nibbering, *Science*, 2009, **326**, 1690–1694.

430 D. Pines, J. Ditkovich, T. Mukra, Y. Miller, P. M. Kiefer, S. Daschakraborty, J. T. Hynes and E. Pines, *J. Phys. Chem. B*, 2016, **120**, 2440–2451.

431 M. J. Cox and H. J. Bakker, *J. Phys. Chem. A*, 2010, **114**, 10523–10530.

432 E. Pines, in *The Chemistry of Phenols*, ed. Z. Rappoport, 2003, John Wiley & Sons: Hoboken, NJ, pp. 491–527.

433 J. R. Platt, *J. Chem. Phys.*, 1949, **17**, 484–495.

434 A. T. Balaban and F. Harary, *Tetrahedron*, 1968, **24**, 2505–2516.

435 *Systematics of the Electronic Spectra of Conjugated Molecules: A Source Book, Papers of the Chicago group, 1949-1964*, ed. J. R. Platt and U. of Chicago, Laboratory of Molecular Structure and Spectra, Dept. of Physics, University of Chicago, Chicago, 1964.

436 E. B. Guidez and C. M. Aikens, *J. Phys. Chem. C*, 2013, **117**, 21466–21475.

437 R. S. Mulliken, *J. Chem. Phys.*, 1955, **23**, 1997–2011.

438 M. Rubio, M. Merchán, E. Ortí and B. O. Roos, *Chem. Phys.*, 1994, **179**, 395–409.

439 M. K. Roos, S. Reiter and R. de Vivie-Riedle, *Chem. Phys.*, 2018, **515**, 586–595.

440 S. Knippenberg, J. H. Starcke, M. Wormit and A. Dreuw, *Mol. Phys.*, 2010, **108**, 2801–2813.

441 F. Bettanin, L. F. A. Ferrão, M. J. Pinheiro, A. J. A. Aquino, H. Lischka, F. B. C. Machado and D. Nachtigallova, *J. Chem. Theory Comput.*, 2017, **13**, 4297–4306.

442 B.-Z. Magnes, N. V. Strashnikova and E. Pines, *Isr. J. Chem.*, 1999, **39**, 361–373.

443 F. Messina, M. Prémont-Schwarz, O. Braem, D. Xiao, V. S. Batista, E. T. J. Nibbering and M. Chergui, *Angew. Chem.*, 2013, **125**, 7009–7013.

444 L. M. Tolbert and J. E. Haubrich, *J. Am. Chem. Soc.*, 1990, **112**, 8163–8165.

445 Y. Shioya, M. Yagi and J. Higuchi, *Chem. Phys. Lett.*, 1989, **154**, 25–28.

446 L. M. Tolbert and J. E. Haubrich, *J. Am. Chem. Soc.*, 1994, **116**, 10593–10600.

447 B. Cohen and D. Huppert, *J. Phys. Chem. A*, 2000, **104**, 2663–2667.

448 B. Cohen, J. Segal and D. Huppert, *J. Phys. Chem. A*, 2002, **106**, 7462–7467.

449 N. Koifman, B. Cohen and D. Huppert, *J. Phys. Chem. A*, 2002, **106**, 4336–4344.

450 B. Cohen, P. Leiderman and D. Huppert, *J. Lumin.*, 2003, **102–103**, 676–681.

451 L. Genosar, T. Lasitza, R. Gepshtein, P. Leiderman, N. Koifman and D. Huppert, *J. Phys. Chem. A*, 2005, **109**, 4852–4861.

452 R. M. D. Nunes, L. G. Arnaut, K. M. Solntsev, L. M. Tolbert and S. J. Formosinho, *J. Am. Chem. Soc.*, 2005, **127**, 11890–11891.

453 H. Yu, O.-H. Kwon and D.-J. Jang, *J. Phys. Chem. A*, 2004, **108**, 5932–5937.

454 K. M. Solntsev, C. E. Clower, L. M. Tolbert and D. Huppert, *J. Am. Chem. Soc.*, 2005, **127**, 8534–8544.

455 A. V. Popov, E.-A. Gould, M. A. Salvitti, R. Hernandez and K. M. Solntsev, *Phys. Chem. Chem. Phys.*, 2011, **13**, 14914.

456 E.-A. Gould, A. V. Popov, L. M. Tolbert, I. Presiado, Y. Erez, D. Huppert and K. M. Solntsev, *Phys. Chem. Chem. Phys.*, 2012, **14**, 8964.

457 J. L. Pérez Lustres, S. A. Kovalenko, M. Mosquera, T. Senyushkina, W. Flasche and N. P. Ernsting, *Angew. Chem., Int. Ed.*, 2005, **44**, 5635–5639.

458 J. L. Pérez-Lustres, F. Rodriguez-Prieto, M. Mosquera, T. A. Senyushkina, N. P. Ernsting and S. A. Kovalenko, *J. Am. Chem. Soc.*, 2007, **129**, 5408–5418.

459 M. Veiga-Gutiérrez, A. Brenlla, C. Carreira Blanco, B. Fernández, S. A. Kovalenko, F. Rodríguez-Prieto, M. Mosquera and J. L. P. Lustres, *J. Phys. Chem. B*, 2013, **117**, 14065–14078.

460 Y. M. Lee, S.-Y. Park, H. Kim, T. G. Kim and O.-H. Kwon, *Methods Appl. Fluoresc.*, 2016, **4**, 024004.

461 S.-Y. Park, T. G. Kim, M. J. Ajitha, K. Kwac, Y. M. Lee, H. Kim, Y. Jung and O.-H. Kwon, *Phys. Chem. Chem. Phys.*, 2016, **18**, 24880–24889.

462 S.-Y. Park, Y. M. Lee, K. Kwac, Y. Jung and O.-H. Kwon, *Chem.–A Eur. J.*, 2016, **22**, 4340–4344.

463 Y. Choi, H. Kim and O. Kwon, *Bull. Korean Chem. Soc.*, 2022, **43**, 501–507.

464 Y.-J. Choi, H.-W. Nho, Y.-J. Kim and O.-H. Kwon, *ChemPhotoChem*, 2024, **8**, e202300164.

465 S.-H. Lee, Y.-J. Choi, Y.-J. Kim, J.-M. Kee and O.-H. Kwon, *Cell Rep. Phys. Sci.*, 2024, **5**, 102155.

466 Y.-J. Kim, S. Rakshit, G. Y. Jin, P. Ghosh, Y. M. Lee, W.-W. Park, Y. S. Kim and O.-H. Kwon, *Chem.–A Eur. J.*, 2017, **23**, 17179–17185.

467 N. Karton-Lifshin, E. Segal, L. Omer, M. Portnoy, R. Satchi-Fainaro and D. Shabat, *J. Am. Chem. Soc.*, 2011, **133**, 10960–10965.

468 N. Karton-Lifshin, L. Albertazzi, M. Bendikov, P. S. Baran and D. Shabat, *J. Am. Chem. Soc.*, 2012, **134**, 20412–20420.

469 N. Karton-Lifshin, I. Presiado, Y. Erez, R. Gepshtein, D. Shabat and D. Huppert, *J. Phys. Chem. A*, 2012, **116**, 85–92.

470 R. Simkovitch, E. Kisin-Finfer, S. Shomer, R. Gepshtein, D. Shabat and D. Huppert, *J. Photochem. Photobiol., A*, 2013, **254**, 45–53.

471 C. Lee, S. Chung, H. Song, Y. M. Rhee, E. Lee and T. Joo, *ChemPhotoChem*, 2021, **5**, 245–252.

472 R. Simkovitch, S. Shomer, R. Gepshtein, D. Shabat and D. Huppert, *J. Phys. Chem. A*, 2013, **117**, 3925–3934.

473 R. Simkovitch, K. Akulov, S. Shomer, M. E. Roth, D. Shabat, T. Schwartz and D. Huppert, *J. Phys. Chem. A*, 2014, **118**, 4425–4443.

474 R. Simkovitch, S. Shomer, R. Gepshtein, D. Shabat and D. Huppert, *J. Phys. Chem. A*, 2014, **118**, 1832–1840.

475 O. Green, R. Simkovitch, L. Pinto da Silva, J. C. G. Esteves da Silva, D. Shabat and D. Huppert, *J. Phys. Chem. A*, 2016, **120**, 6184–6199.

476 L. Pinto da Silva, O. Green, O. Gajst, R. Simkovitch, D. Shabat, J. C. G. Esteves da Silva and D. Huppert, *ACS Omega*, 2018, **3**, 2058–2073.

477 O. Green, O. Gajst, R. Simkovitch, D. Shabat and D. Huppert, *J. Photochem. Photobiol., A*, 2017, **349**, 230–237.

478 O. Green, O. Gajst, R. Simkovitch, D. Shabat and D. Huppert, *J. Phys. Chem. A*, 2017, **121**, 3079–3087.

479 Z. Li, Q. Yang, R. Chang, G. Ma, M. Chen and W. Zhang, *Dyes Pigm.*, 2011, **88**, 307–314.

480 B. Zhu, C. Gao, Y. Zhao, C. Liu, Y. Li, Q. Wei, Z. Ma, B. Du and X. Zhang, *Chem. Commun.*, 2011, **47**, 8656–8658.

481 Z. Luo, B. Yang, C. Zhong, F. Tang, M. Yuan, Y. Xue, G. Yao, J. Zhang and Y. Zhang, *Dyes Pigm.*, 2013, **97**, 52–57.

482 L. Biczók, P. Valat and V. Wintgens, *Phys. Chem. Chem. Phys.*, 1999, **1**, 4759–4766.

483 L. Biczók, P. Valat and V. Wintgens, *Phys. Chem. Chem. Phys.*, 2001, **3**, 1459–1464.

484 L. Biczók, P. Valat and V. Wintgens, *Photochem. Photobiol. Sci.*, 2003, **2**, 230–235.

485 T. Kumpulainen, B. H. Bakker, M. Hilbers and A. M. Brouwer, *J. Phys. Chem. B*, 2015, **119**, 2515–2524.

486 T. Kumpulainen, B. H. Bakker and A. M. Brouwer, *Phys. Chem. Chem. Phys.*, 2015, **17**, 20715–20724.

487 T. Kumpulainen, A. Rosspeintner, B. Dereka and E. Vauthey, *J. Phys. Chem. Lett.*, 2017, **8**, 4516–4521.

488 P. Verma, A. Rosspeintner, B. Dereka, E. Vauthey and T. Kumpulainen, *Chem. Sci.*, 2020, **11**, 7963–7971.

489 A. Yamaguchi, M. Namekawa, T. Kamijo, T. Itoh and N. Teramae, *Anal. Chem.*, 2011, **83**, 2939–2946.

490 B. Hinkeldey, A. Schmitt and G. Jung, *ChemPhysChem*, 2008, **9**, 2019–2027.

491 D. Maus, A. Grandjean and G. Jung, *J. Phys. Chem. A*, 2018, **122**, 9025–9030.

492 R. F. Robbins, *J. Chem. Soc.*, 1960, 2553–2556.

493 D. Maus, *PhD Thesis*, Universität des Saarlandes, Saarbrücken, Germany, 2021.

494 Y. Hu, J. F. Joung, J.-E. Jeong, Y. Jeong, H. Y. Woo, Y. She, S. Park and J. Yoon, *Sens. Actuators, B*, 2019, **280**, 298–305.

495 C. Spies, B. Finkler, N. Acar and G. Jung, *Phys. Chem. Chem. Phys.*, 2013, **15**, 19893.

496 C. Spies, S. Shomer, B. Finkler, D. Pines, E. Pines, G. Jung and D. Huppert, *Phys. Chem. Chem. Phys.*, 2014, **16**, 9104.

497 M. Vester, T. Staut, J. Enderlein and G. Jung, *J. Phys. Chem. Lett.*, 2015, **6**, 1149–1154.

498 M. Vester, A. Grueter, B. Finkler, R. Becker and G. Jung, *Phys. Chem. Chem. Phys.*, 2016, **18**, 10281–10288.

499 J. Knorr, N. Sülzner, B. Geissler, C. Spies, A. Grandjean, R. J. Kutta, G. Jung and P. Nuernberger, *Photochem. Photobiol. Sci.*, 2022, **21**, 2179–2192.

500 N. Sülzner and C. Hättig, *J. Phys. Chem. A*, 2022, **126**, 5911–5923.

501 N. Sülzner and C. Hättig, *Phys. Chem. Chem. Phys.*, 2023, **25**, 11130–11144.

502 N. Agmon, *J. Mol. Liq.*, 2000, **85**, 87–96.

503 R. Simkovitch, S. Shomer, R. Gepshtein and D. Huppert, *J. Phys. Chem. B*, 2015, **119**, 2253–2262.

504 M. Eigen, L. De Maeyer and Z. Elektrochem, *Ber. Bunsenges. Phys. Chem.*, 1955, **59**, 986–993.

505 M. Eigen, W. Kruse, G. Maass and L. Demaeyer, *Prog. React. Kinet. Mech.*, 1964, **2**, 285.

506 N. Sülzner, *Chem*, 2024, **10**, 3276–3278.

507 N. Agmon, *J. Chem. Phys.*, 1999, **110**, 2175–2180.

508 N. Agmon and I. V. Gopich, *Chem. Phys. Lett.*, 1999, **302**, 399–404.

509 K. M. Solntsev, D. Huppert and N. Agmon, *Phys. Rev. Lett.*, 2001, **86**, 3427–3430.

510 E. M. Espinoza, J. A. Clark, C. P. d. Silva, J. B. Derr, G. T. d. M. Silva, M. K. Billones, M. Morales, F. H. Quina and V. I. Vullev, *J. Photochem. Photobiol.*, 2022, **10**, 100110.

511 A. Grandjean, J. L. Pérez Lustres, S. Muth, D. Maus and G. Jung, *J. Phys. Chem. Lett.*, 2021, **12**, 1683–1689.

512 A. Grandjean, J. L. Pérez Lustres and G. Jung, *ChemPhotoChem*, 2021, **5**, 1094–1105.

513 M. Barroso, L. G. Arnaut and S. J. Formosinho, *J. Phys. Chem. A*, 2007, **111**, 591–602.

514 H.-H. Limbach, K. B. Schowen and R. L. Schowen, *J. Phys. Org. Chem.*, 2010, **23**, 586–605.

515 P. M. Kiefer and J. T. Hynes, *J. Phys. Org. Chem.*, 2010, **23**, 632–646.

516 A. J. Kresge, D. S. Sagatys and H. L. Chen, *J. Am. Chem. Soc.*, 1977, **99**, 7228–7233.

517 R. A. Marcus, *J. Phys. Chem.*, 1968, **72**, 891–899.

518 A. Das, P. Ghosh, A. Dutta and P. Sen, *Chem. Phys. Impact*, 2021, **3**, 100044.

519 A. J. Kresge, *Acc. Chem. Res.*, 1975, **8**, 354–360.

520 P. M. Kiefer and J. T. Hynes, *Isr. J. Chem.*, 2004, **44**, 171–184.

521 K. Yates and J. Phys, *Org. Chem.*, 1989, **2**, 300–322.

522 D. N. Silverman, *Biochimica et Biophys. Acta (BBA) – Bioenerg.*, 2000, **1458**, 88–103.

523 K. S. Peters, *Acc. Chem. Res.*, 2009, **42**, 89–96.

524 A. Shabashini, S. Kumar Panja, A. Biswas, S. Bera and G. Chandra Nandi, *J. Photochem. Photobiol., A*, 2022, **432**, 114087.

525 E. Hückel, *Z. Phys.*, 1931, **70**, 204–286.

526 Z. Wen, L. José Karas, C.-H. Wu and J. I-Chia Wu, *Chem. Commun.*, 2020, **56**, 8380–8383.

527 J. Yan, T. Slanina, J. Bergman and H. Ottosson, *Chem.–Eur. J.*, 2023, **29**, e202203748.

528 M. Rosenberg, C. Dahlstrand, K. Kilså and H. Ottosson, *Chem. Rev.*, 2014, **114**, 5379–5425.

529 N. C. Baird, *J. Am. Chem. Soc.*, 1972, **94**, 4941–4948.

530 B. J. Lampkin, Y. H. Nguyen, P. B. Karadakov and B. VanVeller, *Phys. Chem. Chem. Phys.*, 2019, **21**, 11608–11614.

531 C.-H. Wu, L. J. Karas, H. Ottosson and J. I.-C. Wu, *Proc. Natl. Acad. Sci.*, 2019, **116**, 20303–20308.

532 B. Szczepanik, *J. Mol. Struct.*, 2015, **1099**, 209–214.

533 Z. R. Grabowski, W. Rubaszewska and J. Chem, *J. Chem. Soc., Faraday Trans. 1*, 1977, **73**, 11–28.

534 E. R. Davidson and A. A. Jarzęcki, *Chem. Phys. Lett.*, 1998, **285**, 155–159.

535 A. Weller, *P. React. Kinetics Mech.*, 1961, **1**, 187.

536 S. Schulman and Q. Fernando, *Tetrahedron*, 1968, **24**, 1777–1783.

537 J. F. Joung, M. Jeong and S. Park, *Phys. Chem. Chem. Phys.*, 2022, **24**, 21714–21721.

538 D. Himmel, S. K. Goll, I. Leito and I. Krossing, *Angew. Chem., Int. Ed.*, 2010, **49**, 6885–6888.

539 F. Bastkowski, S. Seitz, A. Heering, R. Born, S. Lainela, I. Leito, J. Nerut, J. Saame, V. Radtke, D. Nagy, Z. S. Nagyne, L. Szucs, M. Rozikova, M. Vičarova, L. C. Deleebeeck, A. Snedden, B. Anes, R. Bettencourt, M. F. Camoes, R. Quendera, L. F. Ribeiro, D. Stoica, T. Naykki, L. Liv, E. Uysal and G. Yerleşkesi, *Messunsicherheit praxisgerecht bestimmen – Prüfprozesse in der industriellen Praxis 2021*, VDI Verlag, 2021, pp. 13–22.

540 L. Deleebeeck, A. Snedden, D. Nagy, Z. Szilágyi Nagyné, M. Roziková, M. Vičarová, A. Heering, F. Bastkowski, I. Leito, R. Quendera, V. Cabral and D. Stoica, *Sensors*, 2021, **21**, 3935.

541 V. Radtke, D. Stoica, I. Leito, F. Camões, I. Krossing, B. Anes, M. Roziková, L. Deleebeeck, S. Veltzé, T. Näykki, F. Bastkowski, A. Heering, N. Dániel, R. Quendera, L. Liv, E. Uysal and N. Lawrence, *Pure Appl. Chem.*, 2021, **93**, 1049–1060.

542 K. M. Solntsev, D. Huppert and N. Agmon, *J. Phys. Chem. A*, 2001, **105**, 5868–5876.

543 R. Bhide, C. N. Feltenberger, G. S. Phun, G. Barton, D. Fishman and S. Ardo, *J. Am. Chem. Soc.*, 2022, **144**, 14477–14488.

544 J. Ho and M. L. Coote, *Wiley Interdiscip. Rev.: Comput. Mol. Sci.*, 2011, **1**, 649–660.

545 M. D. Liptak and G. C. Shields, *Int. J. Quantum Chem.*, 2001, **85**, 727–741.

546 J. R. Pliego, *Chem. Phys. Lett.*, 2003, **367**, 145–149.

547 J. Ho and M. L. Coote, *Theor. Chem. Acc.*, 2009, **125**, 3.

548 R. Casasnovas, J. Ortega-Castro, J. Frau, J. Donoso and F. Muñoz, *Int. J. Quantum Chem.*, 2014, **114**, 1350–1363.

549 I. A. Topol, G. J. Tawa, S. K. Burt and A. A. Rashin, *J. Chem. Phys.*, 1999, **111**, 10998–11014.

550 M. D. Liptak and G. C. Shields, *J. Am. Chem. Soc.*, 2001, **123**, 7314–7319.

551 A. M. Toth, M. D. Liptak, D. L. Phillips and G. C. Shields, *J. Chem. Phys.*, 2001, **114**, 4595–4606.

552 M. D. Liptak, K. C. Gross, P. G. Seybold, S. Feldgus and G. C. Shields, *J. Am. Chem. Soc.*, 2002, **124**, 6421–6427.

553 M. D. Tissandier, K. A. Cowen, W. Y. Feng, E. Gundlach, M. H. Cohen, A. D. Earhart, J. V. Coe and T. R. Tuttle, *J. Phys. Chem. A*, 1998, **102**, 7787–7794.

554 C. P. Kelly, C. J. Cramer and D. G. Truhlar, *J. Phys. Chem. B*, 2007, **111**, 408–422.

555 E. Rossini and E.-W. Knapp, *J. Comput. Chem.*, 2016, **37**, 1082–1091.

556 E. Rossini, A. D. Bochevarov and E. W. Knapp, *ACS Omega*, 2018, **3**, 1653–1662.

557 L. C. Kröger, S. Müller, I. Smirnova and K. Leonhard, *J. Phys. Chem. A*, 2020, **124**, 4171–4181.

558 M. Busch, E. Ahlberg, E. Ahlberg and K. Laasonen, *ACS Omega*, 2022, **7**, 17369–17383.

559 J. W. Zheng and W. H. Green, *J. Phys. Chem. A*, 2023, **127**, 10268–10281.

560 J. W. Zheng, E. A. Ibrahim and W. H. Green, pKa Prediction in Non-Aqueous Solvents, *chemRxiv*, preprint, 2024, **https://chemrxiv.org/engage/chemrxiv/article-details/663e53e521291e5d1df186b5**.

561 J. Gao, N. Li and M. Freindorf, *J. Am. Chem. Soc.*, 1996, **118**, 4912–4913.

562 B. Mennucci, *Wiley Interdiscip. Rev.: Comput. Mol. Sci.*, 2012, **2**, 386–404.

563 P. F. Moreira, L. Giestas, C. Yihwa, C. Vautier-Giongo, F. H. Quina, A. L. Maçanita and J. C. Lima, *J. Phys. Chem. A*, 2003, **107**, 4203–4210.

564 B. Szczepanik, S. Styrcz and M. Góra, *Spectrochim. Acta, Part A*, 2008, **71**, 403–409.

565 J. Gao and K. Byun, *Theor. Chem. Acc.*, 1997, **96**, 151–156.

566 O. A. Borg and B. Durbeej, *J. Phys. Chem. B*, 2007, **111**, 11554–11565.

567 O. Anders Borg and B. Durbeej, *Phys. Chem. Chem. Phys.*, 2008, **10**, 2528.

568 D. Jacquemin and C. Adamo, *Density-Functional Methods for Excited States*, Springer International Publishing, Cham, 2016, pp. 347–375.

569 D. Jacquemin, B. Mennucci and C. Adamo, *Phys. Chem. Chem. Phys.*, 2011, **13**, 16987–16998.

570 E. Brémond, M. Savarese, C. Adamo and D. Jacquemin, *J. Chem. Theory Comput.*, 2018, **14**, 3715–3727.

571 P.-F. Loos, A. Scemama and D. Jacquemin, *J. Phys. Chem. Lett.*, 2020, **11**, 2374–2383.

572 D. Jacquemin, E. A. Perpète, I. Ciofini and C. Adamo, *Acc. Chem. Res.*, 2009, **42**, 326–334.

573 D. Jacquemin, V. Wathelet, E. A. Perpète and C. Adamo, *J. Chem. Theory Comput.*, 2009, **5**, 2420–2435.

574 Y. Wang, H. Li and Y. Shi, *New J. Chem.*, 2015, **39**, 7026–7032.

575 J. Yi and H. Fang, *J. Mol. Model.*, 2017, **23**, 312.

576 J. Yi and H. Fang, *Struct. Chem.*, 2018, **29**, 1341–1350.

577 D. Jacquemin, E. A. Perpète, G. Scalmani, I. Ciofini, C. Peltier and C. Adamo, *Chem. Phys.*, 2010, **372**, 61–66.

578 M. Guglielmi, I. Tavernelli and U. Rothlisberger, *Phys. Chem. Chem. Phys.*, 2009, **11**, 4549–4555.

579 G. Bekçioğlu, F. Hoffmann and D. Sebastiani, *J. Phys. Chem. A*, 2015, **119**, 9244–9251.

580 Y. Li, F. Siddique, A. J. A. Aquino and H. Lischka, *J. Phys. Chem. A*, 2021, **125**, 5765–5778.

581 J. D. Coe, B. G. Levine and T. J. Martínez, *J. Phys. Chem. A*, 2007, **111**, 11302–11310.

582 S.-H. Xia, B.-B. Xie, Q. Fang, G. Cui and W. Thiel, *Phys. Chem. Chem. Phys.*, 2015, **17**, 9687–9697.

583 W.-W. Guo, X.-Y. Liu, W.-K. Chen and G. Cui, *RSC Adv.*, 2016, **6**, 85574–85581.

584 D. Jacquemin, I. Duchemin and X. Blase, *J. Phys. Chem. Lett.*, 2017, **8**, 1524–1529.

585 C. A. Guido, B. Mennucci, G. Scalmani and D. Jacquemin, *J. Chem. Theory Comput.*, 2018, **14**, 1544–1553.

586 R. Sarkar, M. Boggio-Pasqua, P.-F. Loos and D. Jacquemin, *J. Chem. Theory Comput.*, 2021, **17**, 1117–1132.

587 A. D. Laurent and D. Jacquemin, *Int. J. Quantum Chem.*, 2013, **113**, 2019–2039.

588 C. Adamo and D. Jacquemin, *Chem. Soc. Rev.*, 2013, **42**, 845–856.

589 D. Jacquemin, E. A. Perpète, G. E. Scuseria, I. Ciofini and C. Adamo, *J. Chem. Theory Comput.*, 2008, **4**, 123–135.

590 A. L. Sobolewski, W. Domcke and C. Hättig, *J. Phys. Chem. A*, 2006, **110**, 6301–6306.

591 C. Suellen, R. G. Freitas, P.-F. Loos and D. Jacquemin, *J. Chem. Theory Comput.*, 2019, **15**, 4581–4590.

592 A. Acharya, S. Chaudhuri and V. S. Batista, *J. Chem. Theory Comput.*, 2018, **14**, 867–876.

593 S. Grimme and M. Parac, *ChemPhysChem*, 2003, **4**, 292–295.

594 A. Prlj, M. E. Sandoval-Salinas, D. Casanova, D. Jacquemin and C. Corminboeuf, *J. Chem. Theory Comput.*, 2016, **12**, 2652–2660.

595 S. Khodia and S. Maity, *Phys. Chem. Chem. Phys.*, 2022, **24**, 12043–12051.

596 A. Ghiami-Shomami and C. Hättig, *J. Comput. Chem.*, 2023, **44**, 1941–1955.

597 A. Klamt, *J. Phys. Chem.*, 1995, **99**, 2224–2235.

598 A. Klamt, V. Jonas, T. Bürger and J. C. W. Lohrenz, *J. Phys. Chem. A*, 1998, **102**, 5074–5085.

599 A. Klamt and F. Eckert, *Fluid Phase Equilib.*, 2000, **172**, 43–72.

600 N. Sülzner, J. Haberhauer, C. Hättig and A. Hellweg, *J. Comput. Chem.*, 2022, **43**, 1011–1022.

601 T. Kloss, J. Heil and S. M. Kast, *J. Phys. Chem. B*, 2008, **112**, 4337–4343.

602 F. Hoffgaard, J. Heil and S. M. Kast, *J. Chem. Theory Comput.*, 2013, **9**, 4718–4726.

603 S. Tsuru, B. Sharma, D. Marx and C. Hättig, *J. Chem. Theory Comput.*, 2023, **19**, 2291–2303.

604 J. M. Toldo, M. T. d. Casal, E. Ventura, S. A. d. Monte and M. Barbatti, *Phys. Chem. Chem. Phys.*, 2023, **25**, 8293–8316.

605 J. C. Tully, *J. Chem. Phys.*, 1990, **93**, 1061–1071.

606 J. Jankowska, M. Barbatti, J. Sadlej and A. L. Sobolewski, *Phys. Chem. Chem. Phys.*, 2017, **19**, 5318–5325.

607 M. Barbatti and K. Sen, *Int. J. Quantum Chem.*, 2016, **116**, 762–771.

608 A. Petrone, F. Perrella, F. Coppola, L. Crisci, G. Donati, P. Cimino and N. Rega, *Chem. Phys. Rev.*, 2022, **3**, 021307.

609 M. Ruckenbauer, M. Barbatti, T. Müller and H. Lischka, *J. Phys. Chem. A*, 2010, **114**, 6757–6765.

610 M. Ruckenbauer, M. Barbatti, T. Müller and H. Lischka, *J. Phys. Chem. A*, 2013, **117**, 2790–2799.

611 D. B. Cordes, S. Gamsey, Z. Sharrett, A. Miller, P. Thoniyot, R. A. Wessling and B. Singaram, *Langmuir*, 2005, **21**, 6540–6547.

612 A. B. Kotlyar, N. Borovok, S. Raviv, L. Zimanyi and M. Gutman, *Photochem. Photobiol.*, 1996, **63**, 448–454.

613 M. Schmitz, M.-S. Bertrams, A. C. Sell, F. Glaser and C. Kerzig, *J. Am. Chem. Soc.*, 2024, **146**, 25799–25812.

614 F. Johannsen, L. Williams, M. H. Chak and M. Drescher, *J. Phys. Chem. Lett.*, 2024, **15**, 7069–7074.

615 A. Clasen, S. Wenderoth, I. Tavernaro, J. Fleddermann, A. Kraegeloh and G. Jung, *RSC Adv.*, 2019, **9**, 35695–35705.

616 A. C. Sedgwick, L. Wu, H.-H. Han, S. D. Bull, X.-P. He, T. D. James, J. L. Sessler, B. Z. Tang, H. Tian and J. Yoon, *Chem. Soc. Rev.*, 2018, **47**, 8842–8880.

617 L. Wimberger, J. Andréasson and J. E. Beves, *Chem. Commun.*, 2022, **58**, 5610–5613.

618 Y. Cheng, X. Ma, J. Zhai and X. Xie, *Chem. Commun.*, 2023, **59**, 1805–1808.

619 P. Utroša, J. A. Carroll, E. Žagar, D. Pahovnik and C. Barner-Kowollik, *Chem.–A Eur. J.*, 2024, **30**, e202400820.

620 A. P. Demchenko, *J. Mol. Struct.*, 2014, **1077**, 51–67.

621 M. Lawrence, C. J. Marzzacco, C. Morton, C. Schwab and A. M. Halpern, *J. Phys. Chem.*, 1991, **95**, 10294–10299.

622 L. M. Tolbert, L. C. Harvey and R. C. Lum, *J. Phys. Chem.*, 1993, **97**, 13335–13340.

623 K. Schäfer and H. Ihmels, *J. Fluoresc.*, 2017, **27**, 1221–1224.

624 J. Othong, J. Boonmak, F. Kielar and S. Youngme, *ACS Appl. Mater. Interfaces*, 2020, **12**, 41776–41784.

625 F. A. d. C. Silva, E. T. Rezende, D. B. Filho, D. d. Brito Rezende, I. M. Cuccovia, L. F. Gome, M. F. P. d. Silva and M. J. Politi, *J. Lumin.*, 2014, **146**, 57–63.

626 P. M. Kiefer and J. T. Hynes, *J. Phys. Chem. A*, 2003, **107**, 9022–9039.

627 E. Sato, K. Chiba, M. Hoshi and Y. Kanaoka, *Chem. Pharm. Bull.*, 1992, **40**, 786–788.

628 S. Hemmer, H. Hui, J. Draeger, J. Menges, E. Schwarz, A. Wrede, J. Oertel, L. Kaestner, G. Jung and S. Urbschat, *A novel fluorescent diagnostic probe as a potential Point-of-Care diagnostic tool to estimate recurrence risk of meningiomas*, 2024, submitted.

629 J. A. Menges, A. Grandjean, A. Clasen and G. Jung, *ChemCatChem*, 2020, **12**, 2630–2637.

630 J. A. Menges, A. Clasen, M. Jourdain, J. Beckmann, C. Hoffmann, J. König and G. Jung, *Langmuir*, 2019, **35**, 2506–2516.

631 D. Han, C. Li, X. Jin, J. Zhou, Y. Xu, T. Jiao and P. Duan, *Adv. Photonics Res.*, 2022, **3**, 2100287.

632 K. Y. Yung, A. J. Schadock-Hewitt, N. P. Hunter, F. V. Bright and G. A. Baker, *Chem. Commun.*, 2011, **47**, 4775–4777.

633 N. Amdursky, Y. Lin, N. Aho and G. Groenhof, *Proc. Natl. Acad. Sci.*, 2019, **116**, 2443–2451.

634 Y. Sha, Z. Guo, Y. Han, Z. Xue, M. Li, Y. Wan, W. Yang and X. Ma, *J. Phys. Chem. C*, 2023, **127**, 14458–14467.

635 S. Heckel, J. Hübner, A. Leutzgen, G. Jung and J. Simmchen, *Catalysts*, 2021, **11**, 599.

636 A. Yucknovsky, B. B. Rich, S. Gutkin, A. Ramanthrikkovil Variyam, D. Shabat, B. Pokroy and N. Amdursky, *J. Phys. Chem. B*, 2022, **126**, 6331–6337.

637 P. Sun, Z. Li, X. Zhang, Y. Liao and S. Liao, *Macromol. Rapid Commun.*, 2024, **45**, 2400054.

638 J. Tripathi, H. Gupta and A. Sharma, Esterification of Carboxylic Acids utilizing Eosin Y as a Photoacid Catalyst,

chemRxiv, preprint, 2024, **https://chemrxiv.org/engage/chemrxiv/article-details/663218ca91aefa6ce1e0070c**.

639 H. Liu, Y. Chen, D. An, X. Zhang and S. Liao, *Synlett*, 2022, **33**, 800–804.

640 J. Saway, A. F. Pierre and J. J. Badillo, *Org. Biomol. Chem.*, 2022, **20**, 6188–6192.

641 N. Otani, K. Higashiyama, H. Sakai, T. Hasobe, D. Takahashi and K. Toshima, *Eur. J. Org Chem.*, 2023, **26**, e202300287.

642 B. Yang, K. Dong, X.-S. Li, L.-Z. Wu and Q. Liu, *Org. Lett.*, 2022, **24**, 2040–2044.

643 A. M. M. Alazaly, A. S. I. Amer, A. M. Fathi and A. A. Abdel-Shafi, *J. Photochem. Photobiol., A*, 2018, **364**, 819–825.

644 S. Kohse, A. Neubauer, A. Pazidis, S. Lochbrunner and U. Kragl, *J. Am. Chem. Soc.*, 2013, **135**, 9407–9411.

645 A. M. Alfaraidi, B. Kudisch, N. Ni, J. Thomas, T. Y. George, K. Rajabimoghadam, H. J. Jiang, D. G. Nocera, M. J. Aziz and R. Y. Liu, *J. Am. Chem. Soc.*, 2023, **145**, 26720–26727.

646 O. Alghazwat, A. Elgattar and Y. Liao, *Photochem. Photobiol. Sci.*, 2023, **22**, 2573–2578.

647 A. de Vries, K. Goloviznina, M. Reiter, M. Salanne and M. R. Lukatskaya, *Chem. Mater.*, 2024, **36**, 1308–1317.

648 J. Bae, H. Lim, J. Ahn, Y. H. Kim, M. S. Kim and I.-D. Kim, *Adv. Mater.*, 2022, **34**, 2201734.

649 A. Yucknovsky, Y. Shlosberg, N. Adir and N. Amdursky, *Angew. Chem., Int. Ed.*, 2023, **62**, e202301541.

650 G. S. Phun, R. Bhide and S. Ardo, *Energy Environ. Sci.*, 2023, **16**, 4593–4611.

651 S. Haghighat, S. Ostresh and J. M. Dawlaty, *J. Phys. Chem. B*, 2016, **120**, 1002–1007.

652 S.-F. Zhou, G.-M. Wu, C.-X. Zhang and Q.-L. Wang, *Adv. Mater. Interfaces*, 2022, **9**, 2101247.

653 F. Wendler, M. Sittig, J. C. Tom, B. Dietzek and F. H. Schacher, *Chem.–A Eur. J.*, 2020, **26**, 2365–2379.

654 M. Bitsch, A. K. Boehm, A. Grandjean, G. Jung and M. Gallei, *Molecules*, 2021, **26**, 7350.

655 H. Chen, K. Wen, Y. Lu, X. Zhang, Y. Shi, Q. Shi, H. Ma, Q. Peng and H. Huang, *Sci. China:Chem.*, 2022, **65**, 2528–2537.

656 L. Kang, H. Zhao, S. Liu, Y. Liu, Y. Liu, D. Chen, H. Qiu, J. Yang, Y. Gu and Y. Zhao, *Eur. J. Med. Chem.*, 2022, **242**, 114669.

657 L. I. Kaberov, M. Sittig, A. Chettri, A. Ibrahim, B. Dietzek-Ivanšić and F. H. Schacher, *Polym. Chem.*, 2023, **14**, 3453–3464.

658 A. Chettri, L. I. Kaberov, N. Klosterhalfen, S. Perera, M. Jamshied, F. H. Schacher and B. Dietzek-Ivanšić, *Chem.–A Eur. J.*, 2024, **30**, e202401047.

659 A. Losi and C. Viappiani, *Chem. Phys. Lett.*, 1998, **289**, 500–506.

660 P. M. Kiefer and J. T. Hynes, *J. Phys. Chem. A*, 2004, **108**, 11793–11808.

661 T. B. McAnaney, X. Shi, P. Abbyad, H. Jung, S. J. Remington and S. G. Boxer, *Biochemistry*, 2005, **44**, 8701–8711.

662 P. M. Kiefer and J. T. Hynes, *J. Phys. Chem. A*, 2002, **106**, 1834–1849.

663 P. M. Kiefer and J. T. Hynes, *J. Phys. Chem. A*, 2002, **106**, 1850–1861.

664 K. M. Solntsev, L. M. Tolbert, B. Cohen, D. Huppert, Y. Hayashi and Y. Feldman, *J. Am. Chem. Soc.*, 2002, **124**, 9046–9047.

665 F. Pavošević, S. Hammes-Schiffer, A. Rubio and J. Flick, *J. Am. Chem. Soc.*, 2022, **144**, 4995–5002.

666 I. Sokolovskii and G. Groenhof, *Nanophotonics*, 2024, **13**(14), 2687–2694.